# Regulation of cell morphogenesis by targeted noise suppression and trafficking of a G protein alpha subunit

Gauri Dixit

A dissertation submitted to the faculty of the University of North Carolina at Chapel Hill in partial fulfillment of the requirements for the degree of Doctor of Philosophy in the Department of Biochemistry and Biophysics

Chapel Hill
2014

Approved by:

Henrik Dohlman

Timothy Elston.

Beverly Errede

Patrick Brennwald

Brian Strahl

## ABSTRACT

GAURI DIXIT: Regulation of cell morphogenesis by targeted noise suppression and trafficking of a G protein alpha subunit
(Under the direction of Dr. Henrik G. Dohlman)

G proteins and their associated receptors form the largest class of proteins that receive and transduce chemical and sensory signals. Regulation of G proteins therefore, is critical to appropriate cellular responses. The work in this thesis evaluates a new function for a known regulator of signaling and identifies a new class of previously unknown regulators that mediate G protein trafficking. Using a yeast model system we demonstrate a novel role for the Regulator of G protein Signaling (RGS) protein in suppression of cell-to-cell variability. Furthermore we identify a novel cascade of ubiquitin-binding domain (UBDs) proteins that serve to deliver the Gα protein from the plasma membrane to the vacuole. Through biochemical assays and single cell analysis we find that the RGS and UBD proteins regulate cellular morphogenesis during signaling. More broadly through this work we were able to uncouple signal and noise in a prototypical stimulus-response pathway and demonstrate for the first time the consequences of G protein trafficking in a non-visual system. This work is important because a thorough understanding of how G protein signaling is spatially and temporally regulated will eventually lead to new drug targets, and more effective or targeted therapeutics.

## ACKNOWLEDGEMENTS

Completion of the work presented here would not have been possible without the support of a lot of people. I would like to begin by thanking my advisor Henrik Dohlman. He has always encouraged me to follow my ideas and helped me grow as an independent scientist. He never let me lose sight of the big picture, particularly when I got caught in the nitty gritty details. I would like to especially thank him for all his patience and for making me a better scientific writer and communicator. I would also like to thank the members of my committee, Tim Elston, Beverly Errede, Patrick Brennwald, and Brian Strahl. They were always available to talk to whenever I needed their help. The work presented here has been greatly influenced by their helpful suggestions and positive feedback.

I would like to thank Laura Hall for early contributions to this work. Thanks to Josh Kelley for his excellent microscopy and troubleshooting skills, help on critical experiments in this thesis work and helpful discussions throughout graduate school. Thanks to John Houser for all his help with the mathematical modeling. I would also like to thank Matt Torres for all his help and guidance with the Gα trafficking paper. Thanks to Rachael Baker for all the help with our manuscript. Without her hard work and patience it would not have been possible to finalize the paper in such a short amount of time. Thanks to Carly Sacks for all her hard work and dedication to the project. Thanks to Tim Elston, Stephen Fuchs, Sarah Clement and Dan Isom, for

providing helpful feedback with experiments and writing. Big thanks to all present and past members of the Dohlman Lab for making it a fun and scientifically charged environment.

Graduate school is a unique experience that brings with it a multitude of emotions- both high and low. Thanks all my friends- both in graduate school and outside for always being supportive no matter what. I would like to especially thank my family- who believed in me more than I can ever believe in myself. Their unwavering support and encouragement helped me get this far. Mummy, papa, didi (and the gang) & Steve- thanks for making this possible. This one's for all of you!

## TABLE OF CONTENTS

## LIST OF TABLES

## LIST OF FIGURES

## LIST OF ABBREVIATIONS AND SYMBOLS

| | |
|---|---|
| $A_{600nm}$ | Absorbance measured at 600nm wavelength |
| α | Alpha |
| ABD-F | 1 mM 4-fluoro-7-aminosulfonylbenzoflurazan |
| ADH1 | Alcohol Dehydrogenase |
| Ala or A | Alanine |
| ATP | Adenosine Triphosphate |
| β | Beta |
| BEM1 | Bud EMergence |
| BUL1 | Binds Ubiquitin Ligase |
| cAMP | cyclic adenosine monophosphate |
| CD | Circular Dichroism |
| CDC | Cell Division Cycle |
| CV | Coefficient of Variation |
| Cys or C | Cysteine |
| Δ | Deletion |
| Δ UD | Deletion of the ubiquitination domain |
| DAG | Diacyl glycerol |
| DIC | Differential interference contrast |
| DDI1 | DNA Damage Inducible |
| *E. coli* | Escherichia coli |
| E1 | Ubiquitin activating enzyme |
| E2 | Ubiquitin conjugating enzyme |

| | |
|---|---|
| E3 | Ubiquitin ligase |
| EC50 | Half maximal effective concentration |
| EDE1 | EH domains and Endocytosis |
| ENT1 | Epsin N-terminal homology |
| ERK | Extracellular Signal-Related Kinase |
| fQCR | Fast Quantitative Cysteine Reactivity |
| FDG | Fluoroscein di-galactoside |
| FUS1 | cell FUSion |
| γ | Gamma |
| G protein | Guanine nucleotide binding protein |
| G6PDH | Glucose-6-phosphate dehydrogenase |
| Gα | G protein alpha subunit |
| GAP | GTPase accelerating protein |
| Gβ | G protein beta subunit |
| GDP | Guanosine diphosphate |
| GEF | Guanine nucleotide exchange factor |
| GFP | Green Fluorescent Protein |
| Gγ | G protein gamma subunit |
| Glu or E | Glutamate |
| GPA1 | G Protein alpha subunit |
| GPCR | G protein-coupled receptor |
| GTP | Guanosine triphosphate |
| HECT | Homologous to E6-AP carboxyl terminus |

| | |
|---|---|
| IB | Immunoblot |
| IP | Immunoprecipitate |
| $IP_3$ | Inositol 1,4,5-trisphosphate |
| kDa | kilo-Dalton (unit of mass) |
| KSS1 | Kinase suppressor of Sst2 mutations |
| MANT-GDP | 2'- / 3'- O- (N'- Methylanthraniloyl)- Guanosine Diphosphate |
| MAPK | Mitogen-activated protein kinase |
| MAPKK | Mitogen-activated protein kinase kinase |
| MAPKKK | Mitogen-activated protein kinase kinase kinase |
| Mg | Magnesium |
| mCherry | Variant of red fluorescent protein |
| PEP4 | CarboxyPEPtidase Y deficient |
| PCR | Polymerase chain reaction |
| PI3K | Phosphatidyl-Inositol-3-Kinase |
| PIP | Phosphatidylinositol 4,5-bisphosphate |
| PKC | Protein kinase C |
| PLC | Phospholipase C |
| REG1 | REsistance to Glucose repression |
| RGS | Regulator of G protein signaling |
| RPN10 | Regulatory Particle non-ATPase |
| RUP1 | Rsp5-Ubp2 interacting Protein |
| RSP5 | Reverses Spt- Phenotype |
| *S. cerevisiae* | *Saccharomyces cerevisiae* |

| | |
|---|---|
| SCF | Skp, Cullin, F-box |
| SDS-PAGE | Sodium dodecyl sulfate-polyacrylamide gel electrophoresis |
| Ser or S | Serine |
| SNARE | SNAP (Soluble NSF Attachment Protein) REceptor |
| SST2 | Supersensitive to pheromone |
| STE | STErile |
| TCA | Trichloroacetic acid |
| TetO | Tetracycline-repressible promoter |
| TEV | Tobacco Etch Virus |
| $T_m$ | Melting Temperature |
| UBA | Ubiquitin Associated Domain |
| Ub | Ubiquitin |
| UD | Ubiquitination Domain |
| UBD | Ubiquitin Binding Domain (containing protein) |
| UIM | Ubiquitin Interacting Motif |
| VPS | Vacuolar Protein Sorting |
| WT | Wild Type |

# CHAPTER I

## INTRODUCTION*

In order to survive and propagate, cells have to respond appropriately to various physical and chemical stimuli in their environment. External stimuli are transduced across the plasma membrane by a variety of signal transduction systems, the most common employing G protein coupled receptors (GPCRs) and their associated heterotrimeric G proteins. From yeast to humans, GPCRs are involved in sensing diverse signals such as hormones, neurotransmitters, light, tastes and odors (Arshavsky et al., 2002; Buck and Axel, 1991; Chandrashekar et al., 2006). GPCRs are expressed in numerous tissues in the body, including the heart and brain. Given their functional importance it is not surprising that aberrant G protein signaling is associated with many human diseases including hypertension, depression and heart disease (Farfel et al., 1999; Spiegel and Weinstein, 2004; Thompson et al., 2008). Consequently, GPCRs represent the protein family most widely targeted by pharmaceutical drugs, claiming over a third of the total share of the drug market (Drews, 2000; Russ and Lampel, 2005; Wise et al., 2002). In order to develop new and more effective drugs, researchers have focused their efforts on identifying new regulators mediating downstream signaling (Cho et al., 2004; Riddle et al., 2005; Zhong and Neubig, 2001).

* All figures contributed by Gauri Dixit

Most studies of G protein signaling are based on examining the average response of a population. The assumption made in each case has been that cellular response is only dependent on the genotype and the surrounding environment. However, emerging data in the last decade have shown that even genetically identical cells exposed to the same environment show individualistic behavior and variation in their phenotypes, a phenomenon called ‘noise’ (Raser and O'Shea, 2004; Raser and O'Shea, 2005). Such cell-to-cell variability greatly increases the number of possible outcomes during signaling. Therefore we aimed to find systems within a signaling pathway that regulate the output and limit the ‘noise’ in the system (Maheshri and O'Shea, 2007). In a yeast model system, this thesis work has examined the role of the Regulator of G protein Signaling (RGS) protein as a noise suppressor. RGS reduced cell-to-cell variability in transcription as well as morphogenesis during signaling, thus establishing a new role for a known signaling regulator.

A relatively new area of research is regulation of the G protein by post translational modifications promoting intracellular trafficking (Wedegaertner, 2012b). While the general process of Gα endocytosis is known, the mediators and consequences of G protein trafficking remain unclear. The work presented here identified a cascade of proteins that mediate trafficking of the yeast Gα from the plasma membrane to the vacuole. The trafficking proteins identified belong to a class of Ubiquitin Binding Domain (UBD) containing proteins. Furthermore we discovered that Gα trafficking is necessary for proper morphogenesis during signaling.

Further understanding how G protein signaling is spatially and temporally regulated will eventually lead to new drug targets, and more effective or targeted therapeutics. The work in this thesis evaluates a new function for a known regulator of signaling (noise suppression by RGS proteins); and identifies a new class of previously unknown G protein regulators (UBD containing proteins) that mediate G protein trafficking. Both RGS and UBD proteins regulate cellular morphogenesis and present future targets for drug intervention. In this introductory chapter special attention will be paid to what is known about noise in eukaryotes and prokaryotes, methods of single cell analysis, as well as recent advances in signaling in single cells and G protein trafficking.

**Heterotrimeric G proteins**

Diverse organisms such as plants, fungi and animals rely on G protein mediated signaling in order to sense and respond to their environment. G protein coupled receptors are seven transmembrane domain containing proteins that detect various environmental stimuli and transmit this information to associated G proteins. G proteins function as molecular switches (Figure 1.1). In the absence of any stimulus they are associated with the receptor as a heterotrimer, composed of the GDP-bound Gα subunit and a Gβγ obligate dimer. Activation of the receptor by extracellular ligand binding promotes conformational changes in the receptor (Katritch et al., 2013). The active receptor acts as a guanine nucleotide exchange factor (GEF) resulting in the exchange of GDP for GTP on the Gα subunit of the heterotrimer. Gα-GTP undergoes conformational changes in three distinct switch

Figure 1.1

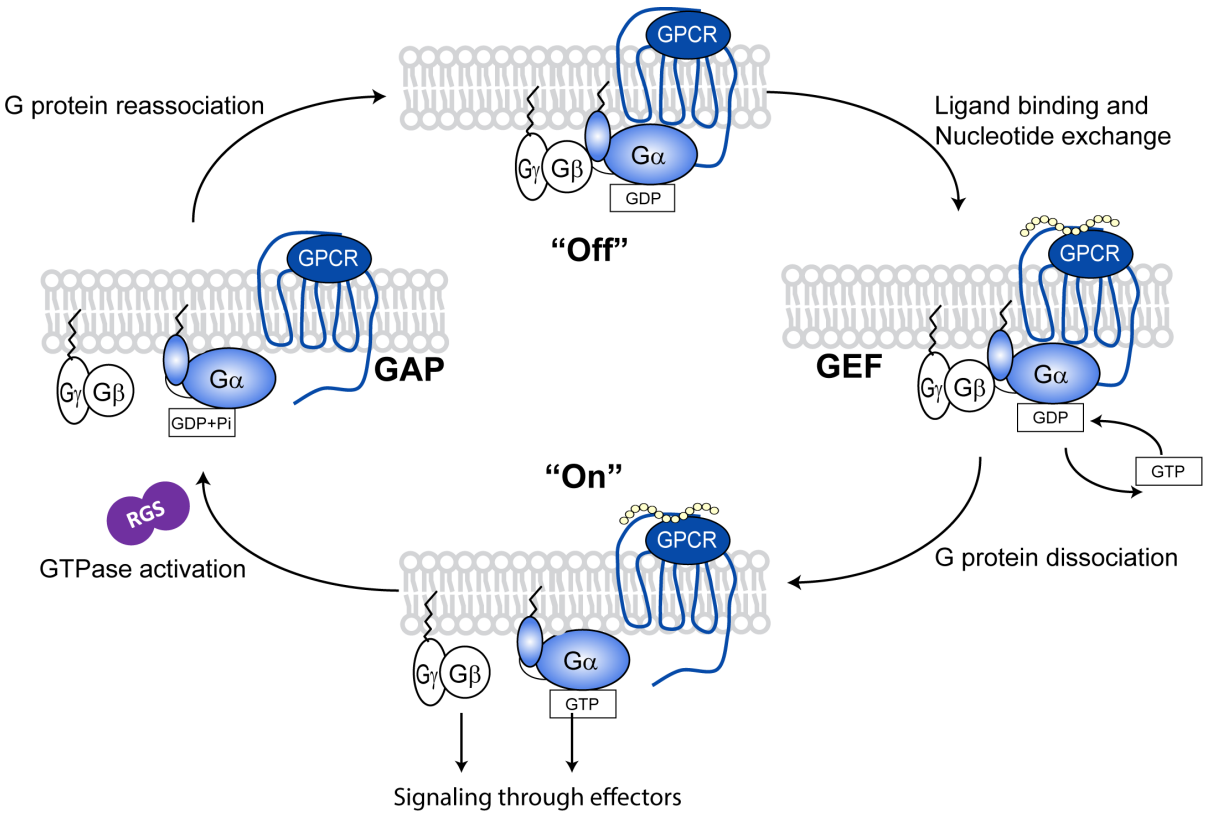


**Figure 1.1 Heterotrimeric G protein activation-inactivation cycle.**
G proteins function as molecular switches in the cell that mediate responses to environmental cues. In the absence of stimulus, Gα-GDP along with Gβγ forms the inactive G protein heterotrimer that is associated with the GPCR at the membrane. Upon ligand binding, the receptor functions as a guanine nucleotide exchange factor (GEF) allowing Gα to exchange GDP for GTP. Ensuing conformational changes promote dissociation of the GTP-bound Gα from Gβγ. Free G protein subunits signal by activating downstream effectors. Signal attenuation occurs upon hydrolysis of GTP bound to the Gα protein. Intrinsic Gα GTPase activity is enhanced by GTPase accelerating proteins (GAP) that mainly belong to the regulator of G protein signaling (RGS) family of proteins. GAPs function by stabilizing the transition state of the reaction. The resulting Gα-GDP reassociated with the Gβγ dimer to turn the pathway off.

regions that cause it's dissociation from the Gβγ dimer. Free Gα-GTP and Gβγ can signal inside the cell by binding downstream effectors resulting in the production of second messengers and activation of protein kinase cascades among other biological effects (Pierce et al., 2002; Sprang, 1997). G protein inactivation is mediated by slow intrinsic GTPase activity (Bourne et al., 1989). Inactivation is often accelerated by Regulators of G protein Signaling (RGS) proteins that function to stabilize the transition state of GTP hydrolysis and therefore act as GTPase accelerating proteins (GAPs) (Siderovski et al., 1996). Thus receptors and GAPs act antagonistically to turn the G protein on and off, respectively. Once inactivated GDP bound Gα reassociates with Gβγ to form the heterotrimeric complex.

Additional ways of fine tuning G protein activation and inactivation exist. For example signal attenuation can occur in mammalian cells through - G protein receptor kinases (GRKs). Free Gβγ recruits GRKs to the membrane. Subsequent phosphorylation of the receptor by GRK promotes recruitment of β-arrestin, receptor inactivation and signal attenuation (Premont et al., 1995). Conversely, G protein activation can be promoted by non-receptor GEFs. These GEFs are thought to act primarily on dissociated Gα subunits adding further complexity to signal dynamics (Garcia-Marcos et al., 2009; Lee and Dohlman, 2008; Siderovski and Willard, 2005).

Mammalian cells have at least 16 different Gα subunit proteins activated downstream of GPCRs. These can be categorized into four sub-families $G\alpha_s$, $G\alpha_i$, $G\alpha_q$ and $G\alpha_{12/13}$ (Gilman, 1987; Hurowitz et al., 2000). The $G\alpha_s$ family (which includes olfactory Gα) promotes the activation of adenylyl cyclase (producing the second messenger cAMP), $Ca^{2+}$ and $K^+$ ion channels and phospholipases C and $A_2$

(Neves et al., 2002). In contrast the $G\alpha_i$ family (that includes transducins) inhibits adenylyl cyclase and promotes MAPK activation (Gainetdinov et al., 2004). $G\alpha_q$ family members primarily mediate activation of phospholipase C and the production of two second messengers formed from the breakdown of PIP2 (phosphatidyl inositol 4,5-bisohosphate), namely diacylglycerol (DAG) and inositol triphosphate ($IP_3$) (Boyer et al., 1994). IP3 promotes the release of $Ca^{2+}$ (second messenger) from the smooth endoplasmic reticulum. Elevated intracellular $Ca^{2+}$ and DAG promote activation of a kinase called Protein Kinase C (PKC) that mediates downstream effects. Lastly, the $G\alpha_{12/13}$ family can stimulate RhoGEFs and regulate activation of the small GTPase Rho. Additionally members of the $G\alpha_{12/13}$ family can stimulate $Na^+$-$H^+$ exchangers in the cell (Tanabe et al., 2004).

GPCRs have been shown to be good targets for therapeutic intervention. However, not many of the intracellular signaling components (including Gα subunits) have been exploited for therapeutics. Therefore an ongoing endeavor for the field is to better understand regulation of signaling and identify new G protein regulators and drug targets. Most of the current knowledge of G protein signaling is based on population based assays. Given the wealth of information pointing towards the existence of cellular heterogeneity and phenotypic variation, a thorough investigation of noise propagation and regulation in G protein signaling is necessary (Wang and Bodovitz, 2010). It will be important to understand not just how drugs act to alter sensitivity of a pathway (by acting as an agonist or antagonist), but also understand how the drug alters cell-to-cell variability and the consequence of such a change in the physiological context.

## Yeast as a Model System for Studying G Protein Signaling

*Saccharomyces cerevisiae (yeast)* is a unicellular eukaryote that has been used as a model organism to study signaling pathways for decades. There are several unique advantages of the yeast system. First, the yeast genome has been sequenced (Goffeau et al., 1996) and the functions of most genes have been annotated. Structural and functional analyses have revealed that most of the yeast signaling components are highly conserved in humans. Examples include the G protein (Nakafuku et al., 1987) and components of the mitogen-activated protein kinase (MAPK) cascade (Chen and Thorner, 2007; Errede and Levin, 1993; Kosako et al., 1993). Not only do most of the pathway components have homologs in humans (Figure 1.2), but yeast and human pathways are also regulated in a similar manner through positive and negative feedback loops. Therefore, discoveries made in yeast will usually be applicable to human G protein signaling.

Additionally, a lot of discoveries important for human physiology were first made in yeast. For example, the founding members of many important proteins were found in yeast including the regulator of G protein signaling protein (Sst2) (Chan and Otte, 1982; Dohlman et al., 1995; Siderovski et al., 1996), cell division cycle proteins (Cdc) (Hartwell et al., 1970), aging-related sirtuin protein (Sir2) (Kennedy et al., 1995), p21-activated kinase (Ste20) (Leberer et al., 1992), vesicle-fusion SNARE proteins (Novick et al., 1980) and the nucleosome-remodeling SWI/SNF complex (Winzeler et al., 1999). Furthermore, yeast are tractable to sophisticated genetic techniques. Yeast cells undergo homologous recombination with high efficiency, which makes it relatively easy to genetically manipulate specific loci (deletions and

Figure 1.2

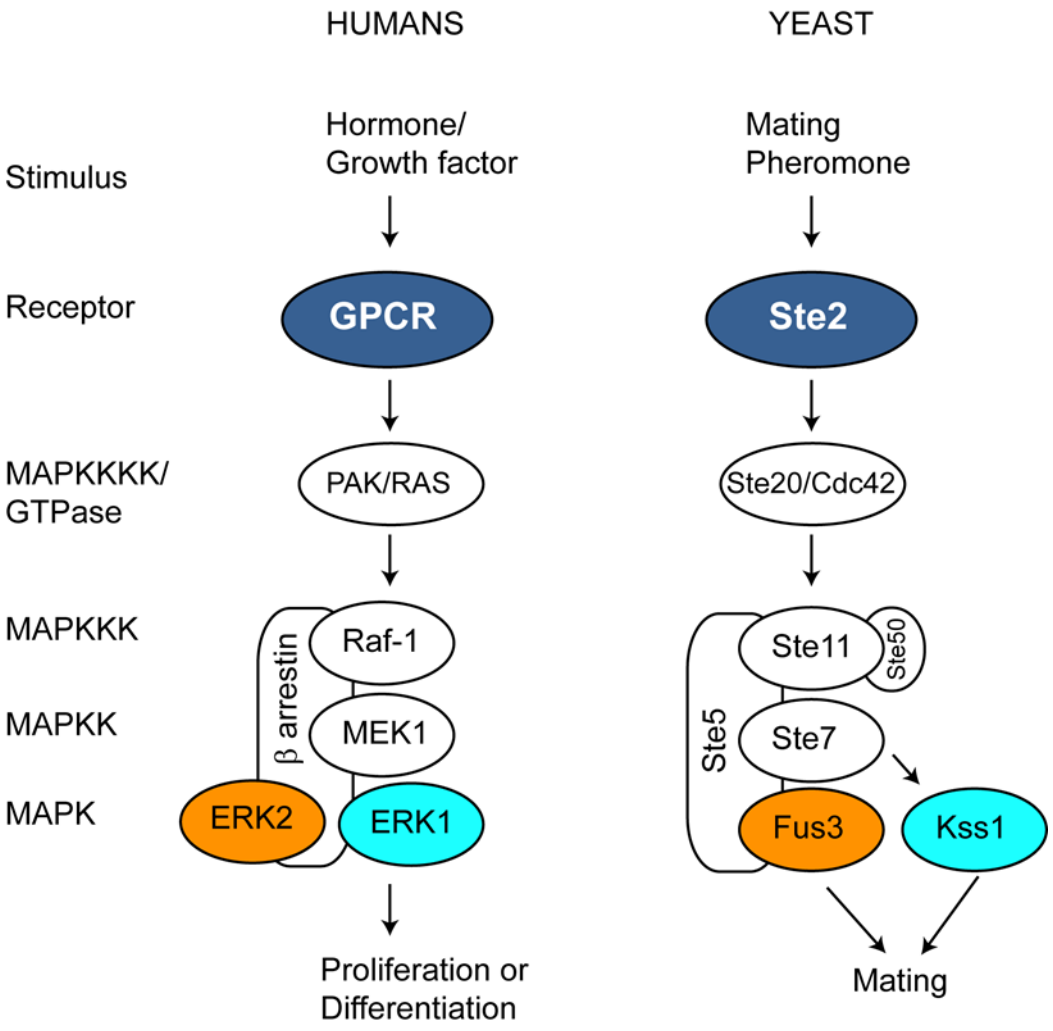


**Figure 1.2 G protein-MAPK signaling pathways are conserved from yeast to humans.** Basic scheme of hormone mediated G protein-MAPK signaling in an example cascade in humans (left) and yeast (right). Yeast and humans share not only the same basic signaling architecture and regulatory mechanisms, but are also made up of homologous protein components. Examples of homologues include Fus3 and Erk2 (yellow); Kss1 and Erk1 (Cyan). Lessons learnt in yeast are likely to fuel future discoveries in humans.
G protein-coupled receptor (GPCR).

targeted point mutations) and track the associated phenotypic changes. In fact, a gene-deletion strain has been made for nearly every non-essential gene in yeast (Giaever et al., 2002) and a drug-repressible strain has been made for nearly every essential gene (Mnaimneh et al., 2004). Additionally GFP tagged versions of every yeast protein allow for high-throughput analysis of protein localization under different conditions (Huh et al., 2003). Together these resources promote addressing many unanswered questions in yeast that would be hard to follow in other systems.

Unlike humans, whose genomes encode more than 800 GPCRs, 20 Gα subunits, 5 Gβ subunits, and 13 Gγ subunits, yeast contain 3 GPCRs and 2 G proteins (Bjarnadottir et al., 2006; Hildebrandt, 1997; Luttrell, 2008). In the yeast *S. cerevisiae*, a single canonical heterotrimeric G protein- MAPK cascade signaling pathway regulates the process of cell mating and therefore presents an attractive model system to study fundamental principles of G protein signaling. The signaling events downstream of the receptor and G protein are well understood. Pathway activation can be measured at various steps including MAPK activation, new gene transcription, cell-cycle arrest and morphological changes. A unique feature of yeast is that they can exist stably as a haploid, making it easy to study recessive gene mutations. Finally, yeast are amenable to study of cell signaling in single cells using quantitative microscopy, flow cytometry and single cell transcriptomics (Colman-Lerner et al., 2005; Paliwal et al., 2007). Recently many studies have been conducted in yeast combining genomic, proteomic and computational analysis to understand nuances of signaling (Fiedler et al., 2009; Ptacek et al., 2005). It is clear through many of these studies that complex events in eukaryotes can be easily

studied in yeast particularly in individual cells, in order to link genotype to phenotype.

To understand how inherent cell-to-cell variability affects signaling responses of the population, it is essential to measure both gene expression and phenotypic parameters in individual living cells in real time over multiple growth cycles. Yeast offers the advantage of having quick doubling times (~90 minutes) and simple yet conserved signaling pathways. Furthermore, yeast signaling pathways have been documented to be 'noisy'. Examples include the pheromone response pathway (Colman-Lerner et al., 2005), galactose induction pathway (Acar et al., 2005) and phosphorus starvation pathway (Raser and O'Shea, 2004). The overall similarity that yeast signaling systems share with humans, make it an ideal model system for noise analysis. Lessons learned about the mechanisms of noise regulation in yeast, may be directly applied to gain insights into noise regulation in complex human systems.

**The Yeast Pheromone Response Pathway**

The pheromone response pathway is a developmental MAPK pathway that is conserved through evolution (Dohlman and Thorner, 2001). Haploid yeast display sexual differentiation and exist as mating type **a** (*MAT***a**) or mating type α (*MAT*α) cells. Both mating types secrete small peptide pheromones, which activate the pheromone response pathway in cells of the opposite mating type (Hicks and Herskowitz, 1976; Wilkinson and Pringle, 1974). Pathway activation results in cell cycle arrest, specific gene expression and morphological changes that ultimately lead to fusion of opposite mating-type cells or mating (Figure 1.3).

Figure 1.3

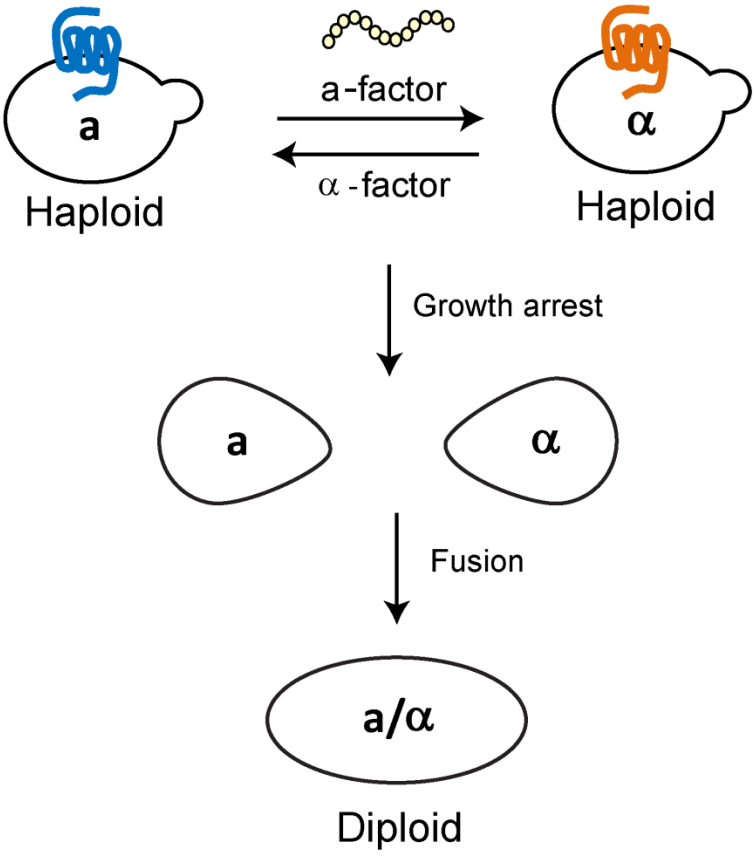


**Figure 1.3 Sexual differentiation and mating in yeast**
Haploid yeast exist in two mating types- *MAT***a** and *MAT*α that communicate by releasing '**a'** and 'α' pheromones respectively. Mating pheromones act by binding cell surface GPCRs to activate a signal transduction program leading to growth arrest in G1, formation of a mating projection or 'shmoo' and eventual fusion to form an a/ α diploid.

*MAT***a** cells produce **a** factor that binds the GPCR Ste3, on *MAT*α cells. On the other hand, *MAT*α cells release α factor that binds the GPCR Ste2 on *MAT***a** cells. Ligand-receptor binding initiates a G protein and MAPK signaling cascade to prepare the cells for fusion to form an **a**/α diploid (Bardwell, 2005). The mating pathway in the yeast *Saccharomyces cerevisiae* is a prototypical GPCR-mediated pathway. Many of the proteins in this pathway are conserved with those in human G protein signaling systems, making yeast a relevant model for G protein signaling studies (Dohlman, 2002). Figure 1.4 shows a simplified scheme of the pheromone pathway. In *MAT***a** cells, the pheromone receptor, Ste2, couples to a heterotrimeric G protein made up of Gpa1 (Gα subunit), Ste4 (Gβ subunit), and Ste18 (Gγ subunit) (Jahng et al., 1988; Miyajima et al., 1987; Whiteway et al., 1989). Pheromone stimulation promotes exchange of GDP for GTP on Gpa1 and causes it to dissociate from the Ste4/18 dimer. Free Ste4/18 activates the MAPK cascade (Zhou et al., 1993) composed of the PAK Ste20, the MAPK kinase kinase Ste11(Chaleff and Tatchell, 1985; Rhodes et al., 1990), the MAPK kinase Ste7 (Teague et al., 1986) and the two partially redundant MAP kinases Fus3 and Kss1(Elion et al., 1990). MAP kinase activation promotes the activation of the transcription factor Ste12 (Elion et al., 1993; Song et al., 1991) which regulates the expression of genes needed for proper mating (Dolan et al., 1989; Errede and Ammerer, 1989; Fields and Herskowitz, 1985; Fields and Herskowitz, 1987). Active Fus3 also phosphorylates the transcriptional repressors Dig1 and Dig2 to relieve the inhibition on Ste12 mediated transcription.

Figure 1.4

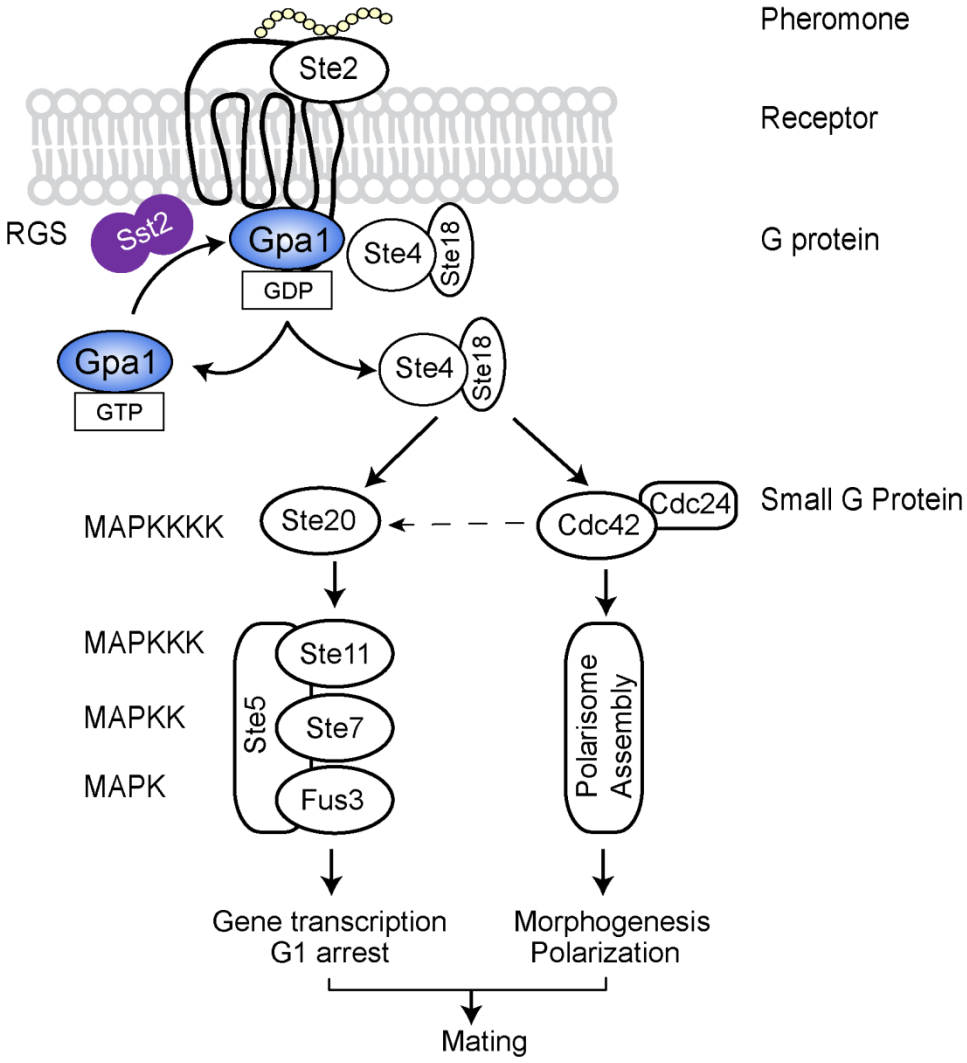


**Figure 1.4 The yeast pheromone response pathway**
The response to mating pheromones in yeast is mediated through a canonical heterotrimeric G protein-MAPK signaling pathway. Binding of α factor pheromone to the receptor Ste2 promotes dissociation of GTP bound Gpa1 and the Gβγ dimer comprised of Ste4 and Ste18. Free Ste4/18 initiates the activation of the MAPK cascade as well as the small G protein Cdc42 (more details are in the text). Phosphorylation and activation of the MAPK Fus3 promotes transcription of mating genes and eventually cell cycle arrest in G1. Activation of Cdc42 promotes cell polarization and morphological changes to prepare the cell to mate.

Free Gβγ Ste4/18 also interacts with the cell cycle regulator Far1 (Chang and Herskowitz, 1990) and the MAPK scaffold Ste5 (Feng et al., 1998; Inouye et al., 1997; Whiteway et al., 1989) at the plasma membrane. Far1 drives cell cycle arrest by inhibiting cyclin-dependent kinase (CDK). Far1 is exported from the nucleus during pheromone stimulation and recruits Cdc24, a GEF for the small G-Protein Cdc42 to the polarity site (Johnson, 1999; Oehlen and Cross, 1998; Simon et al., 1995). Cdc24 in turn promotes activation of Cdc42, which reinforces MAPK activation and drives morphological changes required for proper mating and fusion. Active Fus3 also phosphorylates the regulator of G-protein (RGS) protein, Sst2 (Parnell et al., 2005).

Sst2 accelerates the intrinsic GTPase activity of Gpa1, promoting G protein inactivation and pathway shut off. Although traditionally thought of a just a signal attenuator (Dohlman et al., 1996), more recent evidence suggests that Sst2 performs other functions in the pathway to fine tune signal activation. Supporting this idea are several observations. First Sst2 is one of three non-essential proteins important for cells to track a pheromone gradient (Moore et al., 2008; Segall, 1993). Second, Sst2 promotes membrane recruitment of the MAPK scaffold Ste5 (Yu et al., 2008). Third, through its N terminal DEP domain it can bind the receptor and further modulate the signal response (Ballon et al., 2006). Finally, in the absence of Sst2, cells are unable to mate efficiently, despite being highly sensitive to pheromone (Segall, 1993). Together these data suggest that Sst2 acts both as a positive and a negative regulator of the pathway.

The work in this thesis focuses on the role of Sst2 in suppressing noise in

signaling and maintaining a robust signaling output. To dissect how different functions of Sst2 mediate signal and noise suppression, we used an integrated approach. We employed a Gα mutant (*gpa1*$^{G302S}$) that abrogates binding (due to a single amino acid substitution in the switch1 region) to the RGS protein (DiBello et al., 1998; Lan et al., 1998). This renders the mutant Gα insensitive to inhibition by Sst2; thus we call it the GAP mutant. We also employed a Sst2 mutant (*sst2*$^{Q304N}$) that abrogates binding (due to a single amino acid substitution in the DEP domain) to the receptor (Ballon et al., 2006); thus we call it the receptor uncoupling mutant. We performed several biochemical assays to demonstrate that GAP activity and receptor coupling equally suppress signal sensitivity in a cellular population. However through single cell analysis it is clear that GAP activity also promotes homogeneity in pathway activation and is also required for proper morphogenesis and gradient tracking.

The one common feature of all RGS proteins is the RGS-GAP domain. Therefore the realization that RGS-GAP activity is critical for proper cellular response at the single cell level presents a potential new function for all RGS proteins. There are at least 30 members in the mammalian RGS family classified into subfamilies based on primary sequence and domain composition (Sierra et al., 2000). As researchers probe the therapeutic potential of RGS proteins in humans (Bansal et al., 2007), an important consideration is how altering RGS-GAP activity will affect cellular heterogeneity and signaling fidelity. While the main components of the yeast pheromone pathway have been known for years, questions still remain

about pathway components that fine tune sensitivities, amplitudes and outcomes of signaling both at the level of single cells and the population.

**Noise in biological systems**

Most global signaling analysis currently relies on employing a large number of cells and averaging measured parameters. This approach is done on the assumption that cellular phenotype is determined by genetic makeup and environmental influences alone. However, even genetically identical cells exposed to the same environmental conditions show individualistic behavior and variation in their phenotypes, a phenomenon called ‘noise’ (Elowitz et al., 2002; Lidstrom and Meldrum, 2003; Ozbudak et al., 2002; Raser and O'Shea, 2004; Tawfik, 2010). Therefore while traditional approaches to study cell signaling have the advantage of averaging out natural fluctuations, they are blind to the presence of functionally-important subpopulations with responses significantly distinct from the measured average (Figure 1.5) (Levsky and Singer, 2003; Longo and Hasty, 2006; Wang and Bodovitz, 2010).

Noise in cell populations was first reported in early studies analyzing the heritability of growth rates and chemotactic behavior in bacteria (Kelly and Rahn, 1932; Powell, 1956; Spudich and Koshland, 1976 ); and in the burst size distribution of bacterial viruses (Delbruck, 1945). This early body of work suggested that bacterial populations generate physiological diversity in several characteristics at the individual cell level (Maloney and Rotman, 1973). Since then a lot of studies have tried to understand the origins and consequences of variability. Most studies of

Figure 1.5

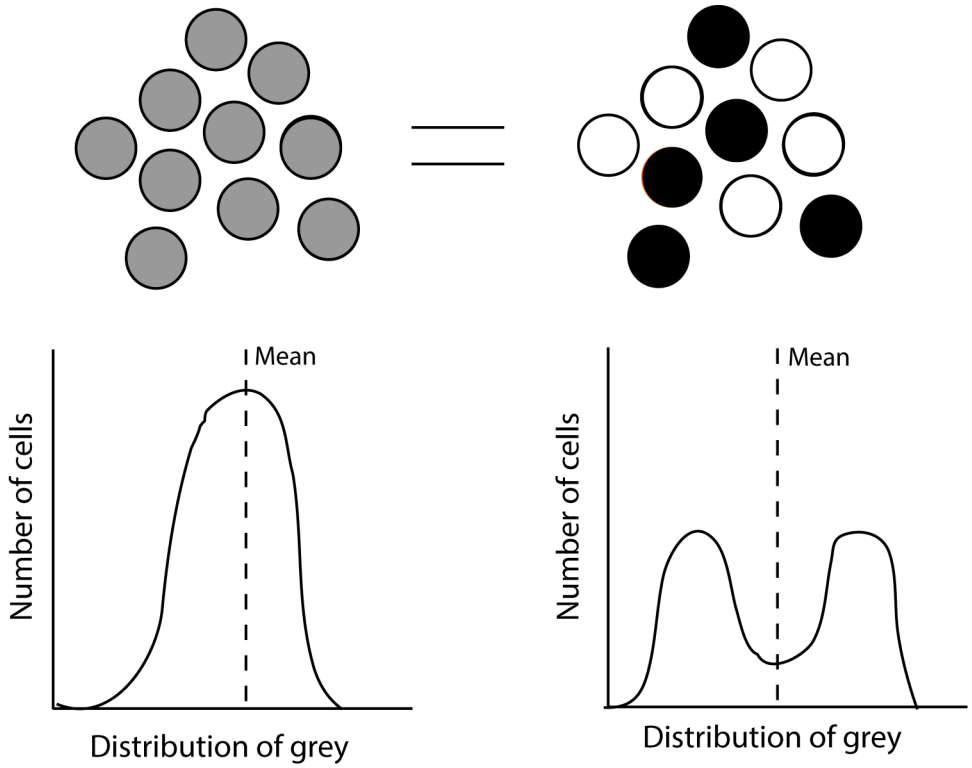


**Figure 1.5 Average behavior of a population versus single cell behavior**
Suppose a population has an initial state (white) and a final (black). In a population average, it may not possible to distinguish between a state in which all cells have an intermediate phenotype (grey) from one in which some are white and the others are black. An intermediate phenotype (grey) implies every cell exists in an in-between state which may or may not be true. (Graphs represent hypothetical data).

single cell analysis have focused on evaluation of noise in the expression of individual genes (Pedraza and van Oudenaarden, 2005; Raj and van Oudenaarden, 2008; Raser and O'Shea, 2005).

Noise can arise from multiple sources, such as variations in the activity of individual genes, from cell-to-cell variations in metabolic activity, or from fluctuating levels of an external signal. Based on the current data on the source of variability, noise is classified as (i) intrinsic or inherent and (ii) extrinsic or external. Intrinsic noise has been mainly attributed to stochastic fluctuations in molecular reactions, due to the small numbers of specific molecules in the cell. Together these make reactions less probable, unpredictable and thus variable (Arkin et al., 1998; Becskei et al., 2005; Blake et al., 2003; Guptasarma, 1995; Kaern et al., 2005; McAdams and Arkin, 1997; McAdams and Arkin, 1999; Ozbudak et al., 2002; Pedraza and van Oudenaarden, 2005; Raser and O'Shea, 2005; Rosenfeld et al., 2005; Smits et al., 2006; Thattai and van Oudenaarden, 2001). Extrinsic noise can arise from the concentration/activity of particular cellular components or differences in cell states including cell size, metabolic state, cell cycle etc. (Colman-Lerner et al., 2005; Elowitz et al., 2002; Pedraza and van Oudenaarden, 2005).

The relative contribution of each source of noise (intrinsic and extrinsic) was first measured in a landmark study by Elowitz et al. (Elowitz et al., 2002). Quantification of noise relied on a ‘dual-reporter assay’ where two fluorescent reporter proteins were driven by identical promoters (Figure 1.6). Comparison of expression levels of the two reporters within the same cell measured intrinsic noise, and the difference in the expression level of the reporters between cells measured

Figure 1.6

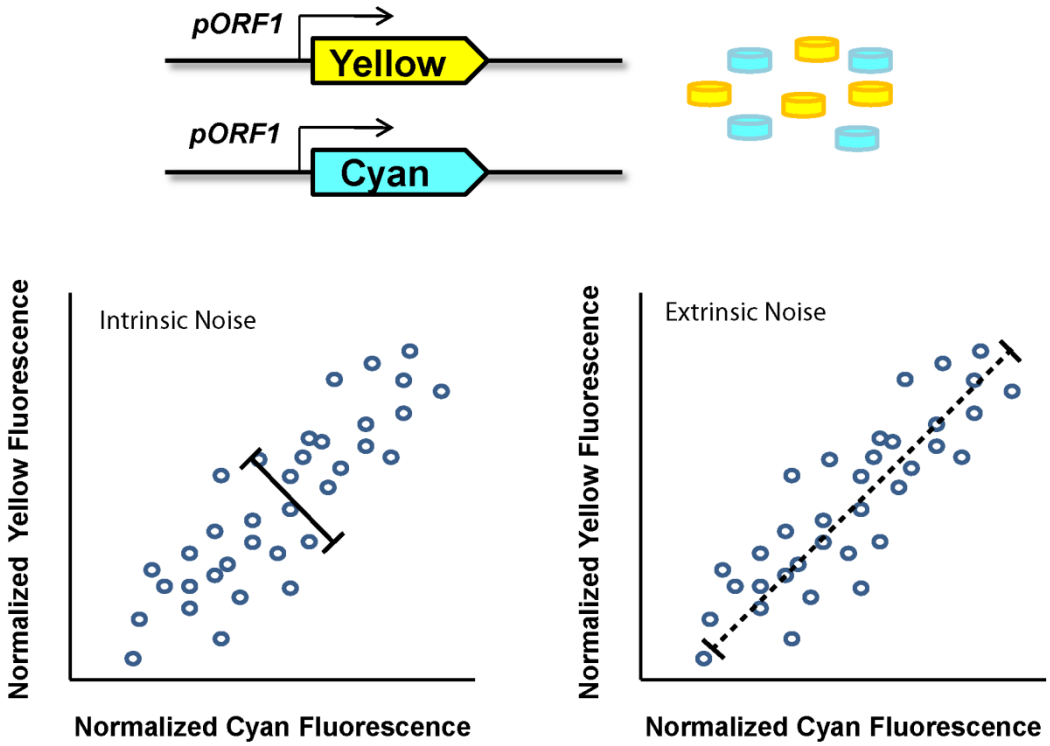


**Figure 1.6 Dual reporter assay to measure intrinsic and extrinsic noise**
Typically the dual reporter assay is employed to quantify the relative contribution of intrinsic and extrinsic noise to the total noise in a system. Two complementary fluorescent reporters (like yellow and cyan fluorescent protein) are chromosomally expressed from identical promoters that are placed equidistant from but located on opposite sides of an origin. CFP and YFP are measured in each cell and a value for mean fluorescence intensity (normalized from the population average) is plotted. Each point represents the normalized CFP and YFP intensities from one cell. The correlated variation between CFP and YFP intensities within single cells I (graph on left) corresponds to intrinsic noise, whereas the uncorrelated variation between cells in a population (graph on right) is extrinsic noise. The actual numeric calculation of total, intrinsic and extrinsic noise from individual cell fluorescence measurements is made using a set of equations detailed in Elowitz et al. 2002. (Graphs represent hypothetical data).

extrinsic noise (Swain et al., 2002). Variability in gene expression is captured as the coefficient of variation (CV) calculated as the standard deviation of individual cells divided by the mean expression. Through this analysis it was first shown that both sources of noise contribute to variation in gene expression in prokaryotes. Using the quantitative foundation described above, a number of studies were conducted to understand the dominant sources of noise in gene expression in eukaryotes (Bar-Even et al., 2006; Colman-Lerner et al., 2005; McCullagh et al., 2010; Raser and O'Shea, 2004). Through these studies it was clear that intrinsic noise is the predominant source of noise in prokaryotes (Elowitz et al., 2002; Kepler and Elston, 2001; Ozbudak et al., 2002; Thattai and van Oudenaarden, 2001) and that extrinsic noise is the dominant source of noise in eukaryotes (Becskei et al., 2005; Blake et al., 2003; Newman et al., 2006; Raser and O'Shea, 2004; Volfson et al., 2006). Recent computational and experimental analysis has also implicated uneven distribution of cellular constituents during mitosis (such as organelles and proteins) as a source of variability in eukaryotes. For example variability in mitochondrial volume and functionality in mammalian cells that was shown to be an even more dominant source of extrinsic noise than cell cycle asynchrony (das Neves et al., 2010; Johnston et al., 2012).

In depth analysis in bacteria and yeast has been done to understand how the rates of transcription, translation and promoter activation control intrinsic noise in gene expression (Sanchez and Golding, 2013). Theoretical predictions backed by experimental data for both systems suggest that infrequent transcription followed by *inefficient* translation results in lower intrinsic noise compared to a case where

infrequent transcription is followed by efficient translation (Blake et al., 2003; Fraser et al., 2004; Ozbudak et al., 2002; Thattai and van Oudenaarden, 2001). Additionally, studies in yeast suggested that noise is strongly dependent upon the transcription rate. These studies demonstrated that transcriptional bursting and slow promoter activation (owing to chromatin remodeling) generate stochasticity in eukaryotic gene expression (Blake et al., 2003; Rajala et al., 2010; Raser and O'Shea, 2004). Supporting this conclusion it was shown in yeast that noise can be manipulated by changing operator sites and distance between the operator sites and the TATA box (Murphy et al., 2007).

*Regulation of gene expression noise*. In cells, expression of a single gene is not an autonomously controlled process. Instead genes function as complex networks in order to adapt and respond to their environment. Therefore once basic principles of noise in gene expression were established, researchers focused their efforts on better understanding the regulation and propagation of noise in gene networks (Munsky et al., 2012; Rinott et al., 2011). The first attempts towards understanding noise regulation in gene networks were made using engineered genetic cascades. Employing mathematical modeling , Thattai et al. were the first to demonstrate how noise is attenuated in an ultrasensitive signaling cascade (Thattai and van Oudenaarden, 2002). The dependence of noise on the length of the signaling cascade was demonstrated by Hooshangi et al. Their results on population heterogeneity in *E. coli* using one, two and three step cascades suggested that signals generated from a short cascade are less noisy than those generated by long cascades (Hooshangi et al., 2005). These results were further

corroborated in a two-step cascade in yeast showing that noise is propagated from upstream to downstream elements (Blake et al., 2003; Pedraza and van Oudenaarden, 2005).

In addition to cascade length, noise can be altered by positive and negative feedback loops. While negative feedback was shown to decrease noise and minimize the effects of fluctuations on downstream processes (at the cost of reducing signaling sensitivity) (Becskei and Serrano, 2000; Dublanche et al., 2006; Kaern et al., 2005; Lidstrom and Konopka, 2010; Thattai and van Oudenaarden, 2004) positive feedback was shown to amplify fluctuations and give rise to bimodal population distributions (Becskei et al., 2001; Isaacs et al., 2003). Subsequent studies modeling positive and negative feedback in more complex circuits however suggested that the role of feedback loops is context dependent- and can have varying effect on noise based on length of the cascades, delay in feedback and the number of feedback loops involved (Brandman and Meyer, 2008; Hooshangi and Weiss, 2006; Hornung and Barkai, 2008). While we have made advances in understanding the regulation of noise in simple synthetic systems, translating this information to more complex systems in eukaryotic cells remains a challenge.

**Cell-to-cell variability: role in regulating cell-fate decisions and diseases**

Large scale studies of mRNA and protein levels in yeast and bacteria have revealed a large amount of variability in the molecular make up of individual cells in an isogenic population (Bar-Even et al., 2006; Newman et al., 2006; Stewart-Ornstein et al., 2012; Taniguchi et al., 2010). Stochasticity, cell cycle, ageing and

epigenetic regulation all contribute to generating cell-to-cell variability in a population. Although variability is thought to be regulated by cellular components and certain feedback loops, it appears that it has not been completely selected against during evolution. In fact functional studies done in a variety of organisms including bacteria, yeast and mammalian cells suggest that noise may be beneficial and play a role in regulating cell fate decisions (Balazsi et al., 2011; Kussell and Leibler, 2005; Losick and Desplan, 2008).

Stochasticity allows bacteria to deploy specialized cells in anticipation of possible adverse changes in the environment (Kussell et al., 2005; Kussell and Leibler, 2005; Thattai and van Oudenaarden, 2004). Striking examples of stochastic decision making include sporulation, acquisition of competence and persistence (Lidstrom and Konopka, 2010). Sporulation and competence are developmental states that only a subset of the population enter when faced with starvation or unfavorable conditions. Studies in *B. subtilis* have shown that entry into these developmental pathways is contingent on threshold levels of key regulatory molecules- a process that is governed stochastically (Maamar and Dubnau, 2005; Maamar et al., 2007; Suel et al., 2006; Suel et al., 2007; Veening et al., 2005; Veening et al., 2008). Likewise, when *E. coli* are treated with antibiotics, most of the population dies rapidly. But the cells that grow more slowly survive the treatment longer, and can switch to fast growth once the antibiotic is removed. The 'persistence' of these slow-growing cells occurs without any genetic mutations (Balaban et al., 2004; Keren et al., 2004; Lewis, 2007).

The above examples illustrate ways that microbial populations hedge their

bets through stochastic gene expression. Bet hedging imparts a fitness advantage in stressful situations that outweighs the cost of producing cells that temporarily stop growing (Avery, 2006). Data from a recent study in yeast supports the notion that slow growing cells are more resistant to stress. In that study increased expression of a metabolic enzyme Tsl1 (trehalose synthase) in a subset of cells was found to positively correlate with stress survival as well as aging (Levy et al., 2012). Like Tsl1 high variability has been observed in the expression of several other stress responsive genes in yeast (Newman et al., 2006). Interestingly mutational analysis has been done to alter gene expression noise for a subset of the stress response genes. Mutations that reduce gene expression noise were found to lower the chance of survival in particular stresses (Blake et al., 2006). Finally, progeny of either fast- or slow-growing cells could ultimately give rise to a population with the entire spectrum of growth-rates showing that, like bacteria, yeast can switch between different growth states (Balaban et al., 2004; Levy et al., 2012; McCullagh et al., 2010).

While stochastic gene expression may benefit microorganisms, it potentially complicates treatments for infection. For example, some promoters in *S. typhimurium* have been shown experimentally to have more variation (be noisier) than others, and the promoters identified with the highest variation control flagella synthesis, a trait associated with virulence (Freed et al., 2008). Therefore better understanding of how to control stochastic gene expression in pathogens, including the slow-growing mycobacteria responsible for tuberculosis (Dhar and McKinney, 2007) might lead to better therapies.

Cell-to-cell variability can lead to multiple steady state phenotypes in multicellular organisms as well. Therefore noise plays a significant role in several developmental processes in mammalian cells. Key examples include embryonic patterning (Sternberg and Horvitz, 1986), mammalian olfactory neuronal receptor choice (Chess et al., 1994; Mombaerts, 2004), distribution of green and red cones in the human retina (Nathans, 1999) and fate decisions in stem cells (Chang et al., 2008; Hoang, 2004; Jan and Jan, 1995). Cellular differentiation is critical for survival. Yet a surprisingly large number of processes, such as acquired & innate immune response to infections and differentiation, are governed by random stochastic events (Feinerman et al., 2008; Gregor et al., 2010; Hu et al., 2011; Johnston and Desplan, 2010). However variability can also be a source of disease (Niepel et al., 2009). Randomness in expression of tumor suppressors may increase genetic instabilities and hence the risk of cancer (Cook et al., 1998; Magee et al., 2003). Furthermore noise has been implicated in the evolution of aggressive cancer cells. Certain melanomas contain rare cells that divide slowly, thus evading chemotherapies that target fast-dividing cells, and these slow-dividing cells can later give rise to daughter cells that proliferate at great rates (Brock et al., 2009). It is therefore not surprising that even in well controlled conditions, the responses of single cells (normal and cancer cells) to stimuli and drugs can vary widely (Cohen et al., 2008; Gascoigne and Taylor, 2008; Orth et al., 2008). Supporting this notion further was a study showing that drug induced apoptosis is also a stochastically determined event that relies on the activity of a procaspase, whose expression was found to be highly variable (Spencer et al., 2009). The importance of single cell

analysis (particularly in gene expression) in human health and disease is clear from numerous examples in the literature. However in order to apply the current knowledge towards manipulating variability and establishing new treatment regimens establish a direct correlation between variability of every protein in the proteome with different cellular outcomes (Cotari et al., 2013a; Wu et al., 2013).

**Methods of single cell analysis**

To a large extent single cell analysis has been possible due to advancements in time-lapse microscopy, quantitative image analysis and fluorescent protein reporters (Falconnet et al., 2011; Kolitz and Lauffenburger, 2012; Longo and Hasty, 2006; Megason and Fraser, 2007; Pelet et al., 2012). In combination with fast maturing and unstable fluorescence reporters, time lapse microscopy allows real time monitoring of the dynamics of gene expression by visualization of single protein molecules (Choi et al., 2008; Elf et al., 2007; Sako, 2006; Yu et al., 2006). Apart from reporting gene expression levels, fluorescent reporters are being used as biosensors that can report on protein-protein interactions (Overton and Blumer, 2000), cellular localization (Yu et al., 2008), protein conformation (Goley et al., 2004; Hagopian, 1970) and protein modifications (Harvey et al., 2008) in single cells. Complementing this approach, are data obtained by fluorescence in situ hybridization (FISH) that monitors the state of gene activation in single cells (Maamar et al., 2007; Raj et al., 2006; Raj et al., 2008; Taniguchi et al., 2010). While quantitative and precise, FISH allows measuring only one to two genes at a time. Therefore researchers are now focusing their efforts towards single cell

transcriptomics (RNA seq) (Nagalakshmi et al., 2008). RNA seq allows monitoring the entire mRNA population in a single cell (Golding et al., 2005; Le et al., 2005; Lipson et al., 2009; Marcus et al., 2006). For example using single cell transcriptomics it was found that mouse immune cells respond to antigen stimulation (LPS) in a heterogeneous fashion (Shalek et al., 2013). What will take the field a step further are advances in high sensitivity mass spectrometry that will enable critical evaluation of single cell proteomes.

Another innovation in single cell analysis is the use of microfluidic devices. Microfluidics allows investigators to maintain uniform conditions (such as pH, $O_2$, nutrients) and minimizes fluctuations that can have confounding effects on noise measurements (Cai et al., 2006; Liu et al., 2009; Paliwal et al., 2007; Ricicova et al., 2013; Taylor et al., 2009). Laser microdissection allows placement of single cells from a population to a pre-determined spot for imaging (Emmert-Buck et al., 1996). When combined with microfluidics, laser microdissection can allow testing the response of individual cells to very precise conditions. However, imaging can be time consuming and limited by the number of cells per field.

An alternative strategy to single cell imaging is using flow cytometry (Cotari et al., 2013b; McCullagh et al., 2010; Sureka et al., 2008; Takahashi and Pryciak, 2008). While it allows collection of quantitative data for a large number of cells and monitoring a large number of proteins at once, flow cytometry cannot be used to follow a single cell over time. Furthermore we do get any information on the cellular morphology or colocalization of markers in individual cells. To combine the benefits of imaging and cytometry, a new technique has been developed called multispectral

imaging flow cytometry (MIFC). In this method the instrument digitally images each cell as it flows through a standard cytometer so that individual cells can be evaluated in terms of morphology, DNA content as well as expression of a fluorescent protein. Though this technique has been successfully employed in yeast, it lacks any information on temporal dynamics of gene expression (Calvert et al., 2008; Gordon et al., 2007).

An unappreciated aspect in the field of noise biology and signaling is the importance of cell morphology as a phenotypic marker. Cellular morphology is under-studied despite the fact that many biological processes were first delineated based on mutants that gave unusual phenotypes upon visual inspection (Hartwell et al., 1973; Jones et al., 2009). Recently a study in endothelial cells demonstrated that, in contrast to the population-averaged behavior, most individual cells follow distinct patterns of temporal cell-shape changes during capillary formation (Parsa et al., 2011). This study further reiterates that shape differences can be qualitative or quantitative markers of physiological states (Pincus and Theriot, 2007). Given the lack of in depth analysis regarding morphological variability, the work in this thesis is unusual in paying special attention to morphological outcomes in single cells responding to pheromone. In Chapter II I describe how RGS-GAP activity regulates noise in morphogenesis to promote gradient tracking. In Chapter III I describe how G protein trafficking regulates morphogenesis upon prolonged pheromone stimulation. Finally in the Appendix, I describe how signal crosstalk between two signaling pathways (mating and energy sensing) delays morphogenesis during mating.

**Noise in cell signaling pathways**

Cells activate several intracellular signaling pathways in response to environmental signals such as stress, hormones and nutrients. Most of these pathways, including the MAPK cascade (Gustin et al., 1998), involve several stages before the final signaling outcome. Each stage of the signaling cascade can add noise to the response- both due to intrinsic noise in biochemical reactions as well as heterogeneity in the abundance of proteins. Simply put, there exist many layers of heterogeneity that can affect the eventual response. Given that appropriate signaling is vital for cellular function and survival it is imperative that we understand how and why signaling systems are noisy.

Noise mediated by a specific stimulus was first suggested in eukaryotic cells responding to glucocorticoids (Ko, 1991). More convincing evidence for noise in signaling was presented later in *Xenopus oocytes* responding to progesterone. When progesterone-induced MAPK activation was measured in a population, there was a gradual increase in phosphorylation in response to an increasing dose of progesterone, suggesting that cells mount a gradual increase in response. However, when examined individually, a cell was either active or inactive (Ferrell and Machleder, 1998). Numerous other examples in mammalian cells have also demonstrated noise in signaling. A study in mammalian cells demonstrated that EGF stimulated AKT activity is bimodal and correlates with PI3K protein level, such that only cells with high PI3K protein can activate AKT (Chen et al., 2012). A related study demonstrated that a homogenous population of cells can display diverse responses to uniform growth factor cues mediated by ERK and AKT signaling (Yuan

et al., 2011). Other critical processes such as TNF mediated NF-κB signaling (Kalita et al., 2011) and cytokine mediated T lymphocyte signaling (Cotari et al., 2013b) have also been shown to be highly heterogeneous in a population. Together these data, along with studies on drug responses (Spencer et al., 2009) in single cells, suggest that cell-to-cell variability allows a population of cells to generate a spectrum of responses from a uniform stimulus.

A large number of analyses focused on noise have been conducted in yeast. One reason for the popularity of yeast is that even modest changes (such as halving the dose of a few genes) have measurable consequences (like growth defects) (Deutschbauer et al., 2005). The first study of noise during signaling in yeast was done for the phosphate starvation pathway (Raser and O'Shea, 2004). This was followed by an innovative analysis of the yeast galactose system- a noisy environmental response network. It was found that in this system cells generate uniform or bimodal (noisy) expression depending on the nutritional stimulus (glucose/galactose) (Biggar and Crabtree, 2001). Decision making was found to be mediated by three key feedback loops (Acar et al., 2008). Subsequent improvements in image analysis have allowed analysis of noise in the yeast osmotic stress response pathway. In the presence of salt induced osmostress, yeast initiate transcription of stress-responsive genes whose expression was found to be variable. Assessment of the source of variability showed a strong contribution of intrinsic noise (Pelet et al., 2012).

*Noise in pheromone signaling*: The most well studied system to understand the origins and consequences of cell-to-cell variability is the yeast pheromone

response pathway (Colman-Lerner et al., 2005; Falconnet et al., 2011; Taylor et al., 2009). Upon pheromone stimulation yeast cells acquire different morphological fates based on assessment of the dose of stimulus (Doncic et al., 2011). Cells either elongate towards the source if the pheromone concentration is low (indicative of a faraway mate) (Moore et al., 2008); or form a mating projection (shmoo) if the source of pheromone is near (Segall, 1993). The final outcome depends on the level of saturation of the receptor and downstream responses (Figure 1.7). The first study to show cell-to-cell differences in pheromone signaling was conducted by Colman et al. who demonstrated that variation is dominated by differences in the capacity of individual cells to transmit signals through the pathway ('pathway capacity') and to express proteins from genes ('expression capacity') (Colman-Lerner et al., 2005). Furthermore they found that MAP kinases regulate variation. While Fus3 suppressed variation at high pheromone levels, Kss1 enhanced variation at low pheromone levels. Subsequently, studies by Paliwal et al. demonstrated that at identical intermediate concentration of pheromone individual cells display a mix of budding, arrested and shmooing morphologies indicative of cellular decision making. Interestingly, pheromone specific gene expression analysis showed that the population had a bimodal expression pattern with highest Fus1 levels in shmooing cells. Furthermore it was shown that positive feedback at the level of the MAPK (Fus3) was responsible for this bimodality and cellular variation (Paliwal et al., 2007).

The role of MAPK in regulating variability was corroborated by an analogous study showing that negative feedback mediated by the MAPK (Fus3 or Kss1) can improve information processing and reduce stochastic noise in pathway output

Figure 1.7

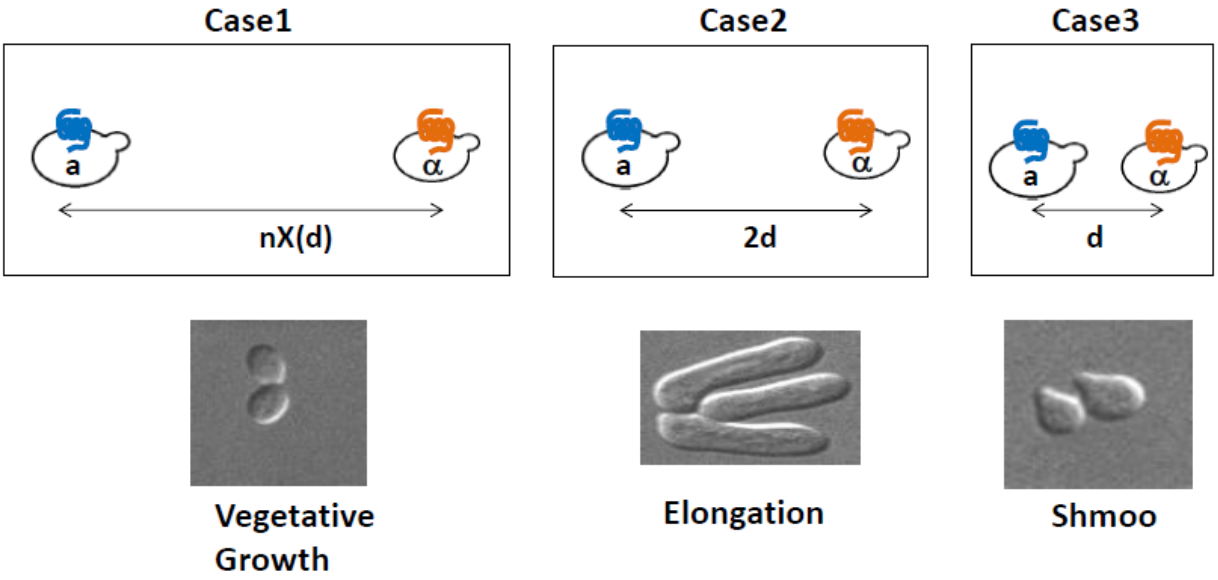


**Figure 1.7 Response to pheromone is a decision making process**
When cells encounter a mating stimulus, whether or not they respond and how they respond is based on assessment of the strength of stimulus. If a mate is far and the stimulus is below detection threshold, cells continue to undergo vegetative growth (case I). If a potential mate is close enough for detection, but far enough that there is differential pheromone binding at the front and back of the cell, cells start to elongate towards the source of pheromone (case II, gradient tracking). Finally, if the mate is close enough to release a large amount of pheromone that promotes saturation of the receptor on the front and back of the cell equally cells form a mating projection or shmoo in preparation of fusion (case III). If ‘d’ is the minimum distance required for shmooing, accordingly 2d should mediate elongation and (n times d ) that represents cells very far apart should maintain budding. Shmooing and elongation take about 2 to 6 hours respectively. Therefore for a successful mating response, cells not only have to make a decision but also stick to the chosen path.

within the first few minutes of pheromone stimulation (Yu et al., 2008). The only pathway component directly shown to minimize variability in the pathway to date is Dig1. Dig1 is a MAPK response regulator that is important for inhibition of Ste12-dependent transcription. Absence of Dig1 increased basal (extrinsic and intrinsic) noise in transcriptional outputs of the mating pathway without much change in the mean output (McCullagh et al., 2010). Finally, a large number of studies focused on pheromone signaling have concluded that differences in population structure (cell size, shape, age, metabolic state and cell cycle) cannot completely account for extrinsic variability during signaling suggesting that noise generation and minimization are partially encoded within the pheromone signaling pathway (Colman-Lerner et al., 2005; Kaufmann and van Oudenaarden, 2007; Ricicova et al., 2013; Volfson et al., 2006; Yu et al., 2008).

Noise is ubiquitious in biological systems. All the evidence presented so far suggests that it has good and bad consequences. Naturally, too much variation can cause indecision particularly in the context of signaling. Therefore to promote robustness during signaling, noise regulation has evolved within the signaling cascades (probably through feedback networks) (Jeschke et al., 2013). Despite the fact that negative feedback has been strongly implicated in noise suppression, few studies have tested this in a canonical G protein signaling cascade. Given the pharmacological relevance of GPCRs and their signaling cascades, studying cell-to-cell variability in these systems has practical implications for drug discovery and design (Thompson et al., 2008). Part of this thesis work was therefore focused on testing molecular and phenotypic noise suppression by the most prominent negative

feedback loop in a prototypical G protein/MAPK signaling cascade.

**G protein ubiquitination and trafficking**

Gα proteins are commonly targeted for post translational modifications such as myristoylation, palmitoylation, phosphorylation and ubiquitination (Chen and Manning, 2001). These modifications are thought to be important for regulating protein-protein interactions, sub-cellular localization and nucleotide binding. While the presence of modified forms of G proteins has been known for a while, less attention has been paid to how these modifications are dynamically altered in response to the environment and what consequence they have for signaling. For example, the yeast Gα Gpa1 has been shown to be phosphorylated and subsequently degraded in a cell cycle dependent manner (Torres et al., 2011). Recently we demonstrated that Gpa1 is also phosphorylated under conditions of starvation. Phosphorylation under nutrient deprivation does not promote Gpa1 degradation. Instead, it leads to a dampened GPCR-mediated pheromone response (Clement et al., 2013).

G protein ubiquitination and its physiological relevance is perhaps one of the least well studied. Early evidence of Gα ubiquitination and its role in mediating proteasomal degradation came from Gt (transducin) in vertebrate photoreceptors (Obin et al., 1996). Subsequently, direct and indirect evidence has shown that $G\alpha_S$ and $G\alpha_{13}$ are also subject to ubiquitination (Fischer et al., 2003; Nagai et al., 2010). Beyond its effect on protein degradation, little is understood about the role of ubiquitination in regulating other functions of human Gα proteins. Given the wealth of information about ubiquitination of Gpa1 (Cappell et al., 2010; Madura and

Varshavsky, 1994; Marotti et al., 2002), it serves as a model to understand G protein ubiquitination and its role in signaling.

Ubiquitin is a small protein that is attached to substrates through the action of three enzymes- E1, E2, and E3 enzymes (Hershko et al., 1983). While E1 and E2 prime the ubiquitin molecule, E3 ligase is responsible for substrate specificity and transfers the ubiquitin onto a lysine residue in the substrate (Hershko et al., 1986). Proteins can either be mono or polyubiquitinated (Chau et al., 1989; Hicke, 2001). Gpa1 is one of few proteins that can be both mono and polyubiquitinated. The site for Gpa1 ubiquitination has been mapped by mass spectrometry to Lysine 165, present in a loop in the helical domain (Marotti et al., 2002). Rsp5 is the E3 ligase enzyme responsible for monoubiquitination of Gpa1 (Torres et al., 2009). This same enzyme has also been shown to monoubiquitinate the receptor Ste2 (Hicke and Riezman, 1996). In each case monoubiquitination results in endocytosis and trafficking to the vacuole for degradation (Figure 1.8) (Wang et al., 2005). However unlike the receptor whose monoubiquitination is agonist dependent (Dunn and Hicke, 2001) Gpa1 is constitutively monoubiquitinated. While much is known about receptor trafficking to the endosome (Hislop and von Zastrow, 2011; Marchese and Trejo, 2013), relatively little is known about G protein trafficking. The most information about trafficking of the Gα and its consequences comes from the visual system. In the visual system trafficking has been shown to fine tune the amount of Gα present at the membrane to mediate a change in the response to light activation (Wedegaertner, 2012a).

Gpa1 (Slessareva et al., 2006) and $G\alpha_S$ (Irannejad et al., 2013) have been

Figure 1.8

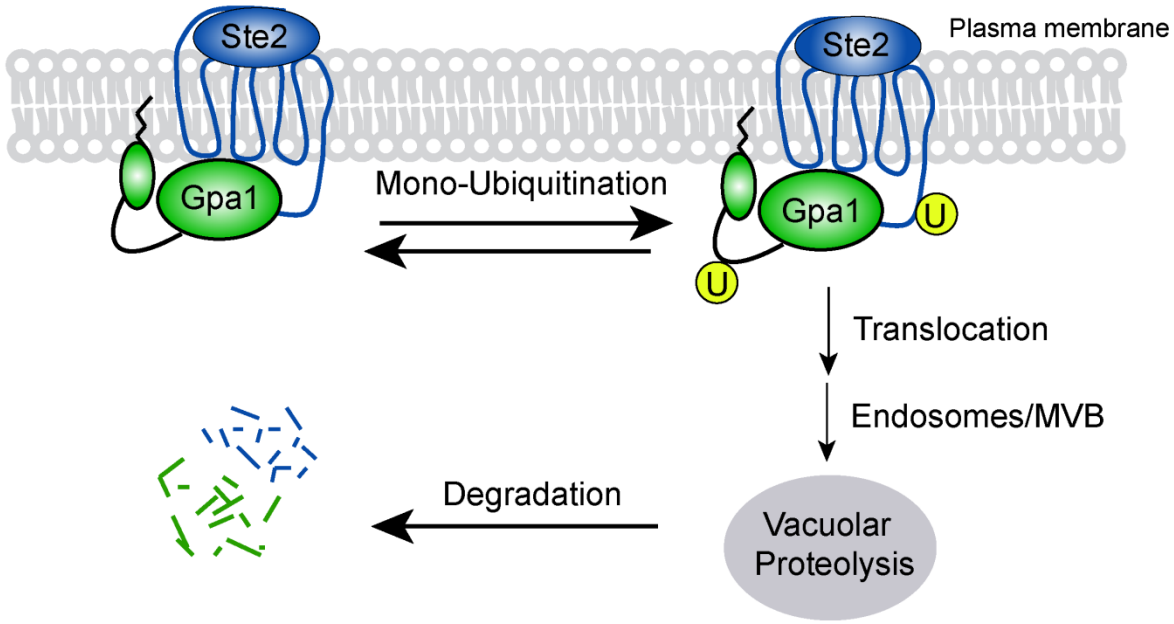


**Figure 1.8 Monoubiquitinated Gpa1 and Ste2 are trafficked to the vacuole**
Gpa1 is monoubiquitinated constitutively and delivered to the vacuole for degradation. Monoubiquitination of Ste2 is enhanced by pheromone resulting in endocytosis and degradation.

shown to be present in an active state in internal membrane compartments. However the components involved in trafficking G proteins to the endomembranes, and how G protein trafficking influences overall signaling, is not well known in any system. Interestingly, how monoubiquitination affects G protein structure or catalytic activity is also not well understood. The work in this thesis addresses some of these questions in yeast combining biophysical and biochemical approaches. We compare Ste2 and Gpa1 trafficking in select mutants to understand whether the two are trafficked together or separately and how that affects pathway activity.

**Ubiquitin Binding Domain containing proteins**

Ubiquitin binding domain (UBD) containing proteins represent a class of cellular proteins that recognize and interact non-covalently with ubiquitin and translate the ubiquitin signal to cellular processes such as degradation by the proteasome, protein endocytosis or targeting to internal membrane compartments (Staub and Rotin, 2006). Ubiquitin has a well-defined structural motif called the ubiquitin fold that is comprised of a β sheet, a $3_{10}$ helix and an α helix. Most UBDs interact with a solvent exposed hydrophobic patch located in the β sheet (Pickart and Eddins, 2004). Almost all UBDs target the same surface of ubiquitin. However different UBDs recognize different lengths of ubiquitin and different amino acids that surround the hydrophobic patch of ubiquitin. Consequently, there is a large array of UBDs with distinct structures and binding affinities for a diverse set of ubiquitinated proteins (Dikic et al., 2009).

The number of UBDs has steadily grown in the last decade, with more than

20 different families of UBDs identified to date present in over 200 proteins (Dikic et al., 2009). Classification of UBDs is based on the structure of their ubiquitin recognition domain as well as the type of ubiquitin that they recognize. Many UBDs (particularly those that recognize monoubiquitinated proteins) use α helical structures to bind the hydrophobic patch in the ubiquitin β sheet. Specific examples of ubiquitin binding domains that bind ubiquitin through α helical structures include UIM (ubiquitin interacting motif), UBA (Ubiquitin associated domain), and CUE (coupling of ubiquitin conjugation to endoplasmic reticulum degradation domain). It is still unclear why so many variants of helical structures exist to bind ubiquitin and regulate signaling. Other UBDs use β sheets in the PH (plekstrin homology domain) to bind the hydrophobic patch of ubiquitin. Examples of such UBD families include GLUE (Gram like ubiquitin binding in EAP45) and PRU (PH receptor for ubiquitin). Still other UBDs contain Zinc Finger domains (NZF) and Ubiquitin conjugating (Ubc) like domains (Hicke et al., 2005; Hurley et al., 2006; Winget and Mayor, 2010). Regardless of the domain it binds, in most cases a ubiquitin moiety binds with only one UBD at a time. It is conceivable that this kind of exclusive binding ensures that each ubiquitin can stimulate only one process at a time for effective ubiquitin signaling.

Spatial control of the membrane bound receptor and Gα proteins can be mediated by endocytosis. The ubiquitin moiety fused to a membrane protein carries with it the necessary information for endocytosis (Hicke, 2001). UBDs serve as the recognition signals or adaptors for ubiquitinated proteins. Ste2 endocytosis in yeast is an example of a well characterized UBD mediated process that serves to regulate

signaling (Hurley and Stenmark, 2011). However, not much information is available for how and which particular UBDs mediate endocytosis of the G protein Gpa1. In this thesis I present a screen of 39 gene deletion mutations of UBDs to identify those that are required for Gpa1 trafficking. Through this work, I identify a seven UBDs that recognize and transport monoubiquitinated Gpa1 to the vacuole. The newly identified UBDs represent a new class of previously uncharacterized G protein binding proteins. Additionally for the first time this work determines the consequence of G protein trafficking in signaling in a non-visual system.

**Summary**

Better understanding how G protein signaling is regulated will eventually lead to new drug targets, and more intelligent drug design. The work in this thesis evaluates regulation of G protein signaling by two protein families. One is a classic regulator of signaling that belongs to the RGS protein family and the other is a new family of previously unknown G protein regulators, the UBD proteins. Both RGS and UBD functions are required for proper cellular morphogenesis during mating in yeast. Due to their role in signal regulation, both RGS and UBD proteins represent potential targets of drug intervention in humans.

The remainder of this thesis is divided into 3 chapters and an Appendix. In Chapter II, “Cellular Noise Suppression by the Regulator of G Protein Signaling, Sst2,” I examine how different functions of the RGS Sst2 suppress cell-to-cell variability in transcription and morphogenesis during pheromone signaling. Using biochemical, single cell and computational approaches we determined that RGS-

GAP activity mediates signal suppression as well as variability in cell fate decisions. In Chapter III “Gα Endocytosis by a Cascade of Ubiquitin Binding Domain Proteins is Required for Sustained Cellular Morphogenesis in Yeast” my collaborators and I examine the effect of the ubiquitination domain on G protein structure and function. I also present a screen of ubiquitin binding domain mutants to determine those that are involved in endocytosis and trafficking of the G protein, receptor or both. This work demonstrates that Gpa1 trafficking is required for proper morphogenesis and efficient signaling and identifies a new putative class of G protein binding proteins. Finally, in Chapter IV, “Conclusions and General Discussion,” I discuss the broad impact of these findings and speculate on the future direction of the field.

## CHAPTER II

# CELLULAR NOISE SUPPRESSION BY THE REGULATOR OF G PROTEIN SIGNALING Sst2[*,◦]

G proteins and their associated receptors process information from a variety of environmental stimuli to induce appropriate cellular responses. Generally speaking, each cell in a population responds within defined limits despite large variation in the expression of protein signaling components. Therefore we postulated that noise suppression is encoded within the signaling system. Using the yeast mating pathway as a model we evaluated the ability of a regulator of G protein signaling (RGS) protein to suppress noise. We found that the RGS protein Sst2 limits variability in transcription and morphogenesis in response to pheromone stimulation. While signal suppression is a result of both the GAP (GTPase accelerating) and receptor binding functions of Sst2, noise suppression requires only the GAP activity. Taken together our findings reveal a hitherto overlooked role of

[*] Elements of the work referenced in this chapter have been submitted for publication: Dixit G, Kelley JB, Houser JR, Elston TE and Dohlman HG. (2014). Cellular Noise Suppression by the Regulator of G Protein Signaling Sst2.

◦ Figures 2.1, 2.2, 2.3A, 2.3B, 2.3C, 2,3D, 2.3E, 2.4, 2.6, 2.7A, 2.7B, 2.8A, 2.8C contributed by Gauri Dixit.
Figures 2.7C, 2.7D and 2.8B contributed by Joshua B. Kelley.
Figures 2.3F and 2.5 contributed by John R. Houser

RGS proteins as noise suppressors, and demonstrate an ability to uncouple signal and noise in a prototypical stimulus-response pathway.

**Introduction**

All eukaryotic cells have the ability to detect external signals and generate an appropriate response. Many of these signals, including most hormones and neurotransmitters, as well as environmental stimuli such as odors, tastes and light, are detected by cell surface receptors coupled to G proteins. Upon activation these receptors promote binding of GTP to the G protein $\alpha$ subunit (G$\alpha$) and dissociation of G$\alpha$ from the G protein $\beta\gamma$ subunits. Regulators of G protein signaling (RGS proteins) promote the hydrolysis of GTP to GDP, thereby terminating the signal (Neves et al., 2002). Thus receptors and RGS proteins act in opposition to one another to control signal output.

G protein signaling systems are conserved across the animal, plant and fungal kingdoms. Among the best characterized is the pheromone response pathway in the yeast *Saccharomyces cerevisiae*. In this example, a G protein-coupled receptor binds to peptide pheromones, which initiates events that prepare haploid cells for mating. As shown in Figure 2.1 *A*, there are two effector systems downstream of the G protein: one that activates a prototypical MAP kinase cascade and the transcription of genes necessary for cell fusion and growth arrest, and a second that triggers Cdc42-dependent morphological changes resulting in either cell expansion towards the source of pheromone (gradient tracking) or formation of a mating projection (shmoo) (Dohlman and Thorner, 2001).

As in most signaling systems, G protein activity is influenced by the strength and duration of the stimulus as well as feedback loops that promote or inhibit signaling over time (Purvis and Lahav, 2013). The dominant source of negative feedback in the pheromone pathway is the RGS protein Sst2, which is strongly induced in response to prolonged pheromone stimulation (Dohlman et al., 1996). Less appreciated are the effects of cell-to-cell differences arising from stochasticity in biochemical reactions, differences in the expression or activity of internal signaling components, as well as heterogeneity in cell states (i.e. cell cycle, cell age and metabolic state) (Becskei et al., 2005; Colman-Lerner et al., 2005; Elowitz et al., 2002; Fraser et al., 2004; Maheshri and O'Shea, 2007; McAdams and Arkin, 1999; Ricicova et al., 2013; Volfson et al., 2006). Such differences greatly increase the number of possible outcomes during signaling. For that reason we asked whether there are systems within signaling pathways to regulate the output and limit the cell-to-cell variability or ‘noise’ in the system (Fraser et al., 2004; Maheshri and O'Shea, 2007). Yeast is especially well suited for investigating noise because it is a unicellular eukaryote (every cell in a population is genetically identical). Therefore each member of the population can be grown under identical environmental conditions and this enables direct correlation between genotype and phenotype at the whole organism level. Furthermore the mating pheromone pathway is among the simplest and most thoroughly understood of any GPCR system (Dohlman and Thorner, 2001)

Here we consider noise suppression by the yeast RGS protein Sst2. Sst2 is the first, and arguably the best-characterized, member of the RGS protein family

(Dohlman et al., 1996). Like other RGS proteins, Sst2 has an RGS-core domain that accelerates G protein GTPase (GAP) activity (Apanovitch et al., 1998). Additionally, Sst2 is one of a subset of RGS proteins containing an N-terminal DEP (Dishevelled, Egl-10, Pleckstrin) domain, which binds to the receptor (Ballon et al., 2006). Both domains are needed for cells to efficiently dampen responses to a pheromone signal. Using single cell analysis we show that Sst2 can suppress noise, that Sst2 acts in a stimulus- and time-dependent manner, and that it acts in both the transcription and morphogenesis branches of the pathway. While signal suppression is mediated equally by the receptor- and G protein-binding functions of Sst2, noise suppression relies exclusively on proper G protein GTPase activity. Taken together these findings reveal that the RGS protein functions as a noise filter. More broadly, these findings reveal that noise suppression and signal suppression are not linked in an obligatory manner, and that signal responses and noise can be regulated independently.

## Results

**Sst2 receptor binding and GTPase- accelerating activities promote desensitization-** Sst2 is well known to diminish pheromone signaling over time. Moreover, Sst2 acts in two ways, by binding to the receptor as well as by promoting G protein GTPase activity (Ballon et al., 2006). Here we examine how these activities affect the signal and the noise, over time, and in space in response to a gradient stimulus. Accordingly, we began by comparing signal suppression in mutants deficient in Sst2-receptor binding (*sst2*$^{Q304N}$ ) (Ballon et al., 2006), GTPase-

## Figure 2.1

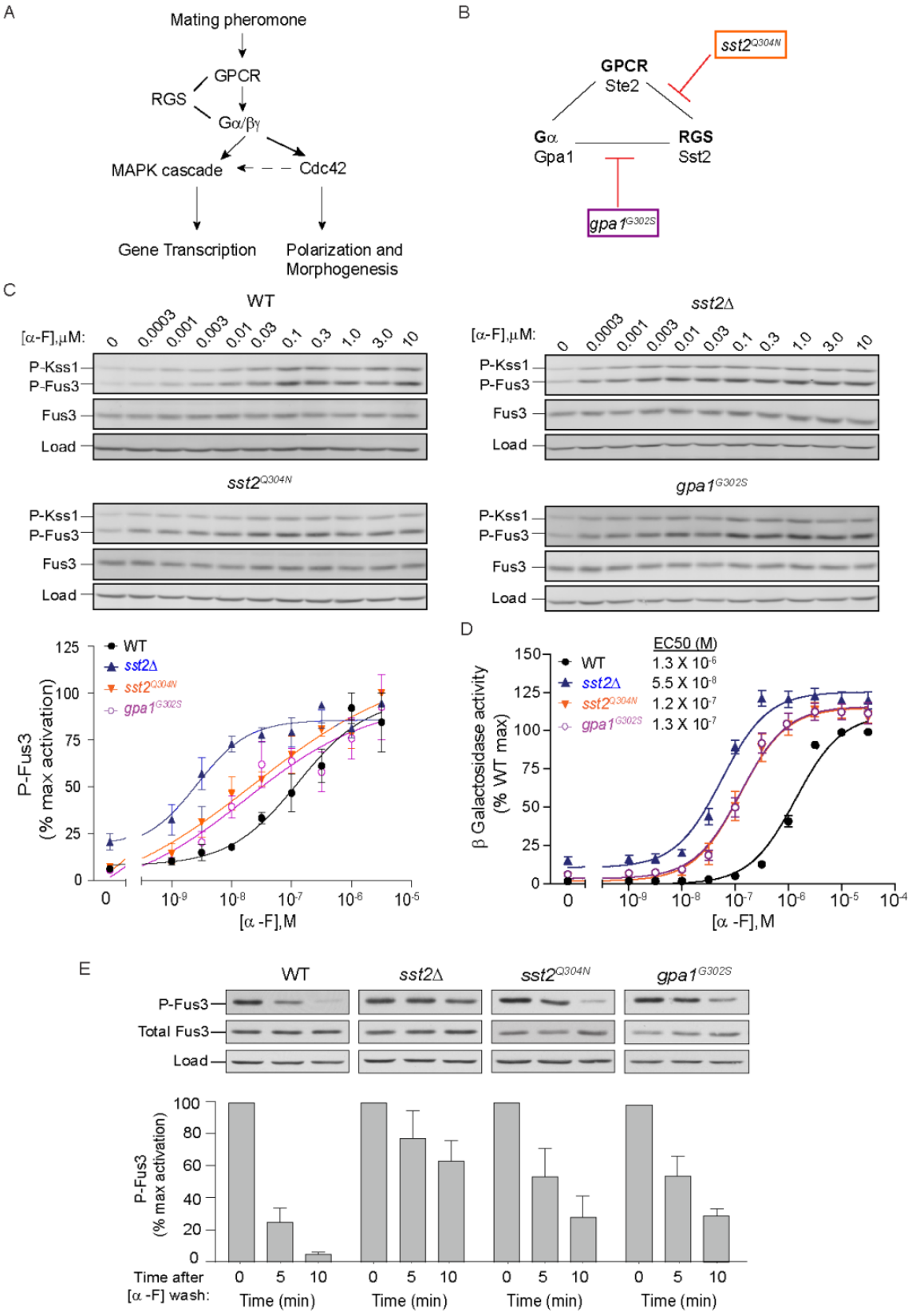
A
Mating pheromone
GPCR
RGS
Gα/βγ
MAPK cascade
Cdc42
Gene Transcription
Polarization and Morphogenesis
B
GPCR
Ste2
sst2Q304N
Gα
Gpa1
RGS
Sst2
gpa1G302S
C
WT
sst2Δ
sst2Q304N
gpa1G302S
[α-F],μM:
0 0.0003 0.001 0.003 0.01 0.03 0.1 0.3 1.0 3.0 10
P-Kss1
P-Fus3
Fus3
Load
P-Fus3 (% max activation)
[α -F],M
D
β Galactosidase activity (% WT max)
EC50 (M)
WT 1.3 X 10-6
sst2Δ 5.5 X 10-8
sst2Q304N 1.2 X 10-7
gpa1G302S 1.3 X 10-7
[α -F],M
E
WT
sst2Δ
sst2Q304N
gpa1G302S
P-Fus3
Total Fus3
Load
P-Fus3 (% max activation)
Time after [α -F] wash:
Time (min)

**Figure 2.1 Binding of the RGS protein to the receptor and G protein contribute equally to signal suppression.**

(A) Schematic of the pheromone response pathway. Upon mating pheromone stimulation, the G protein coupled receptor (GPCR) initiates activation of the G protein heterotrimer, which promotes mating gene transcription (via a MAPK cascade) and cell polarization and morphogenesis (via the small G protein Cdc42). Activated Cdc42 further promotes MAPK signaling while the RGS protein dampens the signal.

(B) Receptor (Ste2), Gα protein (Gpa1) and RGS protein (Sst2) assemble through direct and indirect interactions. The point mutant $sst2^{Q304N}$ disrupts interaction with Ste2 whereas the point mutant $gpa1^{G302S}$ disrupts interaction with Sst2.

(C) *Top*, dose dependence of MAPK activation: Wild type, *sst2*Δ, $gpa1^{G302S}$ or $sst2^{Q304N}$ cells were treated with the indicated concentration (μM) of α factor (α-F), collected at 5 min, and probed by immunoblotting with p44/42 (P-Fus3, P-Kss1), Fus3 and G6PDH (load control) antibodies. *Bottom*, Densitometry of P-Fus3 bands normalized to maximum Fus3 activation.

(D) Transcriptional activation (β-Galactosidase activity) was measured spectrofluorometrically in all strains as in (C). Cells expressing *FUS1-lacZ* were exposed to the indicated concentrations of α factor for 90 min. Shown in inset are the calculated $EC_{50}$ values for each strain.

(E) Time course of MAPK *in*activation. Cells were treated with 3 μM α factor for 30 min, harvested by centrifugation, washed once, resuspended in pheromone-free medium and samples collected at the indicated times. Graphs shown below depict densitometry of P-Fus3 bands. All data are mean ± SEM for three independent experiments.

accelerating activity (*gpa1*$^{G302S}$*)* (DiBello et al., 1998), or both *(sst2*Δ*)* (Figure 2.1 *B*). We monitored pheromone responses at the level of MAPK (mitogen activated protein kinase) activation (immunoblotting), transcriptional induction (β-galactosidase assay) and growth inhibition (halo assay). To measure MAPK activity we used an antibody that recognizes the phosphorylated and fully activated form of Fus3. Kinase activation was greatest in *sst2*Δ cells, followed by the point mutants (*sst2*$^{Q304N}$ and *gpa1*$^{G302S}$*),* and then wild type cells (Figure 2.1 *C* and Figure 2.2 *A*). Likewise in the transcription reporter assay, *sst2*Δ *cells were* ~100 fold more sensitive than wild type cells to pheromone, while the two point mutants (*sst2*$^{Q304N}$ and *gpa1*$^{G302S}$) were each 10 fold more sensitive (Figure 2.1 *D*, compare $EC_{50}$ values). We observed the same rank order of sensitivity in the growth arrest assays (Figure 2.2 *B*).

In addition to the standard assays described above, we employed a new approach to quantify pheromone pathway deactivation. In this method, we stimulated cells with pheromone for 30 min, then washed with pheromone-free medium and monitored MAPK phosphorylation as cells recovered over time. Normally in wild type cells, phospho-MAPK levels drop rapidly and reach pre-stimulation levels after 10 min (Figure 2.1 *E*). Cells lacking Sst2 exhibited sustained MAPK phosphorylation, long after pheromone withdrawal (over 60 min post wash), as expected for a defect in desensitization. The two point mutants (*sst2*$^{Q304N}$ and *gpa1*$^{G302S}$) also exhibited prolonged MAPK phosphorylation. As seen for assays of pathway activation, pathway deactivation was identical in each of the two point mutants and intermediate to that observed in the presence and absence of Sst2.

## Figure 2.2

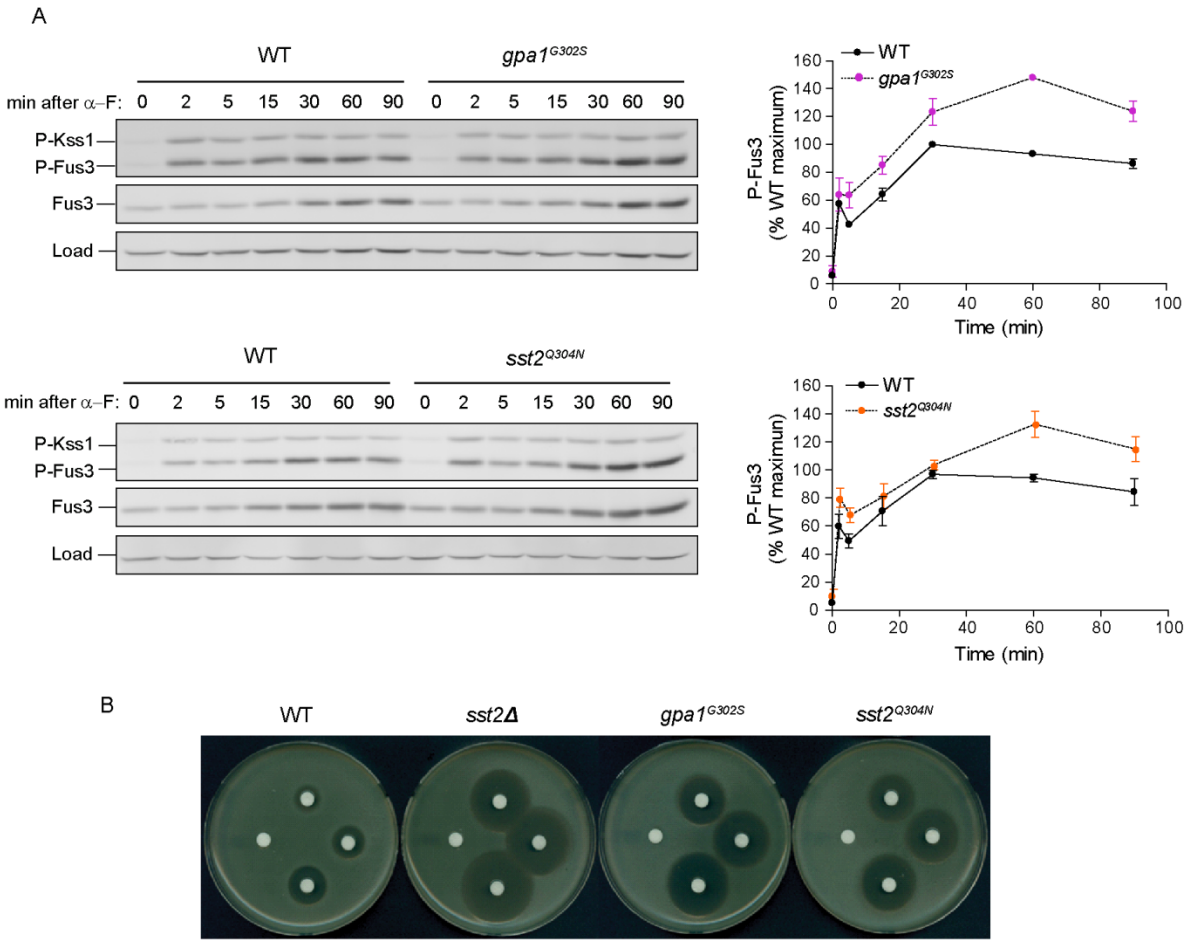


**Figure 2.2 *gpa1*$^{G302S}$ and *sst2*$^{Q304N}$ are equally sensitive to pheromone**

(A) *Left*, Time course of phospho-MAPK activation: Wild type cells and mutant strains *gpa1*$^{G302S}$ or *sst2*$^{Q304N}$ were treated with 3 μM α factor and samples collected at the indicated times. MAPK activation was determined by immunoblotting with phospho-p44/42 (P-Fus3, P-Kss1), Fus3 C terminal (Fus3) and G6PDH (Load) antibodies. *Right*, Densitometry of P-Fus3 bands normalized to the loading control. Results show the mean ± SEM for three individual experiments.

(B) Halo Assay to measure pheromone induced growth arrest. Disks were spotted with 0, 5, 15 and 50 μg α factor.

Thus by four different measures we find that mutants deficient in receptor binding (*sst2*$^{Q304N}$) or GTPase-accelerating activity (*gpa1*$^{G302S}$) are equally sensitive to pheromone. The ability to separate the two known functions of Sst2 allows us to assess the contributions of each to noise suppression, without the confounding effects of differences in overall signaling.

**Sst2 suppresses noise in gene transcription**- Upon activation, the G protein feeds into two branches of the mating pathway, one that promotes new gene transcription and a second that promotes polarized expansion towards the source of pheromone (gradient tracking). Since gene expression is by far the best studied and most established measure of noise (Elowitz et al., 2002; Raser and O'Shea, 2005) we first focused our efforts on measuring transcription in the presence and absence of Sst2. For these experiments we employed a microfluidic chamber where cells are maintained in a uniform environment to minimize fluctuations in pheromone concentration (Hao et al., 2008). As shown in Figure 2.3 *A*, the pheromone is delivered by passive diffusion from feeder channels perpendicular to the direction of flow on either side of the growth chamber. This minimizes flow across the cells so that they remain stationary during the course of the experiment. To monitor transcription we selected two native gene promoters each fused to a fluorescent reporter: GFP driven by the *FUS1* promoter and mCherry driven by the *ADH1* promoter (Figure 2.3 *B*). Whereas FUS1-GFP reports on pheromone-driven transcription, ADH1-mCherry is constitutively produced and therefore reports on the overall expression capacity of the cell (Colman-Lerner et al., 2005). As expected, GFP expression increased in response to pheromone while mCherry was essentially

unchanged (Figure 2.3 *C*, left). We then quantified GFP and mCherry expression in individual cells, normalized GFP relative to mCherry in each cell and calculated the coefficient of variation (CV) for the population at discrete time points. Normalizing pathway response (GFP) with a reference reporter (mCherry) accounts for any cell-to-cell differences in protein expression capacity and corrects for instrument fluctuations, non-uniform field illumination and differences in cell size and the focal plane being imaged. This experimental platform allows us to measure pathway specific noise (Colman-Lerner et al., 2005) and also differentiate biochemical noise within a single cell (intrinsic noise) from variability within the population (extrinsic noise).

We began by measuring total noise in the absence of stimulus. As compared to wild type, the *sst2*Δ mutant exhibited a significant 50% increase in cell-to-cell variability (Figure 2.3 *D*). Using the same assay we saw an identical increase in the "benchmark" *dig1Δ* strain, reported previously to elevate CV in the absence of pheromone (Figure 2.3 *D*) (McCullagh et al., 2010). An equivalent increase in baseline variability was seen in the absence of GAP activity ($gpa1^{G302S}$) but not in the absence of receptor binding ($sst2^{Q304N}$) (Figure 2.3 *D*). The increase in CV was not due to a global increase in gene expression noise as determined by comparing the normalized mean GFP and mCherry intensities in wild type and *sst2*Δ cells (Figure 2.4 *A*). Moreover, the CV remained relatively constant over time (Figure 2.4 *B*), demonstrating that basal noise is unaffected by progression through the cell cycle. We conclude that GAP activity, but not receptor binding, acts to suppress cell-to-cell variability in the absence of stimulus.

## Figure 2.3

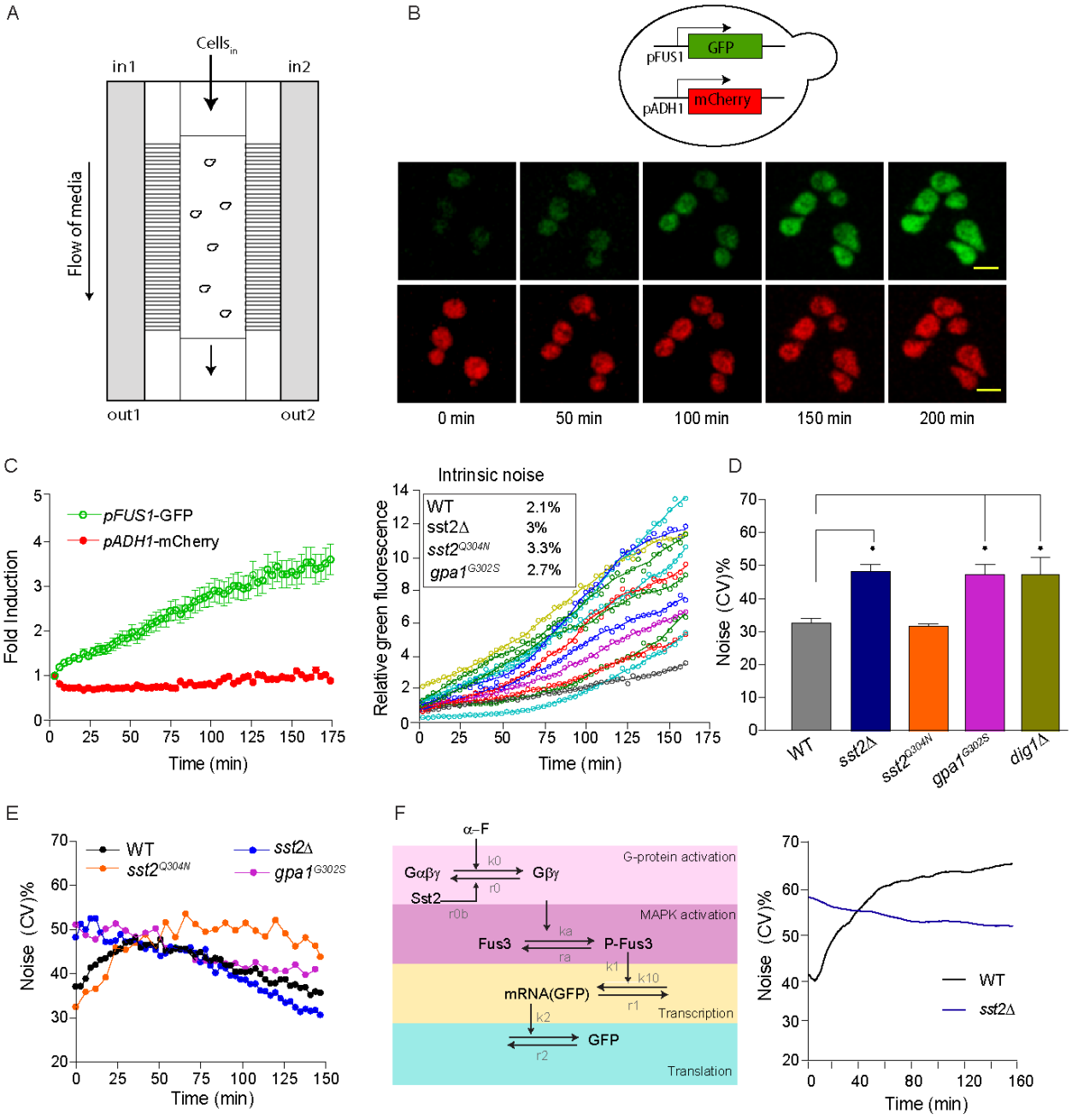
A
Cells$_{in}$
in1
in2
Flow of media
out1
out2
B
pFUS1
GFP
pADH1
mCherry
0 min
50 min
100 min
150 min
200 min
C
pFUS1-GFP
pADH1-mCherry
Fold Induction
Time (min)
Intrinsic noise
WT 2.1%
sst2Δ 3%
sst2Q304N 3.3%
gpa1G302S 2.7%
Relative green fluorescence
Time (min)
D
Noise (CV)%
WT
sst2Δ
sst2Q304N
gpa1G302S
dig1Δ
E
WT
sst2Q304N
sst2Δ
gpa1G302S
Noise (CV)%
Time (min)
F
α–F
Gαβγ
Gβγ
Sst2
k0
r0
r0b
G-protein activation
MAPK activation
Fus3
P-Fus3
ka
ra
k1
k10
mRNA(GFP)
r1
Transcription
k2
GFP
r2
Translation
Noise (CV)%
WT
sst2Δ
Time (min)

**Figure 2.3 RGS-GAP activity suppresses noise in gene expression.**
(A) Schematic of the microfluidic chamber.
(B) *Top*, Transcriptional reporter assay: pheromone pathway specific reporter *FUS1*-GFP was integrated at the *FUS1* promoter; reference reporter *ADH1*-mCherry was integrated at the *ADH1* promoter. *Bottom*, Activation of pheromone-dependent gene expression: Wild type cells were treated with 150 nM α factor. GFP and mCherry fluorescence was visualized by confocal microscopy at the indicated times. Scale bar, 5 μm.
(C) *Left*, Quantification of fold induction of GFP and mCherry in wild type cells in response to pheromone treatment. Data show mean +/- SD for at least 50 individual cells. *Right*, Representative single cell traces of relative GFP (GFP fluorescence/mCherry fluorescence) for individual wild type cells over time, showing minimal intrinsic fluctuations within single cells. Inset, measurements for average intrinsic noise over time (see Supplemental Experimental Procedures) for cells treated with 150 nM α factor.
(D) Bar graphs showing the CV of basal (relative) GFP expression in wild type, *sst2*Δ, $gpa1^{G302S}$, $sst2^{Q304N}$ and *dig1*Δ cells in the absence of pheromone. Student's t-test was used to calculate P values (* $P<0.05$). CV calculated from three independent experiments with at least 100 individual cells per experiment.
(E) Dynamic change in CV over time following treatment with 150 nM α factor. Fluorescence and CV measurements were made every 3 min for wild type cells and every 6 min for mutant strains (see Figure S2).
(F) *Left*, Model of the pheromone pathway featuring core components with key reactions and rates highlighted. Model assumes cell-to-cell variability in the abundance or activity of pathway components at the level of the MAPK and above. Parameters derived from the literature were optimized to those that best matched the data in (E). See Experimental Procedures for details of parameter optimization. The reactions, as well as final parameter values, used for the model for calculating CV are provided in Table S4 of Supplemental Information. *Right*, Stochastic simulations were run using BioNets as described in the experimental procedures to calculate CV over time for wild type and *sst2*Δ cells under pheromone stimulation.

In a previous study it was concluded that loss of Sst2 results in receptor *independent* G protein activation in a subset of the population (Siekhaus and Drubin, 2003). While indicative of noise, their measurements relied on plasmid-borne transcription reporters, which are inherently noisy (Lobner-Olesen, 1999), and were made only in the absence of stimulus.

Given that Sst2 can alter signal dynamics (Figure 2.1 *E*), we next considered how Sst2 affects the dynamics of noise. Accordingly, we monitored reporter activity in cells treated with pheromone. Shown in Figure 2.3 *C* (right) are representative traces for relative GFP intensities in single cells over time. Visual inspection clearly showed that cell-to-cell variability, but not fluctuations within each cell, was the dominant source of noise. To further measure intrinsic fluctuations we fit a smooth curve to each trace and calculated the deviation of the data from this curve (see Supplemental Experimental procedures for details). By this measure we confirmed that there was little difference in intrinsic noise between the four strains. Additionally, in each case intrinsic noise had a very low contribution to total noise.

We then turned to measures of total noise. Following treatment with pheromone, noise in wild type cells increased initially but then declined after approximately 40 min (Figure 2.3 *E*). In contrast, *sst2*Δ cells exhibited high basal noise that declined immediately after the addition of pheromone. A similar change in CV was evident in the absence of GAP activity (*gpa1*$^{G302S}$) but not in the absence of receptor binding (s*st2*$^{Q304N}$) (Figure 2.3 *E*). Thus, while receptor binding and GAP activity are both needed to suppress the pheromone signal, and they contribute equally to signal regulation, GAP activity alone suppresses transcriptional noise.

We then performed additional experiments using lower doses of pheromone that better matched the elevated sensitivity of the *sst2* mutant. For wild type cells at saturating pheromone, the noise increased and then decreased, while at non-saturating pheromone the noise increased and remained elevated (Figure 2.4 *C*). In *sst2*Δ cells the noise decreased over time, and this decrease was more pronounced at higher (saturating) pheromone concentrations (Figure 2.4 *D*). There was no further decrease even at the highest concentrations of pheromone (compare *sst2*Δ in Figures 2.3 *E* and 2.4 *D*). These results show that noise is higher at the non-saturating concentrations of pheromone, and the same pattern holds for the *sst2*Δ mutant and wild type strains.

We postulated that the initial increase in CV after pheromone stimulation was due to variability in the abundance of early pathway components (Newman et al., 2006). In the absence of pheromone, expression and therefore cell-to-cell variability of the reporter is dependent on the basal activity of the transcriptional machinery but independent of other signaling components (basal MAPK activation is negligible). However, in the presence of pheromone, the MAPKs are activated and expression of the reporter is dependent on MAPK activation in individual cells, which is variable. Thus the dominant source of variability may shift, in a dynamic manner, from components downstream of the MAPK to variable components upstream of the kinase. This shift could lead to an initial increase in cell-to-cell variability following stimulation. This increase in CV is followed by a gradual decrease after 30-40 min of stimulation. Coincident with this transition is a pheromone-dependent redistribution of Sst2, wherein the protein moves from the cytoplasm to the plasma membrane

## Figure 2.4

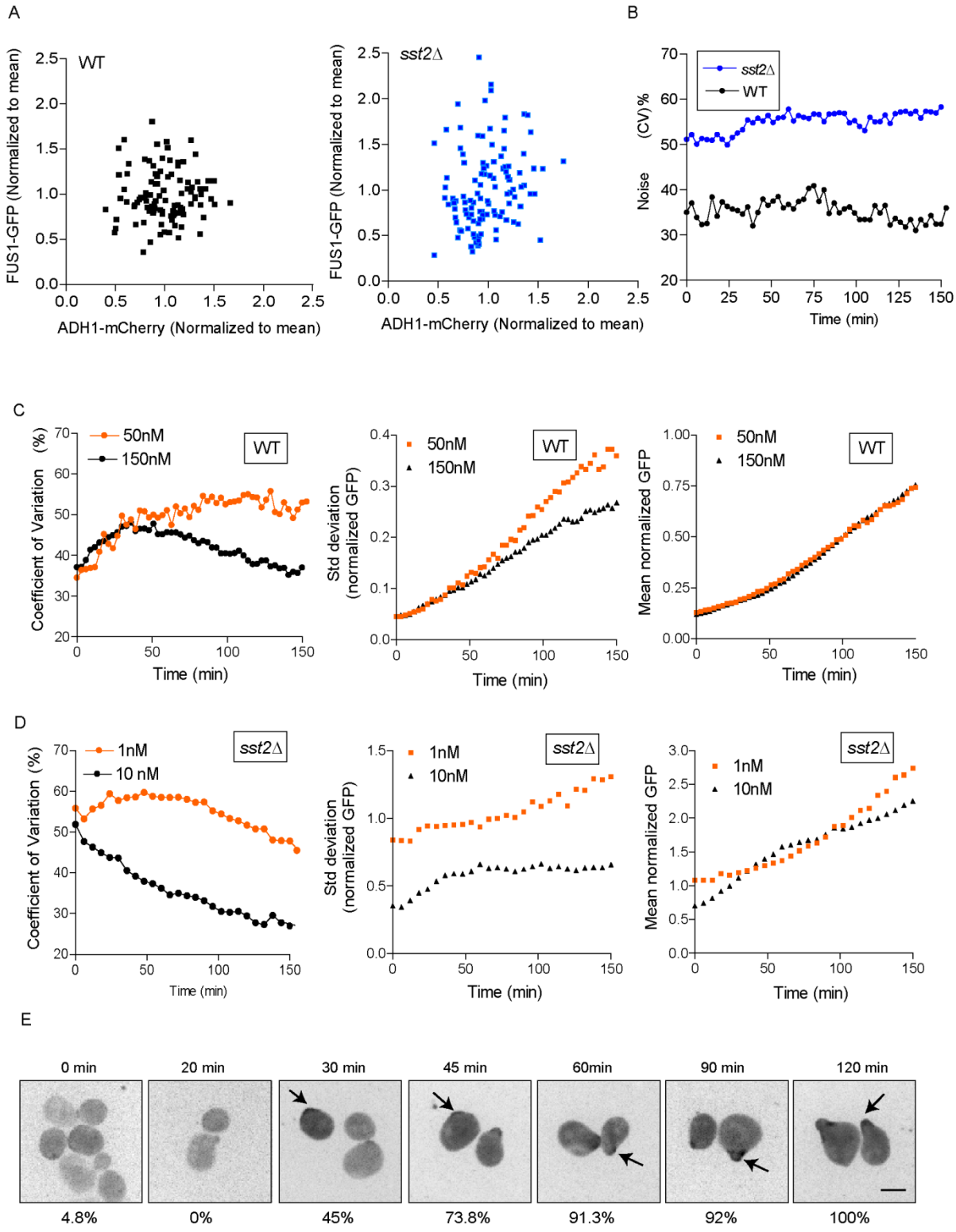
A
WT
FUS1-GFP (Normalized to mean)
ADH1-mCherry (Normalized to mean)
sst2Δ
B
sst2Δ
WT
(CV)% Noise
Time (min)
C
50nM
150nM
WT
Coefficient of Variation (%)
Std deviation (normalized GFP)
Mean normalized GFP
Time (min)
D
1nM
10 nM
sst2Δ
E
0 min
20 min
30 min
45 min
60min
90 min
120 min
4.8%
0%
45%
73.8%
91.3%
92%
100%
% of wild type cells with Sst2 -GFP membrane localization

**Figure 2.4 Noise analysis of pheromone pathway specific gene expression.**
(A) Scatter plots demonstrating pheromone pathway specific (*FUS1*-GFP) and pathway independent (*ADH1*-mCherry) noise in wild type and *sst2*Δ cells. Each point represents the mean fluorescence intensities from one cell.
(B) Change in CV over time in the absence of pheromone in wild type and *sst2*Δ cells. Fluorescence and CV measurements were made every 3 min.
(C) *Left*, Increase in CV in wild type cells upon α factor treatment is sustained when cells are treated with a low dose of pheromone. Cells were stimulated with either 50 nM (low) or 150 nM (high) α factor and imaged every 3 min. CV was calculated as standard deviation of mean (mCherry normalized) GFP (*middle*) divided by the mean (mCherry normalized) GFP over time (*right*)**.**
(D) Left, *sst2*Δ cells exhibit sustained high CV when treated with a low dose of pheromone. *sst2*Δ cells were stimulated with either 1 nM (low dose) or 10 nM (high dose) α factor and imaged every 6 min. CV was calculated as standard deviation of mean (mCherry normalized) GFP (*middle*) divided by the mean (mCherry normalized) GFP (right). Note that the initial mean fluorescence and standard deviation are different at the two doses owing to differences in the laser power outputs on separate days.
(E) Sst2-receptor binding at the membrane is initiated 30 min post pheromone stimulation. Wild type cells expressing GFP-tagged Sst2 were either left untreated or treated with 10 μM (saturating dose) α factor in a shaking culture flask. Samples were collected and imaged on agar pads for Sst2-GFP at the indicated times. Representative GFP (inverted fluorescence) images are shown for each time with the percentage of cells demonstrating Sst2-membrane localization at the bottom of each image. Arrows point to polarized Sst2-GFP. Scale bars, 5 μm,

and becomes concentrated at the mating projection where receptors and G proteins are located (Figure 2.4 *E*). In contrast, sst2$^{Q304N}$ remains cytoplasmic at all times (Ballon et al., 2006) possibly accounting for the sustained elevated noise exhibited by the mutant. In the absence of Sst2, basal signaling and MAPK activation is permanently elevated (Figure 2.1 *C* & *D*) and, consequently, so is variability in protein expression. In this situation there is no transition between late and early sources of variability and the CV does not increase after pheromone addition.

To better understand noise dynamics we built several stochastic models based on the core signaling cascade shown in Figure 2.3 *F* (left) and containing various control mechanisms that might regulate noise. These alternative models featured the core pathway components alone (model A) or the same components with pheromone induced stabilization/destabilization of the MAPK (model B), positive feedback at the level of the MAPK (model C) or negative feedback mediated by the MAPK (model D) (Figure 2.5). Details of the models can be found in the Supplemental Information and important modeling parameters are provided in Supplemental Table IV. All four models were evaluated for their ability to capture the changes in noise exhibited by wild type cells treated with pheromone (Figure 2.3 *F* and Figure 2.5). All incorporate intrinsic fluctuations due to the random nature of biochemical reactions in the cell. However none of these models were able to capture the qualitative behavior of the CV for wild type cells, suggesting another source of variability is responsible for the noise properties of the pathway. To investigate this we used the used the core signaling cascade (Model A, Figure 2.5) and added cell-to-cell variability in upstream signaling components. In this case the

## Figure 2.5

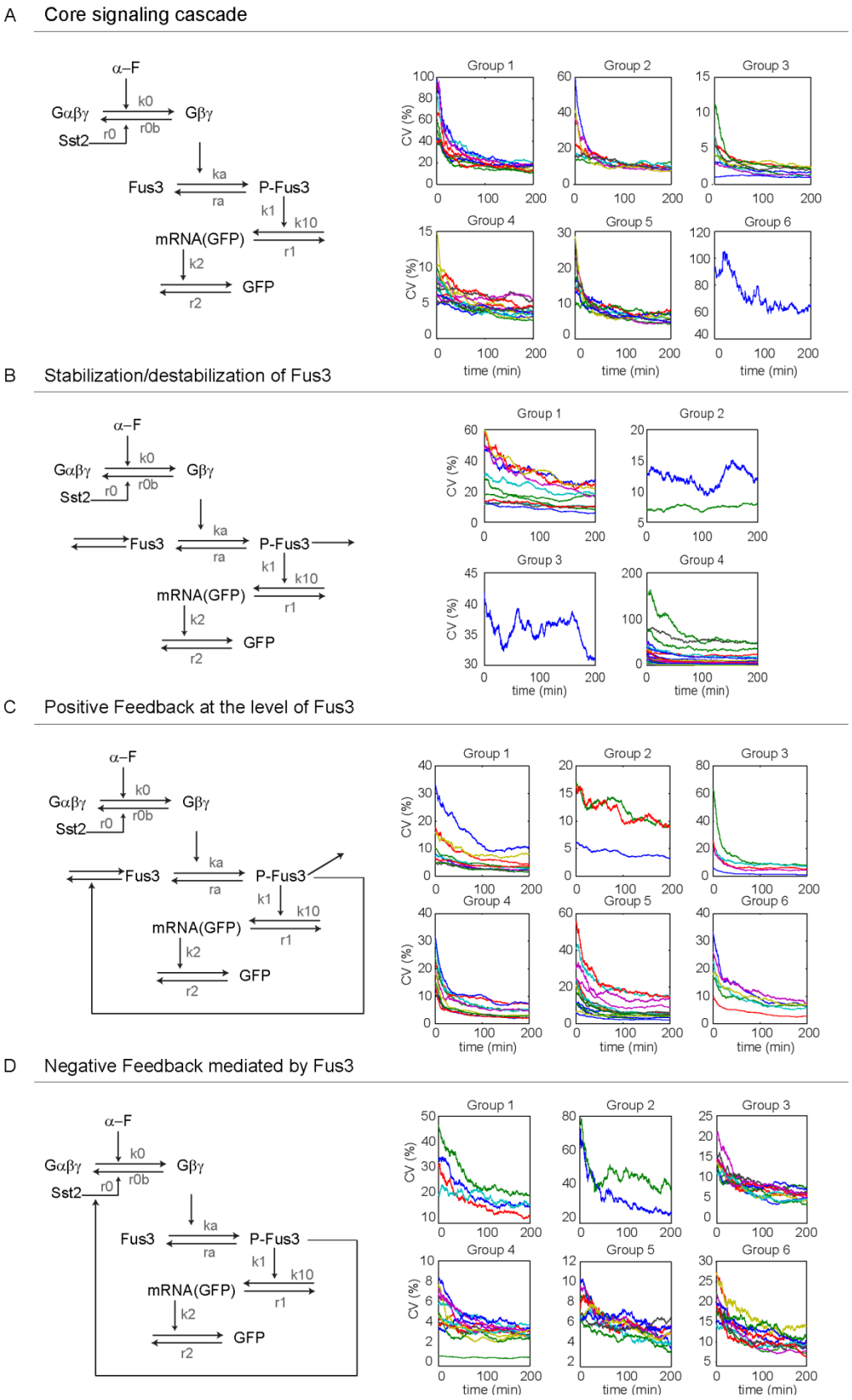
A
Core signaling cascade
α–F
k0
Gαβγ
Gβγ
r0b
Sst2
r0
ka
Fus3
P-Fus3
ra
k1
k10
mRNA(GFP)
r1
k2
GFP
r2
Group 1
Group 2
Group 3
Group 4
Group 5
Group 6
CV (%)
time (min)
B
Stabilization/destabilization of Fus3
C
Positive Feedback at the level of Fus3
D
Negative Feedback mediated by Fus3

**Figure 2.5 Alternative models tested (left) and corresponding simulations (right) that were unable to capture the dynamic changes in CV of the GFP reporter in wild type cells*$_{\varphi}$.**

(A) *Left*, Model of pathway activation that includes the core signaling cascade: G-αβγ, Fus3, Sst2, mRNA, and GFP. *Right*, Simulations of dynamic changes in CV for wild type cells using the basic activation model.

(B) *Left*, Model of pathway activation that includes pheromone mediated stabilization or destabilization of Fus3 in the core signaling cascade. *Right*, Simulations of dynamic changes in CV for wild type cells with the stabilization/destabilization (of Fus3) model.

(C) *Left*, Model of pathway activation that includes positive feedback where activated Fus3 leads to synthesis of more Fus3 in the core signaling cascade. *Right*, Simulations of dynamic changes in CV for wild type cells using the positive feedback model.

(D) *Left*, Model of pathway activation that includes negative feedback whereby Fus3 increases Sst2 activity, which in turn lowers G protein activity in the core signaling cascade. *Right*, Simulations of dynamic changes in CV for wild type cells using the negative feedback model.

* All four models incorporate intrinsic fluctuations due to the random nature of biochemical reactions in the cell.

$_{\varphi}$ For each of these models 50 parameter sets were chosen from a normal distribution centering on average values derived from the literature. For each model the 50 simulations were grouped using the MATLAB kmeans clustering algorithm with the “distance” option set to “correlation”.

abundance of the MAPK, Fus3, and the G protein were randomly chosen from normal distributions centering on average values derived from the literature (with a 30% variance). Stochastic simulations of the revised model (Figure 2.3 *F*) were compatible with the experimental data provided in Figure 2.3 *E*.

Our model generates results that are consistent with several important properties of the pathway. First, the model predicts that basal noise is increased by stochastic activation of the G protein and decreased by Sst2-mediated inactivation of the G protein. In support of this prediction, cells that lack Sst2 exhibit elevated basal G protein activity, elevated expression of upstream signaling components, and consequently increased variability in basal Fus3 activity, all contributing to the elevated initial CV. Second, in cells treated with pheromone, noise becomes elevated due to variable expression of the pathway components upstream of the transcriptional machinery. As shown in Figure 2.3 *F*, our model captures (i) the qualitative difference in the starting CV in the presence and absence of Sst2, (ii) the pheromone-dependent increase in CV when Sst2 is present and, (iii) the immediate decrease in CV when Sst2 is absent. For the sake of simplicity we only considered Sst2 GAP activity and not receptor binding. In addition we did not model the change in CV at later times, which is likely influenced by more complex events, such as the redistribution of Sst2 to the plasma membrane (Figure 2.4 *E*) or feedback regulation.

**Sst2 suppresses noise in morphogenesis** - Having shown that Sst2 limits transcriptional noise, we next considered whether Sst2 also limits variability in morphogenesis. As noted above, the G protein initiates signaling through two pathways, one that is mediated by the MAPK Fus3, leading to new gene

transcription, and a second that is mediated by the small G protein Cdc42. Cdc42 drives cell polarization during budding as well as in preparation for mating (Moskow et al., 2000; Pruyne and Bretscher, 2000). Thus the pheromone-dependent changes in cell morphology are an important indicator of the cellular decision-making process. Upon pheromone stimulation the population transitions from a one state system comprised of budding cells (vegetative growth) to a three state system comprised of budding cells, elongated cells and shmooing cells. In wild type cells, the two new states are temporally distinct, with the elongated growth stage emerging last (Figure 2.6, left). It has been shown previously that these elongated cells expand in the direction of a gradient stimulus, presumably in an effort to reach a distant mating partner (Erdman et al., 1998; Hao et al., 2008). In contrast, cells lacking Sst2 display a variety of morphologies (Figure 2.6, right) including circular, elliptical, peanut and irregular shapes. Given this heterogeneity in cell shape, we postulated that Sst2 suppresses variability in morphogenesis and that noise suppression enables effective decision making in response to a pheromone gradient.

Thus the results presented above reveal that Sst2 suppresses variability in cellular morphogenesis, particularly in the elongation phase where cells can expand towards a pheromone stimulus. It has been shown previously that Sst2 is required to properly track a pheromone gradient (Segall, 1993). We therefore hypothesized that gradient tracking relies on Sst2-mediated noise suppression during morphogenesis. To test our theory we quantified the behavior of our mutants in a microfluidics chamber capable of producing a linear pheromone gradient. For these experiments we used pheromone concentrations matched to the sensitivity of the individual

## Figure 2.6

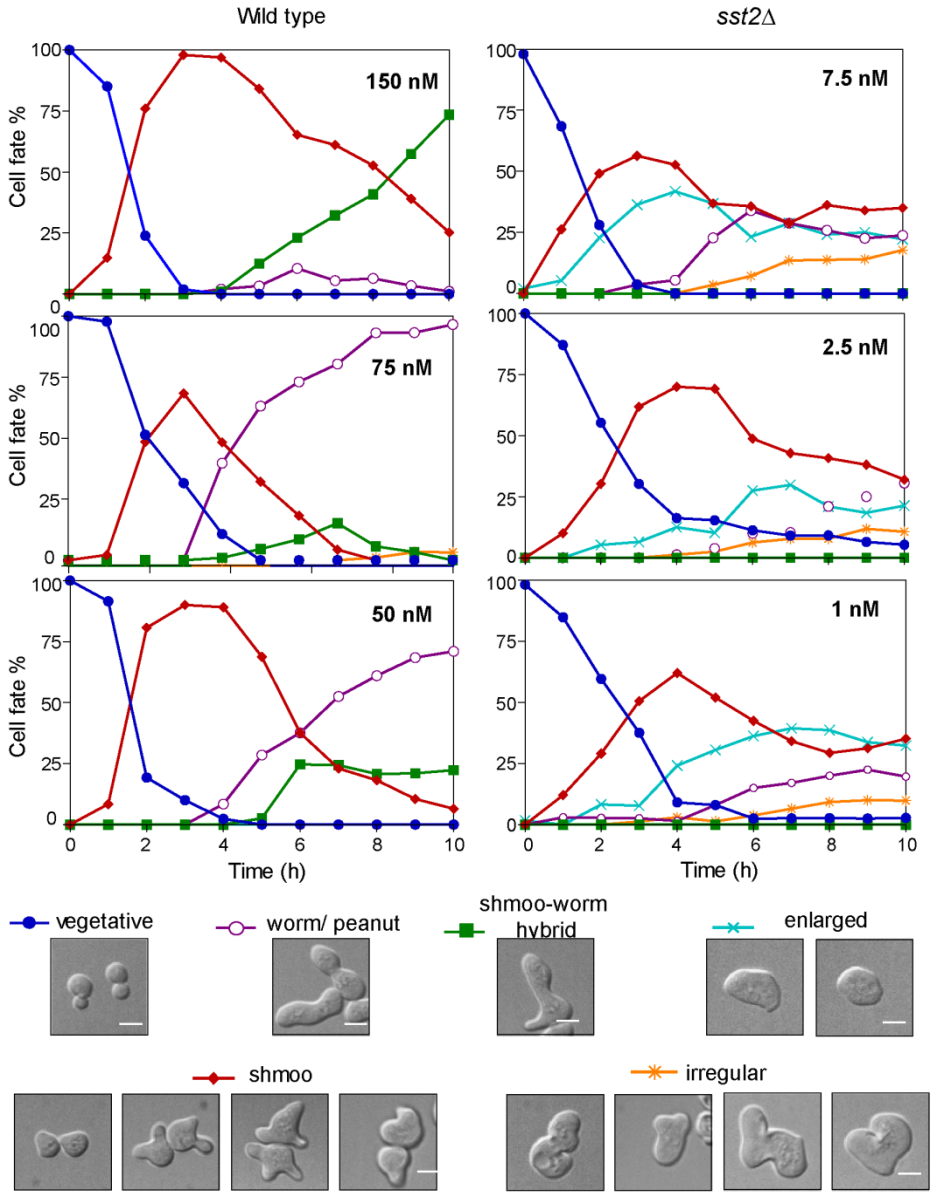


**Figure 2.6 Sst2 limits heterogeneity in pheromone dependent cell fate (morphology).** Wild type (left) and *sst2*Δ cells (right) were treated with the indicated doses of pheromone in a microfluidic chamber and morphological fates determined every hour up to 10 h. Cells were categorized as follows: (1) vegetative (G1/S/G2/M), (2) worm or peanut (elongating), (3) shmoo-worm hybrid, (4) enlarged (circular or ellipse), (5) shmoo (one, two or three projections and cells with a projection that is rotating), and (6) irregular (undefined shapes). Key, representative images for each morphological class. Each graph contains data from one experiment with at least 100 cells monitored over time. Scale bar, 5 μm.

strains; 0-150 nM for wild type, 0-50 nM for *gpa1*$^{G302S}$ and *sst2*$^{Q304N}$, and a 0-7.5 nM for *sst2*Δ. To monitor directionality of growth we used a GFP-tagged version of the protein Bem1, which binds active Cdc42 and therefore localizes to the polar cap (Madden and Snyder, 1998). To assess gradient tracking we focused on cells residing in the region of the chamber with the largest linear difference in pheromone concentration, as evaluated by the intensity of a dye contained in pheromone solution (Figure 2.7 *A*). Cell polarization was then monitored over 5 min intervals (Figure 2.7 *B*) and quantified by measuring the final angle of polar cap orientation (represented as an angle distribution histogram, Figure 2.7 *C*). As expected, wild type cells oriented properly, typically within -/+ 45° of the gradient, while cells lacking Sst2 oriented randomly. Of the two point mutants, only loss of Sst2 GAP activity (*gpa1*$^{G302S}$) produced any defects in gradient tracking (Figure 2.7 *C*). Thus the mutants that exhibit an increase in transcription noise also exhibit a defect in gradient tracking. If increased pheromone sensitivity alone conferred a defect in gradient tracking, the individual point mutants should have behaved similarly. Taken together our findings indicate that noise suppression, but not signal suppression, is associated with proper chemotropic growth.

We considered two potential mechanisms for a failure to track a gradient. In the first scenario, cells are unable to determine the source of the pheromone and elongate in random directions. In the second, cells are able to sense directional cues, but are unable to maintain polarization in the correct direction. To distinguish between these two possibilities, we monitored the time-dependent (dynamic) changes in cell morphology and polar cap movement. We began with the two

**Figure 2.7**

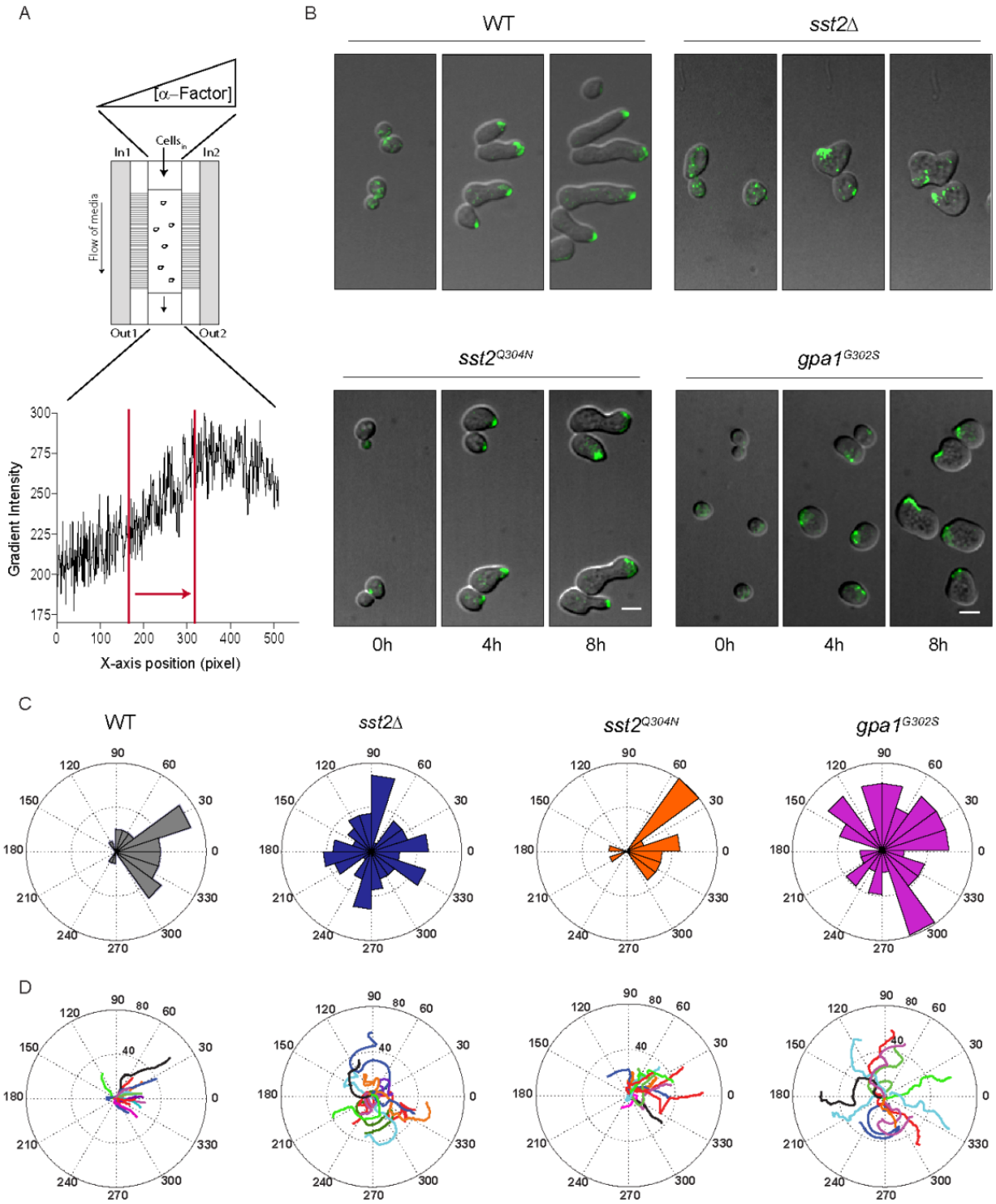
A
[α–Factor]
In1
Cells
In2
Flow of media
Out1
Out2
Gradient Intensity
X-axis position (pixel)
B
WT
sst2Δ
sst2Q304N
gpa1G302S
0h
4h
8h
C
WT
sst2Δ
sst2Q304N
gpa1G302S
D

**Figure 2.7 RGS-GAP activity promotes directed polarization and proper gradient tracking**.

(A) *Top*, Schematic of gradient tracking. A gradient was created in the chamber by passive diffusion of pheromone-containing medium from the right channel (In2) and pheromone-free medium in the left channel (In1). *Bottom*, pheromone gradient profile in the microfluidic chamber visualized by the dye cascade blue. Cells were monitored in the region of steepest gradient (bounded by red lines). Arrow points in the direction of highest pheromone.

(B) Merged DIC and fluorescence (Bem1-GFP) images collected at 5 min intervals for 8 h, in the pheromone gradient described in (A). Cells were exposed to the following gradients to promote elongated growth: wild type (0-150 nM), *sst2*Δ (0-7.5 nM), $gpa1^{G302S}$ and $sst2^{Q304N}$ (0-50 nM). Scale Bar, 5 μm.

(C) Histograms for the frequency distribution of the final angle of cell polarization with respect to the pheromone gradient. Zero represents perfect alignment toward the gradient. Results show mean data for two independent experiments, n=50 approx.

(D) Polar plots of ten representative cells tracked over time. Center represents t=0.

mutants unable to track a gradient, *sst2*Δ and *gpa1*$^{G302S}$. In both cases over 50% of cells were unable to elongate towards high pheromone as the polarity site frequently changed direction (Figures 2.7 *B* and *C*). Furthermore the random changes in polar cap orientation were evident from the beginning of the stimulus. As before, the two GAP-deficient mutants also exhibited heterogeneous morphologies. In contrast, wild type cells and the receptor binding mutants (s*st2*$^{Q304N}$) elongated properly towards the gradient and exhibited unaltered morphologies. The inability of *sst2Δ* and *gpa1*$^{G302S}$ to continuously move toward the gradient is documented in Figure 2.7 *D*, which shows the time averaged path of the polar cap for a representative set of wild type and mutant cells. Finally we measured the persistence in Bem1 polarization over 8 h in a gradient. For this analysis we defined persistence as the ratio of final displacement to total distance traveled. In accordance with the data presented above, the polar cap was most persistent in wild type cells (0.42 ± 0.02) followed by the Sst2-receptor binding mutant (0.25 ±0.01), the Sst2-GAP activity mutant (0.18 ± 0.01) and finally the *sst2*Δ cells (0.13 ±0.01). We conclude that Sst2 GAP activity promotes directional persistence of the polar cap during gradient tracking, and does so by suppressing morphological variation.

Successful mating is contingent upon the ability to reliably sense the source of pheromone, to induce mating genes and to form a stable mating projection (or shmoo) for fusion with a mating partner. Since loss of GAP activity results in increased variability in transcription as well as in morphology, we sought to examine the consequences of these defects with regard to mating. Accordingly, we tested the ability of cells to maintain polarization in saturating pheromone (mimicking the

presence of a nearby mate). As shown in Figure 2.8 *A* and movies S1-S4, wild type cells and mutants deficient in receptor binding (*sst2*$^{Q304N}$) were able to form well-defined shmoos and the polar cap did not change orientation over time. These results imply that cells, once they are properly polarized, are able to maintain the orientation of the polar cap. In contrast, cells lacking Sst2 did not form well-defined shmoos and the polar cap randomly changed orientation, implying a defect in maintenance of polar cap orientation. Once again, mutants deficient in GAP function (*gpa1*$^{G302S}$*)* showed a defect similar to that of *sst2*Δ cells.

We then measured the ability of cells to maintain polarization as a frequency distribution of the angle of orientation during shmooing in individual cells. While wild type and *sst2*$^{Q304N}$ cells exhibited low noise in orientation (measured as the standard deviation of the distribution), *sst2*Δ and *gpa1*$^{G302S}$ cells exhibited a high noise in orientation of polarization (Figure 2.8 *B*). Consistent with a defect in locating a potential mating partner, loss of GAP activity resulted in a severe reduction in mating efficiency (Figure 2.8 *C*). As in previous assays, the receptor binding mutant (*sst2*$^{Q304N}$) showed no defects in orientation or mating ability despite its increased sensitivity to pheromone. Taken together, our data establish that Sst2, and in particular Sst2 GAP activity, is a suppressor of noise. Sst2 acts in both the absence and presence of a pheromone stimulus, regulates noise in a dynamic manner and suppresses noise in transcription as well as in morphogenesis. Based on these findings, we propose that noise suppression - but not signal suppression - is required for proper gradient detection and morphogenesis.

**Figure 2.8**

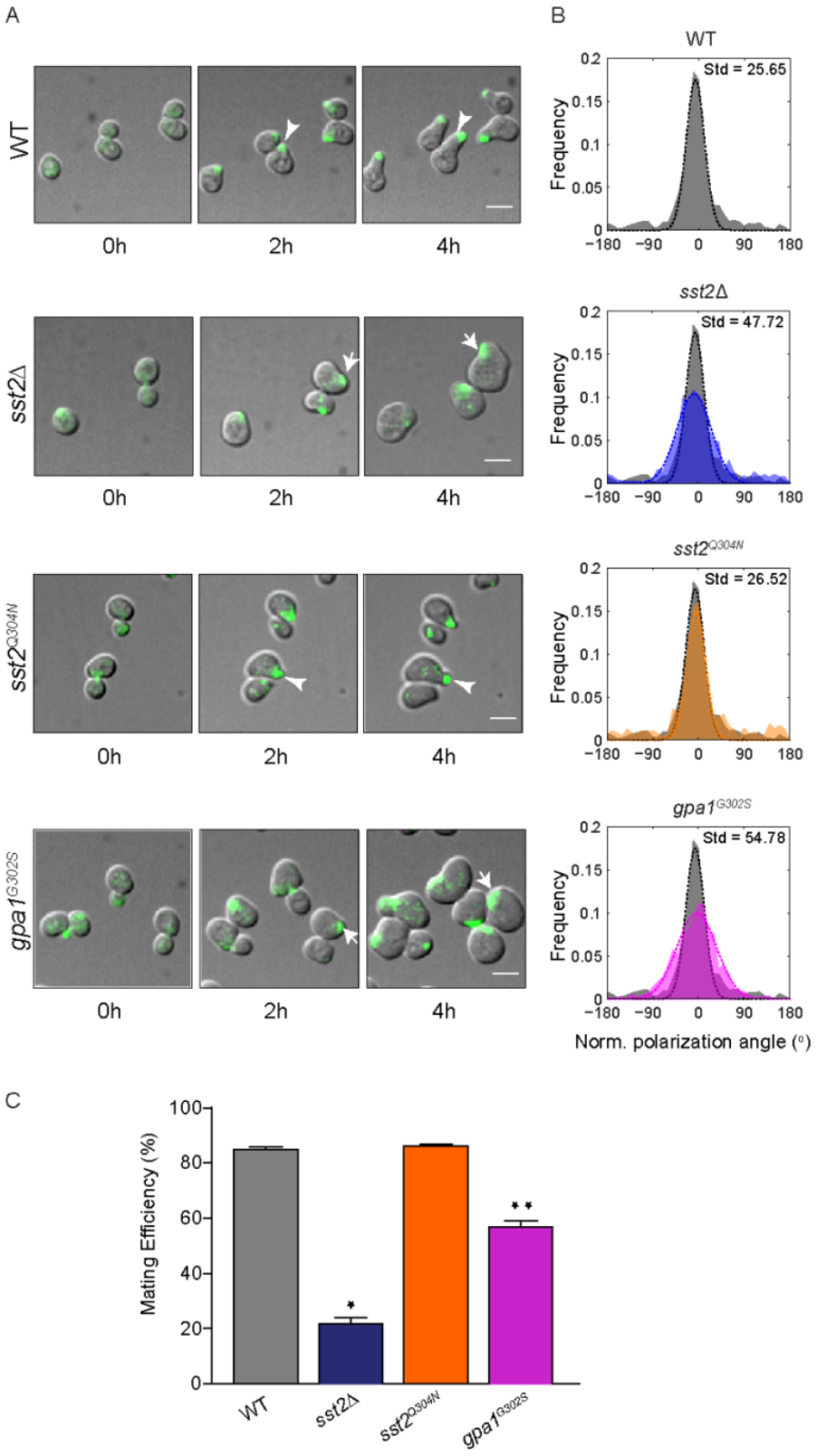
A
B
C
WT
sst2Δ
sst2Q304N
gpa1G302S
0h
2h
4h
Std = 25.65
Std = 47.72
Std = 26.52
Std = 54.78
Frequency
Norm. polarization angle (°)
Mating Efficiency (%)

**Figure 2.8 RGS-GAP activity promotes persistent polarization and proper mating efficiency**

(A) Merged DIC and fluorescence (Bem1-GFP) images of cells treated with high pheromone concentrations (150 nM) to promote shmoo formation, collected at 5 min intervals for 4 h. Arrows indicate the site of Bem1 polarization.

(B) Frequency distribution of the mean normalized angle of polarization during shmooing in individual cells measured over a 3 h period. The distribution for each mutant is laid over the distribution for wild type cells (in grey). The data for each strain were fit to a single Gaussian and a standard deviation (Std) was calculated.

(C) Mating-efficiency assay. Data are mean ± SEM of three independent experiments. Student's t-test was used to calculate P values (* $P<0.05$).

## Discussion

It has long been recognized that cellular behavior is a consequence of genetically-encoded and environmental cues. However, advances in single cell analysis have revealed that even genetically identical cells, grown under identical conditions, can exhibit widely divergent behaviors. Furthermore, it is evident that much of the observed variability in eukaryotic cells is due to “extrinsic” sources of noise, as opposed to the “intrinsic” noise inherent in biochemical processes (Raser and O'Shea, 2004; Volfson et al., 2006). Consistent with these broader findings, it has been demonstrated previously that extrinsic noise is the dominant source of variation in the mating pheromone pathway, at least at the level of transcription (Colman-Lerner et al., 2005), and that the transcription regulator Dig1 is a major contributor to noise suppression (McCullagh et al., 2010). Here we show that the RGS protein Sst2 suppresses noise and, more specifically, does so by accelerating G protein inactivation. In our experimental system we found that Sst2 and Dig1 contribute similarly to limiting variability in transcription (Figure 2.3 *D*). In addition we were able to show that Sst2 suppresses noise in the presence of pheromone and limits variability in cellular morphogenesis as well as in transcription.

We chose to focus on Sst2 for several reasons. First, deletion of Sst2 has the largest effect of any known gene on the pheromone signal, and it was therefore likely to be a major contributor to noise (Chasse et al., 2006). Second, Sst2 acts early in the pathway and any effects on noise were likely to be propagated (amplified) to downstream events, adding substantially to the variability of the final readout. Third, Sst2 expression is induced following pheromone stimulation and,

consequently, signaling is attenuated over time. Theoretical analysis, based on stochastic models, had predicted that such feedback inhibition events would improve noise filtering (Becskei and Serrano, 2000; Dublanche et al., 2006; Thattai and van Oudenaarden, 2001). Thus, Sst2 represented an opportunity to test some longstanding theories about the origins of cell-to-cell variability. Fourth, Sst2 regulates both branches of the pheromone signaling pathway. While gene expression is the most common and convenient measure of cellular noise, it seemed likely that noise would impact other cellular responses such as chemotropism and morphogenesis. Finally, whereas transcriptional changes occur over minutes, changes in cell morphology can take much longer. A good understanding of the various time scales of pathway output is necessary to fully understand the causes and consequences of noise regulation (Purvis and Lahav, 2013).

One conclusion of our work is that noise is dynamically regulated. Whereas past studies have focused on noise under standard (unstimulated) growth conditions, we show that Sst2 regulates noise in both the presence and absence of a pheromone stimulus. This is important because noise levels may confer enhanced phenotypic diversity when cells are challenged by various environmental cues (Avery, 2006). Moreover we show that transcriptional noise increases and then decreases with prolonged pathway activation, and that these trends persist at various doses of pheromone. Our model predicts that prior to pheromone stimulation, noise is suppressed by Sst2 because the GAP activity of this protein ensures that basal MAPK activity is minimal. Therefore, variability due to fluctuations in upstream pathway components (both activity and abundance) is not propagated

through the pathway. Treatment with pheromone “unmasks” these pathway specific fluctuations leading to an increase in cell to cell variability.

Another aspect of our work is the attention paid to cellular morphogenesis. Whereas previous investigations have focused on transcriptional noise, we also analyzed variations in cellular morphogenesis, through Cdc42 activation of projection formation in single cells. Indeed, our analysis of gradient tracking and of mating projection formation indicates that pheromone super-sensitivity, by itself, does not impede mating (Jackson and Hartwell, 1990). Rather, morphological variability, random changes in polarization, and an inability track a gradient can account for the overall deficiency in mating. Thus we consider noise suppression to be biologically significant in yeast. Given the broad conservation of G protein signaling, noise suppression by RGS proteins is likely to be biologically significant in plants and in other animals including humans.

The third, and perhaps most important, advance is the realization that noise suppression and signal suppression are not linked in an obligate manner. By selectively uncoupling Sst2 from its two known binding partners, in each case by a single amino acid substitution, we identified conditions that produce equivalent signal outputs but widely different noise characteristics. To our knowledge there is no other example of a system that exhibits these characteristics. In this regard, it was surprising to us that cellular noise suppression mechanisms can be so easily subverted, and that there are so few redundancies to buffer such behaviors.

While it is clear that signal and noise suppression are mediated by Sst2-GAP activity, the mechanism by which Sst2-receptor interaction suppresses signaling

remains to be addressed. Another question is how changes in noise, particularly transient increases or decreases in noise such as those reported here, might benefit the population. Theoretical work has suggested that phenotypic variation may be particularly useful in a rapidly changing environment (Kussell and Leibler, 2005; Thattai and van Oudenaarden, 2004). Accordingly, noise in the pheromone response might allow a portion of cells to delay responses to the mating signal and continue cell proliferation. These proliferating cells will not mate, but would be at a growth advantage if there were no suitable mating partner to be found. Thus extrinsic sources of noise may serve as both an impediment to predictable behavior as well as a means to promote survival in uncertain growth conditions.

Finally, the realization that an RGS protein can function as a noise suppressor is significant because it represents a new function for a well-established signaling protein. Insofar as these findings may represent a general activity of RGS proteins, they are potentially important in understanding human physiology and pharmacology. RGS4, the protein most closely related to Sst2, has been proposed as a drug target for the treatment of schizophrenia and Parkinson's disease among other disorders (Gu et al., 2007; Roman et al., 2007). Given that any drug should confer a predictable response, the potential of RGS proteins as drug targets should be carefully considered.

In conclusion, noise in biological systems has long been recognized, but it has been difficult to understand its causes and functional consequences. Investigating the sources of such behaviors is made especially difficult given the challenges of studying a phenomenon that is - by definition - unpredictable. Only by

removing noise control mechanisms, as we have done here, can we begin to understand what happens if noise suppression fails and such variations occur unchecked. In this regard, our experimental platform will allow investigators to analyze the properties of a well-defined signaling pathway under high noise conditions, and to evaluate the performance and efficiency of cellular decision-making systems that rely on noisy chemical cues and imprecise information. A deeper understanding of the processes that suppress noise will allow us to eventually develop a theoretical framework for predicting their occurrence.

## Experimental Procedures

**Strains, Plasmids and Growth of Cultures**. Standard procedures for the growth, maintenance and transformation of yeast and bacteria were used throughout. The yeast (*Saccharomyces cerevisiae*) strains used in this study were BY4742 (MAT$\alpha$ *leu2Δ lysΔ his3-1 ura3Δ*), BY4741 (MAT**a** *leu2Δ met15Δ his3-1 ura3Δ*) and its derivatives (Brachmann et al., 1998). A table of strains, plasmids, and primers as well as details of plasmid construction can be found in Supplemental Experimental Procedures. All cells were grown at 30°C in yeast extract peptone medium (YPD) or synthetic complete medium (SC) containing 2% (w/v) dextrose. Plasmid-transformed cells were grown in synthetic complete medium that lacked the appropriate nutrient.

**Plasmid Construction.** The pRS406 ADH1-mCherry and pRS405 ADH1-mCherry integrating vectors were constructed in two steps, both employing mega-primer cloning (Unger et al., 2010). First, mCherry was PCR amplified using pRS405

STE2-mCherry as the template and the following primers: mCherryMega (F) and mCherryMega (R). The primers introduced sequences at the N and C termini of mCherry complementary to the *ADH1* promoter and *ADH1* terminator sequences in pRS316 ADH1. Subsequently, *ADH1*p-mCherry-$ADH1_t$ was PCR amplified from pRS316 ADH1-mCherry with primers [ADH1_XhoI (F) and ADH1_SacI (R)] that also introduced terminal XhoI/SacI sites and overhangs that direct $ADH1_p$-mCherry-$ADH1_t$ into the MCS of pRS406 and pRS405. pRS406 $sst2^{Q304N}$ was made by PCR amplification of *SST2* +/- 500 bp from the gDNA of wild type cells using primers sst2 (F) and sst2 (R) that introduced BamHI and KpnI sites for directional cloning into pRS406. Single point mutation of $sst2^{Q304N}$ was constructed by QuikChange (Stratagene) mutagenesis using primer sst2-Q304N-F and its complement.

**Strain Construction.** The *sst2Δ* (BY4741 *sst2Δ*::KanMX4) strain from Research Genetics did not produce a consistent phenotype. It was remade by PCR amplification of the KanMX cassette of pFA6KanMX and transformation into wild type BY4741 (Wach et al., 1994). The GAP insensitive Gpa1 strain $(gpa1^{G302S})$ was constructed as described earlier (Lambert et al.). The receptor uncoupling strain ($sst2^{Q304N}$) was constructed by transformation of pRS406 $sst2^{Q304N}$ (linearized by AscI) followed by pop-out of the wild type allele on 5-Fuoroorotic acid-containing medium. All constructs were verified by nucleotide sequence analysis.

**Generating dual reporter strains with pathway specific GFP and reference mCherry**. Pathway specific GFP reporter was integrated at the *FUS1* promoter by transformation of pRS303 FUS1-GFP linearized by digestion with XcmI. Positive clones with one *FUS1*-GFP integration were selected by growth on SCD–

His medium and transformed with PacI-digested pRS406 ADH1-mCherry that integrated at the *ADH1* promoter. Transformants selected on medium lacking uracil were deemed positive only if they had a single integration as assessed by mCherry fluorescence intensity. This process was applied to all other strains except *gpa1*$^{G302S}$ which was transformed with pRS405 ADH1-mCherry.

**Generating reporter strains to monitor polarization.** *BEM1*-GFP was PCR amplified from the GFP-tagged library strain (Huh et al., 2003). Briefly, genomic DNA was isolated and used as a template for PCR with primers [Bem1His (F) and Bem1His (R)] that amplified a portion of the C' of *BEM1* along with GFP and *HIS3*. The PCR product was transformed in wild type, *sst2Δ, gpa1*$^{G302S}$ *and sst2*$^{Q304N}$ cells, and selected on medium lacking histidine.

**Pheromone Sensitivity Assays.** Pheromone sensitivity was measured as growth inhibition using an agar diffusion (halo) bioassay (Sprague, 1991) and by a transcriptional reporter assay (Hoffman et al., 2002) as described earlier. Briefly for the halo assay, filters were spotted with 0, 5, 15 or 50 µg α- factor and laid onto cells mixed with soft agar. For the transcriptional reporter assay, cells transformed with pRS423FUS1-LacZ were stimulated with different doses of pheromone for 90 min and β-galactosidase activity was measured spectrofluorometrically.

**Quantitative Mating Efficiency Assay**. Mating efficiency assays were conducted as described earlier (Sprague, 1991). Briefly, MAT**a** (BY4741) and MATα (BY4742) cells were grown to mid log phase, counted and mixed in equal numbers, allowed to adhere to nitrocellulose discs (Millipore) and incubated on YPD plates for 4 h. Subsequently, cells were harvested and plated onto diploid selective (SCD-Met-

Lys) and non-selective plates (SCD). Mating efficiency was calculated by dividing the number of diploid colonies from the total number of colonies.

**Cell Extract Preparation and Immunoblotting**. Briefly, cells either untreated or treated with 3 μM α factor for different durations (2, 5, 15, 30, 60 and 90 min) were harvested in TCA (5% final concentration), washed with 10 mM $NaN_3$, collected by centrifugation and the resulting pellets frozen at -80°C. For MAPK inactivation measurements, cells were treated with 3 μM α factor for 30 min, harvested by centrifugation, washed once, resuspended in pheromone-free medium and harvested at the times indicated. Cell extracts were prepared by glass bead lysis in TCA as described before (Hao et al., 2007). Protein concentration was determined by Dc protein assay (Bio-Rad). Proteins were resolved by 10% SDS-PAGE, transferred to nitrocellulose and detected by immunoblotting with p44/42 MAPK antibodies at 1:500 (9101L, Cell Signalling Technology), Fus3 antibodies at 1:500 (sc-6773, Santa Cruz Biotechnology, inc.) and anti-G6PDH at 1:50,000 (A9521, Sigma-Aldrich). Immunoreactive species were detected by chemiluminescence detection (Thermo Scientific Pierce ECL Plus) of horseradish peroxidase-conjugated antibodies (anti-rabbit, 170-5046 or anti-goat,sc-2768, Santa Cruz) at 1:10,000. Blots were scanned using Typhoon Trio+ (GE healthcare) and band intensity was quantified using Fiji (National Institute of Health).

**Single Cell Transcription Reporter Assay in Microfluidics Chambers.** A microfluidics device similar to the one described earlier was constructed (Hao et al., 2008). Cells containing the two reporters (pathway specific GFP and reference mCherry) were grown to $A_{600nm}$ ~0.4 after maintaining them at exponential growth for

at least 12-15 h. Cells were then loaded onto the microfluidics chamber ensuring a dispersed distribution of cells and stimulated with 150 nM pheromone (high dose for the chamber). The response was monitored by imaging DIC, GFP (488 laser) and mCherry (561 laser) every 6 min (unless otherwise noted) for 150 min. A 60X PlanApo objective under oil immersion was used and images were captured by an Olympus Spinning disc confocal microscope equipped with a motorized XYZ stage and EM CCD camera. MetaMorph software (Universal Imaging Corporation, Downington, PA) was used for image analysis. Image quantification was done using SchnitzCell (Matlab) software (Elowitz et al., 2002), but with custom modifications made mainly to the segmentation code to allow detection of yeast that are of varied morphology compared to bacterial cells. Relative green fluorescence was calculated by dividing the GFP intensity by the mCherry intensity. Noise was calculated as the coefficient of variation (CV) of the relative fluorescence of the population.

**Intrinsic Noise Calculation.** We calculated the trend-line for the single cell GFP intensity traces over time, using the MATLAB “smooth” function, with a span of 7 time points and a “lowess” fit. The absolute value of the difference of the actual data from the smoothed line was divided by the value of the smoothed line to determine the coefficient of variation at each time point. There was little variation in intrinsic noise over time, so the coefficients of variation for all time points were averaged for all cells to determine the average coefficient of variation for each strain.

**Analysis of polarization during gradient tracking and shmooing.** Early-mid log phase yeast cells containing the polarity marker Bem1-GFP were grown and loaded onto a microfluidics chamber as described above. A pheromone gradient was

generated as described previously (Hao et al., 2008). The specific dose of pheromone used to generate the gradient varied depending upon the pheromone sensitivity of the strain. Uniform pheromone (300 nM) was used for analysis of polarization during shmooing.

**Morphology analysis at uniform pheromone.** Log phase cells were loaded onto a microfluidic chamber at low density. Cells were stimulated with saturating pheromone (150 nM for wild type cells and 7.5 nM for *sst2*Δ), intermediate pheromone (75 nM for wild type cells and 2.5 nM for *sst2*Δ) or low-intermediate pheromone (50 nM for wild type cells and 1 nM for *sst2*Δ). DIC images were taken every 6 min for 10 h to track changes in cell morphology. Morphological cataloging was done by manually binning cells in predefined classes using ImageJ to visualize cells over time.

**Image Analysis for cell polarization during gradient tracking.** Images were analyzed with FIJI (Fiji Is Just Imagej) for cell tracking and polar plot generation from live cell microscopy. The GFP channel was registered based on the DIC channel using “descriptor based series registration.” The Bem1-GFP images were then thresholded to select just the polar cap. The “Analyze Particles” function was used to obtain the centroid of each polar cap throughout the time course. Using MATLAB, the polar caps were assigned to their respective cells by starting with the last time point, and comparing all of the centroids to the centroids of the previous time point. The distances of each object were calculated from the previous time point, and the object that was closest in the preceding time point was assigned to the same cell as in the current time point. This pairwise comparison of polar caps by

time points was iterated through the entire time series. The polar plots were generated by time averaging the x,y positions of the polar caps over 10 time points (50 min). The starting point for each cell was set to zero, and the x,y positions were converted to polar coordinates and plotted using the MATLAB polar plot function. Measurements for final angles of orientation during gradient tracking were calculated from the difference in x and y positions between two points (the final time averaged position and the position 1 h earlier) using the MATLAB atan2 function. Persistence was calculated as the ratio of the direct distance between the first and last x,y position and the total distance traveled, defined as the sum of the distances between each consecutive x,y position.

**Shmoo Angle Determination**. In order to determine the orientation of the polar cap during mating projection formation, cell masks were created using FIJI to define cells, and were then analyzed by custom MATLAB script. Briefly, for each time point and in each cell two regions of interest (ROI) were defined by thresholding at the 95$^{th}$ percentile and 75$^{th}$ percentile of Bem1 intensity. The angle of orientation was determined using the angle defined by the centroid of the 95% threshold ROI and the centroid of the 75% threshold ROI. Each cell was then normalized to an average of zero by subtracting the average angle of orientation of the cell from each data point. A Gaussian was fit to each distribution, and the constant c was used as the standard deviation of the distribution, where the Gaussian is written $f(x) = ae^{-\frac{(x-b)^2}{2c^2}}$.

**Mathematical modeling.** Stochastic simulations were run using BioNets to generate an executable file (Adalsteinsson et al., 2004). The executable, when

called, runs the Gillespie algorithm for a particular set of reactions. A custom MATLAB (Mathworks) script was developed in order to quickly run an ensemble of simulations for a given parameter set(s) while easily keeping track of the results. The reactions, as well as parameter values, used for the model for calculating CV are provided in Table S4 of Supplemental Information. Parameters were derived from the literature whenever possible (Ghaemmaghami et al., 2003). Parameters were further optimized to find those that best matched the data. Parameters were optimized by random selection from a $\log_{10}$ normal distribution, where the mean was taken as the literature-derived values and the standard deviation was taken as 0.5. For each parameter set an ensemble of 50 simulations was run. For each of the 50 ensemble simulations, and to model cell-to-cell variability, the total levels for G protein and MAPKs were chosen randomly from a normal distribution where the average was taken from literature derived values and the standard deviation was set to 30%. To find the parameter sets that best agreed with the data, parameters were searched for those that gave the smallest RMS distance between the observed CV for both the wild type and *sst2*Δ cases. We also explored the potential of several other simple models that did not rely on cell-to-cell variability, to reproduce our observed CV. The details of these simulations can be found in Supplemental Experimental Procedures. These other simple models did not give the increase in CV over time under pheromone stimulation.

Ordinarily the variability of protein expression, measured by the coefficient of variation (CV), is expected to decrease as the average protein concentration increases. The fact that the CV of pheromone-dependent gene expression increases

transiently under pheromone stimulation (at the same time that the average GFP concentration increases) is unexpected. Further, deleting the negative regulator, Sst2, changes the dynamic behavior of the noise: basal noise increases and pheromone induction only results in a decrease in CV over time. To help elucidate the mechanism of the increase in CV over time in wild type cells, and the decrease in CV over time in *sst2*Δ cells, we built several simple nonlinear models. In our basic model free Gβγ activates Fus3 by phosphorylation which in turn promotes transcription and eventually translation of the GFP reporter. Additionally, there is Fus3-independent transcription and translation. Sst2 promotes the re-association of Gβγ to Gα, shutting off the pathway. Importantly, the total level of the MAPK Fus3 and G protein are randomly chosen, from a normal distribution, for each simulation with the variance being 30%. The mean of the distribution is taken from reported values of the protein concentrations (Ghaemmaghami et al., 2003). Each individual simulation corresponds to an individual cell. See details of parameters used in Table 2.4.

To further convince ourselves that the change in CV was not due to some other, simple, mechanism we investigated several other models including a simple activation cascade including (A) transcription/translation, (B) stabilization/destabilization of Fus3, (C) positive and (D) negative feedback, as described in Figure 2.5. We also simulated a stochastic version of a detailed model of transcriptional regulation downstream of the MAPK (Houser et al., 2012). Crucially, in these models, the cell-to-cell variability of protein concentrations is assumed to be negligible. As seen in Figure 2.5, none of these other models were

able to capture the qualitative behavior of variability in wild type cells over time that we observed. This further strengthens our initial model of variability although we cannot completely rule out some other mechanism completely.

## Table 2.1: Strains used in Chapter II

| Strains | Parent | description |
|---|---|---|
| BY4741 | | MAT**a** *leu2*Δ *met15*Δ *his3*Δ *ura3*Δ |
| BY4742 | | MATα *leu2*Δ *lys2*Δ *his3*Δ *ura3*Δ |
| sst2Δ | BY4741 | *sst2Δ*::KanMX4 |
| gpa1G302S | BY4741 | $gpa1^{G302S}$::*URA3* |
| sst2Q304N | BY4741 | $sst2^{Q304N}$ integrated and 5 FOA selected |
| WT $FUS1_p$GFP $ADH1_p$ mCherry | BY4741 | $FUS1_p$GFP::*HIS3* $ADH1_p$ mCherry::*URA3* |
| *sst2*Δ $FUS1_p$GFP $ADH1_p$ mCherry | BY4741 | *sst2Δ*::KanMX $FUS1_p$GFP::*HIS3* $ADH1_p$mCherry::*URA3* |
| $gpa1^{G302S}$ $FUS1_p$GFP $ADH1_p$ mCherry | BY4741 | $gpa1^{G302S}$::*URA3* $FUS1_p$GFP::*HIS3* $ADH1_p$mCherry::*LEU2* |
| $sst2^{Q304N}$ $FUS1_p$GFP $ADH1_p$ mCherry | BY4741 | $sst2^{Q304N}$ integrated $FUS1_p$GFP::*HIS3* $ADH1_p$ mCherry::*URA3* |
| WT Bem1-GFP | BY4741 | *BEM1*-GFP::*HIS3* |
| *sst2*Δ Bem1-GFP | BY4741 | *sst2Δ*::KanMX4 Bem1-GFP::*HIS3* |
| $gpa1^{G302S}$ Bem1-GFP | BY4741 | $gpa1^{G302S}$::*URA3* Bem1-GFP::*HIS3* |
| $sst2^{Q304N}$ Bem1-GFP | BY4741 | $sst2^{Q304N}$ Bem1-GFP::*HIS3* |

## Table 2.2: Plasmids used in Chapter II

| Name | Description | Source |
|---|---|---|
| pRS406 $gpa1^{(81\text{-}1538)G302S}$ | YIp $Amp^R$ *URA3* $gpa1^{(81\text{-}1538)G302S}$ | (Lambert et al.) |
| pRS406 $sst2^{Q304N}$ | YIp $Amp^R$ *URA3* $sst2^{Q304N}$ | This study |
| pRS423 FUS1-lacZ | 2 µm $Amp^R$ *HIS3 FUS1*-lacZ | (Hoffman et al., 2000) |
| pRS303 FUS1-GFP | YIp $Amp^R$ *HIS3* $FUS1_p$GFP | (Siekhaus and Drubin, 2003) |
| pRS316 ADH1 mCherry | CEN $Amp^R$ *URA3* $ADH1_P$-$ADH1_T$ | This study |
| pRS406 ADH1 mCherry | YIp $Amp^R$ *URA3* $ADH1_P$-$ADH1_T$ | This study |
| pRS405 ADH1 mCherry | YIp $Amp^R$ *LEU2* $ADH1_P$-$ADH1_T$ | This study |

**Table 2.3: Oligonucleotide primer sequences used in Chapter II**

| Name | Sequence 5'-3' |
|---|---|
| sst2 del (F) | GTTATAGGTT CAATTTGGTA ATTAAAGATA GAGTTGTAAG CGTACGCTGCAGGTCGAC |
| sst2 del (R) | GTGCAATTGTACCTGAAGATGAGTAAGACTCTCAATGAAA ATCGATGAATTCGAGCTCG |
| sst2 (F) | ATGC**GGATCC**GTGCTTATAA CTTTAAGAAA AACCAGCGTC |
| sst2 (R) | ATGC**GGTACC**ATGAATGAATTTGCGTTCAATCCC |
| sst2-Q304N(F) | TTACAACAAAGGCTATATGG***AAC***TGGATAATGGACTGTACTGAT |
| sst2-Q304N(R) | ATCAGTACAGTCCATTATCCA***GTT***CCATATAGCCTTTGTTGTAA |
| mCherryMega (F) | CAAGCTATACCAAGCATACAATCAACTatggtgagcaagggcgaggagg |
| mCherryMega (R) | GGCGAAGAAGTCCAAAGCTCTGGCGttacttgtacagctcgtccatgccgc |
| mCherry406 (F) | CCCCC**CTCGAG**GTCGACGGTATCGATAAGCgggaacaaaagctggtaccaagcttagatcc |
| mCherry406 (R) | CAAAAGCTG**GAGCTC**CACCGCGGTGGCGGCCGCgatccgtgtggaagaacgattacaacagg |
| ADH1_xhoI (F) | ATG C**CT CGA G**GA AGG TGA GAC GCG CAT AAC CGC |
| ADH1_SacI (F) | GAC T**GA GCT C**AT CCG TGT GGA AGA ACG ATT ACA ACA GG |
| Bem1His (F) | TGTCTGAGGAAGAGTTAGAAA |
| Bem1His (R) | AGTATCTTTGGGCTGCGGTTA |

* Red sequence binds pFA6-KanMX. Lower case binds mCherry and upper case binds pRS316ADH1. Restriction enzyme sites are indicated in bold letters.

## Table 2.4: Model parameter values and reactions

| Parameter Name | Description | Best Value | Mean in random search | Reaction |
|---|---|---|---|---|
| k0 | Dissociation of Gβγ from Gα: Pheromone dependent input | 3 e-4 1/sec | 2e-3 1/sec | Gαβγ -> Gβγ + Gα |
| k1 | Fus3 dependent transcription | 8.2e-6 1/sec | 2 e-05 1/sec | P-Fus3 -> P-Fus3 + mRNA |
| k10 | Fus3 independent transcription | 0.0013 1/sec | 2e-3 1/sec | -> mRNA |
| k2 | Translation rate | 0.004 1/sec | 1.5e-3 1/sec | mRNA -> mRNA + GFP |
| ka | Activation/phosphorylation rate of Fus3. Dependent on Gβγ | 7.6e-4 (1/sec*molec) | 5e-3 1/(sec*molec) | Fus3 + Gβγ -> P-Fus3 + Gβγ |
| r0 | Sst2 dependent association of Gα, Gβγ | 4 (1/sec*molec) | 5 (1/sec*molec) | Sst2 + Gβγ + Gα -> Sst2 + Gαβγ |
| r0b | Sst2 independent association of Gα, Gβγ | 0.004 (1/sec*molec) | .005 1/(sec*molecule) | Gβγ + Gα -> Gαβγ |
| r1 | Degradation rate of mRNA | 0.0017 1/sec | 0.0017 1/sec | mRNA |
| r2 | Degradation rate of GFP | 1.6e-04 1/sec | 1.6e-04 1/sec | GFP -> |
| ra | Deactivation /de-phosphorylation rate of P-Fus3 | 0.11/(sec* molec) | 0.1 1/(sec*molec) | P-Fus3 -> Fus3 |
| Total Fus3 | | 8000 molec/cell | 8000 molec/cell | *Source: (Ghaemmaghami et al., 2003) |
| Total G protein | | 8000 molec/cell | 8000 molec/cell | |

# CHAPTER III

## Gα Endocytosis by a Cascade of Ubiquitin Binding Domain Proteins is Required for Sustained Morphogenesis and Proper Mating in Yeast [*,◦]

Heterotrimeric G proteins are well known to transmit signals from cell surface receptors to intracellular effector proteins. There is growing appreciation that G proteins are also present at endomembrane compartments, where they can potentially interact with a distinct set of signaling proteins. Here, we examine the cellular trafficking function of the G protein $\alpha$ subunit in yeast, Gpa1. Gpa1 contains a unique 109 amino acid insert, within the α-helical domain, that undergoes a variety of posttranslational modifications. Among these is monoubiquitination, catalyzed by the NEDD4 family ubiquitin ligase Rsp5. Using a newly optimized method for G protein purification, together with biophysical measures of structure and function, we show that the ubiquitination domain does not influence enzyme activity. By screening a panel of 39 gene deletion mutants, each lacking a different ubiquitin-binding domain protein, we identify seven that are necessary to deliver Gpa1 to the

[*] Elements of the work referenced in this chapter have been submitted for publication: Dixit G*, Baker, RA*, Sachs CM, Torres MP and Dohlman HG. (2014). Gα Endocytosis is Required for Sustained Cellular Morphogenesis in Yeast (* equal contribution).

◦ Figures 3.1, 3.2, 3.7 *D* and Table 3.4, contributed by Rachael Baker. Figures 3.3, 3.6, 3.7A, 3.7B 3.7C, 3.8 contributed by Gauri Dixit. Figure 3.4 jointly contributed by Gauri Dixit, Carly Sachs and Mathew P Torres

vacuole compartment including four proteins (Ede1, Bul1, Ddi1 and Rup1) previously not known to be involved in this process. Finally, we show that proper endocytosis of the G protein is needed for sustained cellular morphogenesis and mating in response to pheromone stimulation. We conclude that a cascade of ubiquitin-binding proteins serves to deliver the G protein to its final destination within the cell. In this instance, and in contrast to the previously characterized visual system, endocytosis from the plasma membrane is needed for proper signal transduction rather than for signal desensitization.

**Introduction**

Gα proteins are enzymatic switches that are part of a multi-component signaling complex. The complex typically consists of a seven transmembrane G protein coupled receptor (GPCR), a guanine nucleotide binding protein (Gα) and an associated dimer consisting of β and γ subunits (Gβγ) (Sprang, 1997). Signaling is turned on and off based on receptor activation, which in turn dictates the nucleotide-bound state of the Gα protein. When Gα is GDP-bound, Gβγ is sequestered and signaling pathways are off (Sprang, 1997). When Gα releases GDP and binds GTP, Gβγ dissociates and the signaling pathways are turned on. Subsequent GTP hydrolysis is accelerated by regulators of G protein signaling (RGS proteins) (Berman et al., 1996; Kleuss et al., 1994; Ross and Wilkie, 2000; Siderovski and Willard, 2005). Large Gα proteins contain a Ras-like domain as well as an independently folded α-helical domain (Sprang, 1997). Within this group of proteins there is a well-established role for the Ras-like domain in specifying interactions with

Gβγ, effectors and RGS proteins (Coleman et al., 1994; Siderovski and Willard, 2005; Sprang, 1997). However, recent evidence has shown that the α-helical domain is also important for signal modulation (Dohlman and Jones, 2012). Accordingly, structure determinations have revealed differences in the α-helical domain of $G\alpha_i$ when bound to GDP and GTPγS (Mixon et al., 1995; Van Eps et al., 2011; Westfield et al., 2011).

Apart from the regulation of GTP binding and hydrolysis, G proteins are regulated by targeted delivery to subcellular compartments (Wedegaertner, 2012). G protein trafficking can be either constitutive or stimulus dependent. Stimulus-dependent movement of Gα and Gβγ to various endomembrane compartments has been observed in several systems including the visual system in drosophila and mammals (Frechter et al., 2007; Wedegaertner, 2012) as well as certain non-visual systems (Chisari et al., 2007; Wedegaertner et al., 1996). In the yeast *Saccharomyces cerevisiae,* the Gα Gpa1 is constitutively trafficked to endosomes, where it binds to and activates a phosphatidylinositol 3-kinase, as well as to the vacuole, where the protein is eventually degraded (Backer, 2008; Slessareva et al., 2006). More recently, work by Irannejad et al. demonstrated that mammalian $G\alpha_s$ is present and active at the endosomal membrane as well as at the plasma membrane (Irannejad et al., 2013; Murphy et al., 2009). However, the functional importance of Gα trafficking is not well-established (Wedegaertner, 2012).

In order to fully understand the consequences of G protein trafficking, we must first understand how such trafficking events are regulated. Much of the spatial control of GPCRs and G proteins is dependent upon post-translational modification

by monoubiquitination. For example, the yeast Gβ (Ste4) and GPCR (Ste2) are monoubiquitinated after stimulation with the mating pheromone α-factor (Hicke, 1999; Hicke and Riezman, 1996; Zhu et al., 2011). Both proteins are subsequently removed from the plasma membrane and delivered to the vacuole (Hicke, 1999; Shaw et al., 2001; Zhu et al., 2011). For Ste2 this process is mediated in part by endocytic adaptor proteins containing a ubiquitin binding domain (UBD) (Shih et al., 2000; Sloper-Mould et al., 2001). Although structurally diverse, UBDs share the ability to bind non-covalently to ubiquitin-conjugated substrates and serve to transport monoubiquitinated proteins through the various stages of endocytosis (Husnjak and Dikic, 2012). While the general process of monoubiquitination-mediated endocytosis is well understood, questions remain concerning the specific protein components that are important for trafficking of the G protein.

The yeast model system, in which many ubiquitination and cellular trafficking components were originally identified, can facilitate understanding of the interconnections between G protein signaling, monoubiquitination and trafficking (Dohlman and Thorner, 2001; Wang and Dohlman, 2006). Pheromone binds to Ste2, which is coupled to Gpa1 (Gα) and Ste4/Ste18 (Gβγ). When Gα is activated, Gβγ dissociates and stimulates a kinase cascade leading to activation of the yeast MAPK Fus3. A second branch of the pathway leads to activation of a Rho family GTPase, Cdc42 (Dohlman and Thorner, 2001). Together these processes result in cell cycle arrest, new gene transcription, and morphological changes that facilitate mating (Dohlman and Thorner, 2001). Pheromone pathway signaling is attenuated by the pheromone-dependent monoubiquitination and endocytosis of the GPCR Ste2

(Hicke and Riezman, 1996). As with the receptor, monoubiquitination leads to the endocytosis and eventual vacuolar degradation of Gpa1 (Torres et al., 2009b). In contrast to Ste2, monoubiquitination of Gpa1 is not dependent on pheromone stimulation. Both proteins are monoubiquitinated by the same ubiquitin ligase, Rsp5 (Dunn and Hicke, 2001; Torres et al., 2009b).

While the Ras-like and α-helical domains are highly conserved across species, Gpa1 possesses a unique 109 amino acid insert (ubiquitination domain (UD)) within the α-helical domain. The UD contains the known sites of phosphorylation as well as the primary residue for both monoubiquitination and polyubiquitination (Cappell et al., 2010; Marotti et al., 2002). Given that the α-helical domain modulates the activity of some G proteins, we considered whether the UD could influence the activity as well as the cellular distribution of Gpa1. Here we show that the UD does not influence G protein catalytic activity or downstream MAPK signaling, but is needed for proper trafficking of Gpa1 to the vacuole. Our screen of 39 gene deletion mutations revealed seven UBD-containing proteins that are required for Gpa1 trafficking. Four of these proteins are required for trafficking of Gpa1 but not Ste2, thus demonstrating that constitutive endocytosis of these proteins occurs by distinct mechanisms. Finally, we show that Gα endocytosis from the plasma membrane is required for sustained cellular morphogenesis and efficient mating.

## Results

**Structural contributions of the ubiquitination domain to Gpa1.** Gpa1 is

distinct from other Gα proteins because of the UD. A comparison of available genome sequences shows that the UD is found among *Saccharomycotina*, but is not present in other eukaryotes (Figure 3.1 *A*). Based on sequence alignment with Gα proteins, the ubiquitination domain is at the end of the A/B helix in the α-helical domain (Figure 3.1*B*). Previous analysis has shown that the UD is the site of post-translational modifications including phosphorylation, monoubiquitination and polyubiquitination (Li et al., 2007; Marotti et al., 2002; Torres et al., 2011).

In order to be modified, amino acids must be accessible to the modifying enzyme. The ability to modify a given amino acid requires that the residue be present at the surface of the protein or in a region lacking secondary structure. Indeed, phosphorylation and ubiquitination often occur on intrinsically disordered regions of proteins (Predrag et al., 2010). Therefore, we postulated that the UD is without substantial secondary structure. To test our hypothesis we employed a series of biophysical measurements of protein conformation. First, we used circular dichroism to determine the contribution of the UD to the secondary structure content of Gpa1. This analysis revealed no difference between Gpa1 with or without the UD (Figure 3.1*C*). Precise removal of the UD resulted in expression comparable to that of the full length protein, whereas removing just one additional amino acid abolished expression entirely. We infer that the UD does not contribute to the structure of the adjoining helical domain.

Figure 3.1

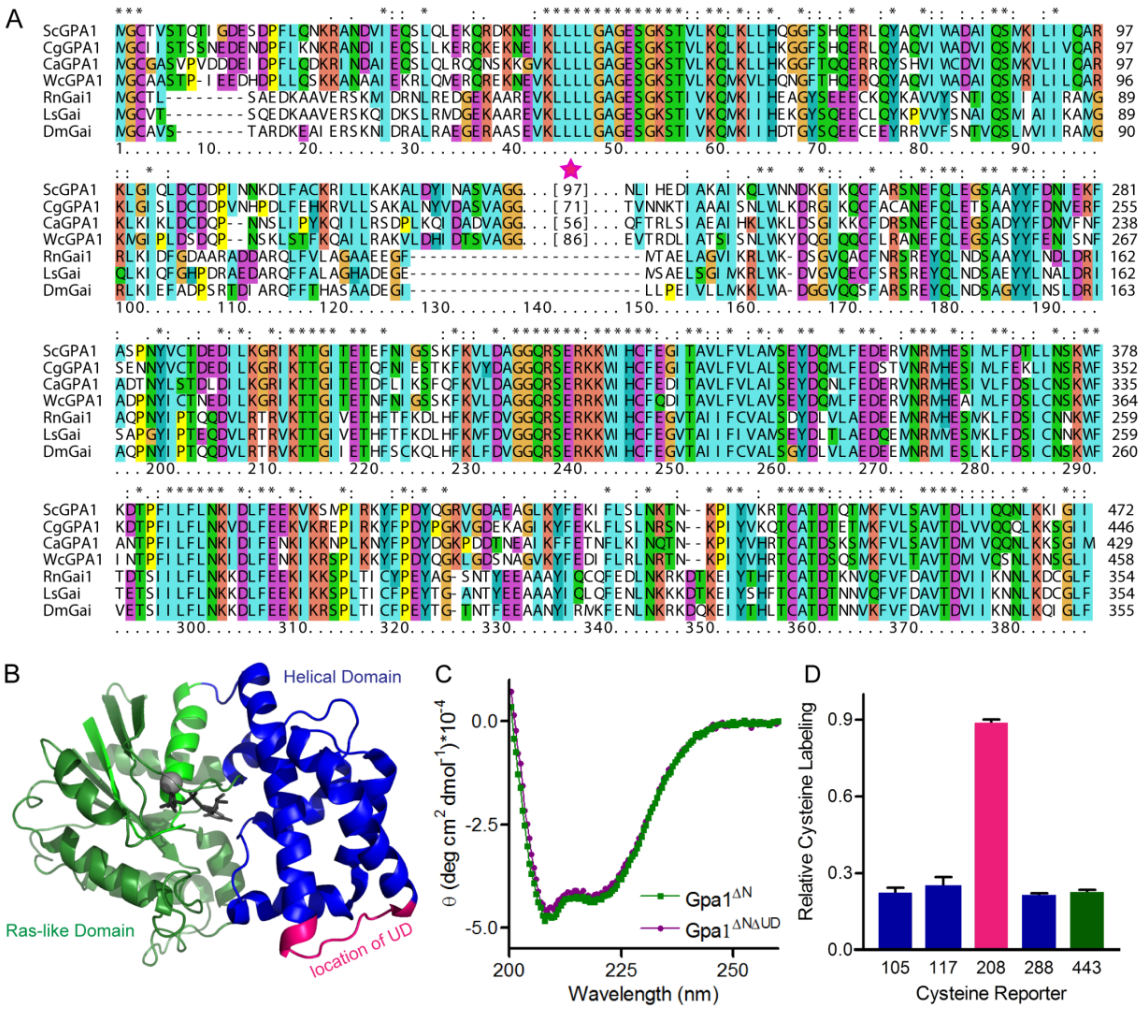


**Figure 3.1 Conservation of the ubiquitination domain.**

(A) Sequence alignment of Gpa1-like Gα proteins from yeast *Saccharomyces cerevisiae* (Sc), other *Saccharomycotina* (*Candida glabrata* (Cg), *Candida albicans* (Ca), *Wickerhamomyces ciferrii* (Wc)) as well as $G\alpha_i$ from rat (*Rattus norvegicus* (Rn)), snail (*Lymnaea stagnalis* (Ls)) and fruit fly (*Drosophila melanogaster* (Dm)).

(B) Structure of $G\alpha_i$ (PDB: 1GIA) showing the location of the Gpa1 ubiquitination domain (magenta) based on the sequence alignment. The Ras-like domain is shown in green and the α-helical domain is shown in blue. Magnesium and GTP analog shown in grey.

(C) Secondary structure content of $Gpa1^{\Delta N}$ and $Gpa1^{\Delta N\Delta UD}$ measured by circular dichroism.

(D) Relative labeling of five cysteines in GTPγS-bound Gpa1. Results are the mean ± SEM. Coloring according to that used in (B).

To further assess whether the UD contains unfolded regions, we asked whether resident cysteines were especially accessible to labeling with a small modifier 4-fluoro-7-aminosulfonylbenzoflurazan (ABD-F) (Isom et al., 2013). Gpa1 is an ideal candidate for this method because it contains cysteines dispersed throughout the protein. There are two in the Ras-like domain (Cys333 and Cys443), four in the helical domain (Cys105, Cys117, Cys258, and Cys288) and one in the UD (Cys208). Using this method, we detected ABD-F labeling for five of the seven cysteines. As seen in Figure 3.1*D*, cysteines within the well-folded helical domain are highly protected, while the cysteine in the UD is highly exposed (value close to one). These results are consistent with the circular dichroism data suggesting that the UD lacks secondary structure. Taken together, our results are consistent with the hypothesis that the UD is an evolutionarily unique, structurally distinct, and largely unstructured domain.

**Functional contributions of the ubiquitination domain to Gpa1 activity.** The α-helical domain is known to be influence G protein nucleotide exchange activity (Jones et al., 2012). The UD is adjacent to the A/B helix of the helical domain - a region whose dynamics were previously shown to promote the rapid, receptor-independent, nucleotide exchange activity of *A. thaliana* Gpa1 (Jones et al., 2012). However, it is not known whether the UD regulates the enzymatic activity of *S. cerevisiae* Gpa1. To address this question we used the cysteine reactivity method to measure the thermal stability of Gpa1 in the presence and absence of the UD. As shown in Figure 3.2 *A*, removing the ubiquitination domain did not alter Gpa1 thermal stability, despite the loss of 109 amino acids. We then measured the ability

of guanine nucleotides to bind Gpa1 in the presence and absence of the UD. For these experiments we used the fluorescent nucleotide analog MANT-GDP. The rate of nucleotide exchange was measured as a loss of fluorescence over time as Gpa1 released MANT-GDP and bound unlabeled GDP, added in excess. As shown in Figure 3.2 *B*, the rate of nucleotide dissociation was not altered by the absence of the UD. Finally we measured the rate of GTP hydrolysis using a method that monitors a nucleotide-dependent change in the intrinsic fluorescence of Gpa1 (Higashijima et al., 1987). Using this assay, we observed similar rates of GTP hydrolysis in the presence and absence of the UD (Figure 3.2 *C*). Together, these data suggest that the UD does not alter the structure or enzymatic activity of Gpa1.

**A cascade of Ubiquitin Binding Domain (UBD) proteins transport Gpa1 to the vacuole***.* The data presented above indicate that the UD does not directly contribute to the structure and enzymatic function of Gpa1. However the UD functions as a site of phosphorylation, polyubiquitination (for targeting to the proteasome) and monoubiquitination (for trafficking to the vacuole). Gpa1 is monoubiquitinated by the Rsp5 ubiquitin ligase (Wang et al., 2005). However, the proteins involved in Gpa1 endocytosis, and specifically those that recognize monoubiquitin within the UD, are not known. Accordingly, we embarked on a search for proteins that recognize the monoubiquitinated form of Gpa1.

Monoubiquitin-mediated trafficking pathways are often comprised of ubiquitin binding domain (UBD) containing proteins (Hurley and Stenmark, 2011). In most cases, multiple UBD-containing proteins are involved in the passage of a monoubiquitinated protein to its final destination (Husnjak and Dikic, 2012).

Figure 3.2

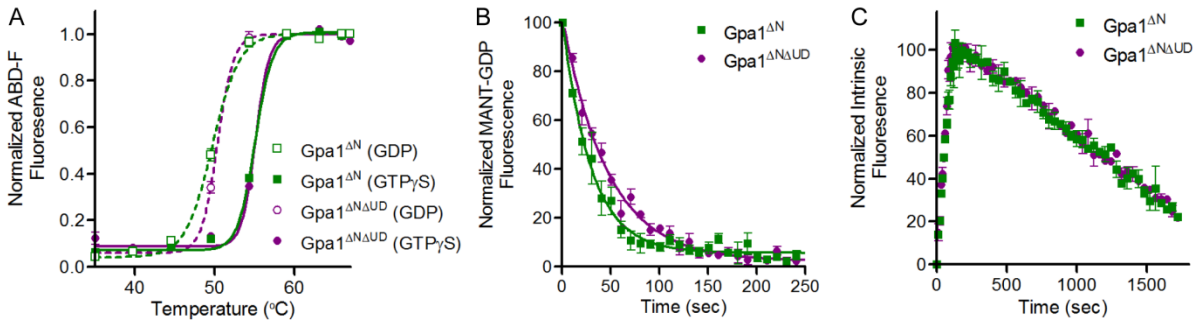


**Figure 3.2 The ubiquitination domain does not contribute to Gpa1 activity**.
(A) Thermal stability of Gpa1$^{\Delta N}$ and Gpa1$^{\Delta N\Delta UD}$ measured by ABD-F labeling and fQCR. Data are normalized to the maximum fluorescence intensity for each curve and results are the mean ± SEM (n=4).
(B) Intrinsic nucleotide dissociation rates for Gpa1$^{\Delta N}$ and Gpa1$^{\Delta N\Delta UD}$ pre-loaded with MANT-GDP. The rate of GDP dissociation was monitored as a decrease in MANT-GDP fluorescence upon the addition of unlabeled GDP. Data are fit to an exponential dissociation curve. Results are the mean ± SEM (n=3).
(C) Intrinsic tryptophan fluorescence measure of GTP binding and hydrolysis for Gpa1$^{\Delta N}$ and Gpa1$^{\Delta N\Delta UD}$. Data are normalized to the maximum signal achieved in each experiment upon completion of binding. Results are the mean ± SEM (n=3).

Moreover, the route of endocytosis appears to be dictated in part by the identity of the monoubiquitinated protein (Husnjak and Dikic, 2012). Numerous UBDs have been previously defined (Hicke et al., 2005) and are now included in the protein descriptions found in the Saccharomyces Genome Database (SGD; www.yeastgenome.org). Using UBD proteins known at the start of this project, we screened a comprehensive set of gene deletion strains for endocytosis and trafficking defects affecting the delivery of Gpa1 from the plasma membrane to the vacuole. Since Gpa1 and Ste2 are targeted for internalization by the same ubiquitin ligase, we also examined trafficking of Ste2, with the expectation that both proteins share the same trafficking machinery components. Accordingly, we monitored the localization of GFP-tagged Gpa1 (Gpa1-GFP, Green) and Ste2 (Ste2-GFP) in a total of 39 UBD deletion strains (Dikic et al., 2009; Winzeler et al., 1999). Gpa1-GFP was introduced by homologous recombination at the *PEP4* locus, thereby inactivating the master vacuolar protease (*pep4Δ*) and preserving the GFP signal after delivery to the vacuole (Wang et al., 2005). Ste2-GFP was expressed from the native *STE2* locus.

As a proof of concept we first monitored GFP localization in the absence of Vps23, Vps27, Vps9, or Rpn10. Major trafficking defects were observed for both Gpa1-GFP and Ste2-GFP in the absence of Vps23 or Vps27, two known components of the ESCRT (Endosomal Sorting Complexes Required for Transport) machinery (Figure 3.3) (Hurley, 2010; MacGurn et al., 2012). Trafficking defects were also observed for Ste2-GFP following deletion of Vps9, a protein required for efficient endocytic trafficking of proteins (Donaldson et al., 2003). Finally, deletion of

Figure 3.3

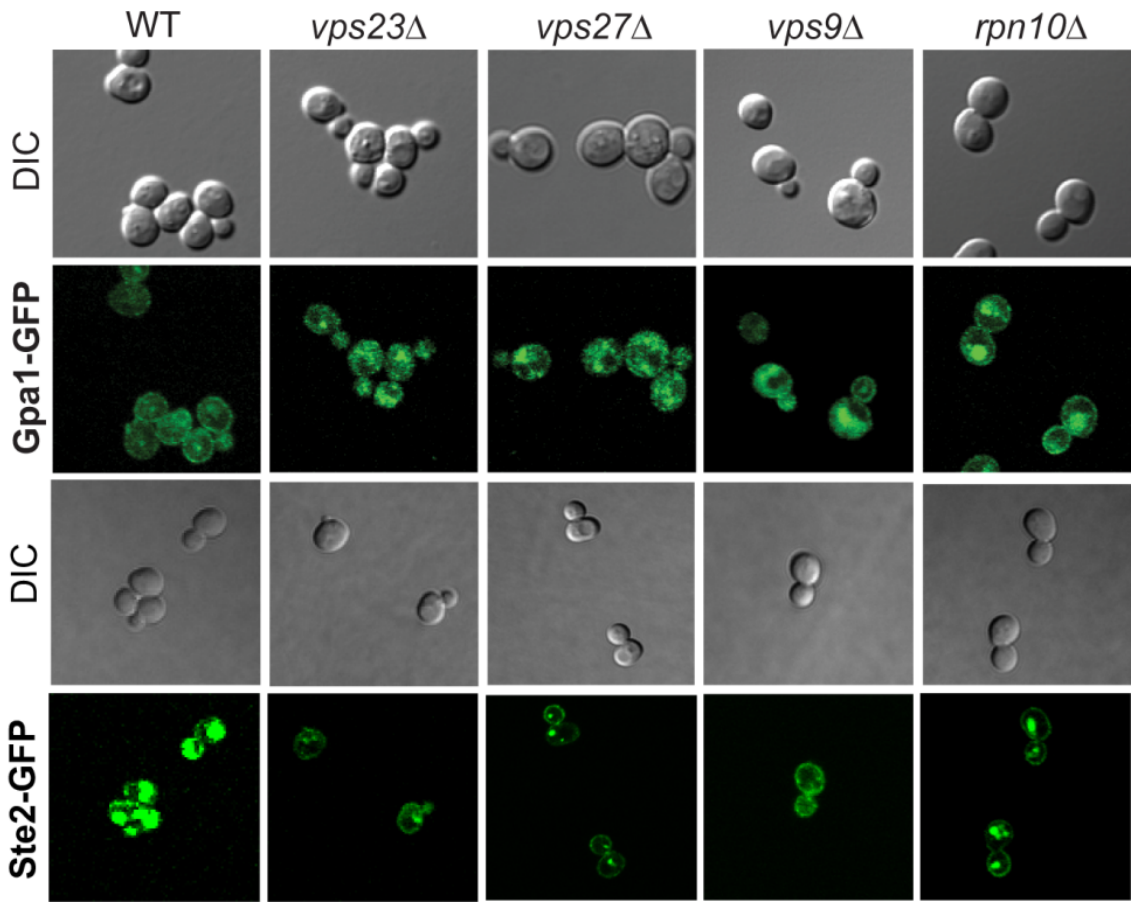


**Figure 3.3 Vacuolar protein sorting complex proteins that disrupt trafficking of Gpa1 and Ste2.**
Differential interference contrast (DIC) and GFP images showing Gpa1-GFP and Ste2-GFP in the absence of ESCRT (Endosomal Sorting Complexes Required for Transport) complex proteins Vps23 and Vps27; only Ste2-GFP trafficking is disrupted in the absence of Vps9. Trafficking of neither Gpa1 nor Ste2 is affected in the absence of the polyubiquitin binding proteasomal protein (*rpn10*Δ).

the polyubiquitin binding proteasomal protein Rpn10 did not affect trafficking of the receptor or G protein (Figure 3.3), indicating that the screen specifically monitors the fate of monoubiquitinated proteins.

Having validated the screening approach, we conducted a more comprehensive screen of the known UBD-containing proteins in yeast (Figure 3.4 *A*). Our general strategy was to look for UBD mutants that prevent accumulation of GFP in the vacuole. As shown in Figure 3.4 *B*, vacuoles were visualized by pulse-staining with an amphiphilic styryl dye (FM4-64, Red), which initially incorporates into the plasma membrane and gradually accumulates in the lumen of the vacuole (Betz et al., 1996). In wild type cells Gpa1-GFP was present at the plasma membrane but not in vacuoles, consistent with our previous findings (Wang et al., 2005) (Figure 3.4 *B*, left panel). In *pep4*Δ cells Gpa1-GFP accumulated in the vacuole, indicative of monoubiquitin-dependent vacuolar translocation (Figure 3.4 *B*, middle panel). Of the 39 UBD deletion strains tested, seven exhibited Gpa1-GFP mislocalized to puncta within the cytoplasm (Figure 3.4 *B*, right panel). Major trafficking defects were observed in the absence of Vps36, a component of the ESCRT machinery (Hurley, 2010). Additionally, defects in Gpa1 localization were seen upon deletion of the following: Bul1, the ubiquitin binding component of the Rsp5 ubiquitin ligase (Yashiroda et al., 1996); Ede1, a component of the early endocytic machinery (Gagny et al., 2000); Ddi1, a DNA damage inducible v-SNARE binding protein regulating exocytosis (Liu and Xiao, 1997); and Rup1, a regulator of Rsp5 (Lam and Emili, 2013) (Figure 3.4 *C*) Defects in Ste2-GFP trafficking were likewise observed in the absence of Vps36. However, three of the UBD deletions

Figure 3.4

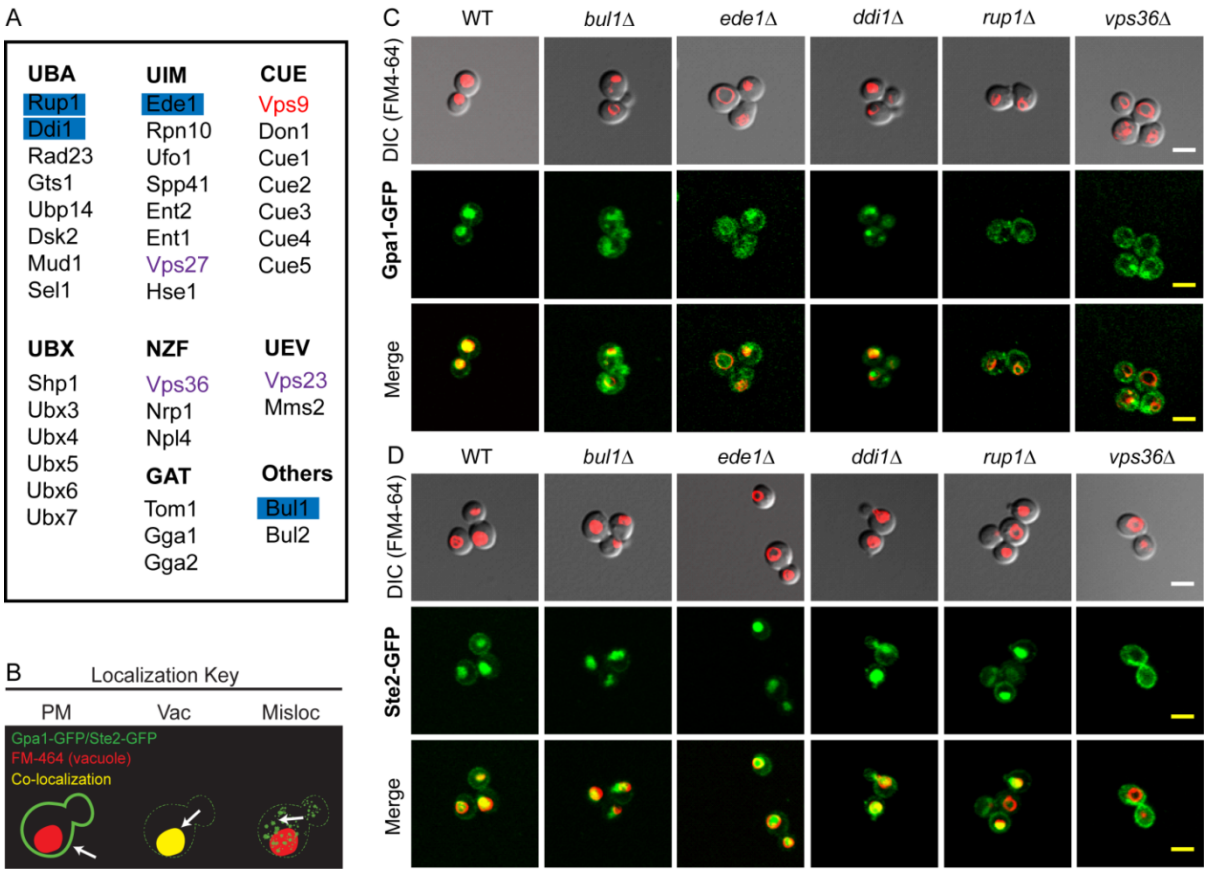


**Figure 3.4 Screen for Gpa1 translocation mutants identifies components of the endocytosis and vacuolar trafficking machinery**

(A) Table of all UBD-containing proteins screened. Proteins are sorted by the type of UBD they contain: UBA, ubiquitin associated; UIM, ubiquitin interacting motif; CUE, coupling of ubiquitin conjugation to endoplasmic reticulum; UBX, ubiquitin regulatory X; NZF, Npl4 zinc finger; GAT, [GGA(Golgi localized, gamma-ear containing) ADP-ribosylation factor-binding protein, and TOM (target of Myb)]; UEV, ubiquitin-conjugating enzyme E2 variant.

(B) General scheme of the genetic screen to identify binding partners of Gpa1-ubiquitin. A total of 39 deletion mutants, each lacking a specific ubiquitin-binding domain-containing (UBD) protein, were separately transformed with plasmids encoding either Gpa1-GFP (pRS406-GPA1-GFP) or Ste2-GFP (pRS406-STE2-GFP). Gpa1 and Ste2 localization was monitored by DIC and fluorescence microscopy, in the presence of a vacuolar dye (red, FM4-64). In the absence of endocytosis the proteins are retained at the plasma membrane (green, left panel). Following delivery to the vacuole (Vac), the proteins colocalize with FM4-64 (yellow, middle panel). If trafficking is disrupted at any point, the proteins are mislocalized (Misloc) to puncta in the cytoplasm (right panel). Microscopy of mutants that mislocalized Gpa1-GFP (C) but not Ste2-GFP (D). Mutant *vps36*Δ is shown as an example of a UBD that affects trafficking of both Gpa1 and Ste2. Scale bar, 5 μm.

that affected Gpa1 trafficking had no effect on Ste2 endocytosis (Figure 3.4 *D*). In total, we identified seven UBD proteins necessary for proper vacuolar delivery of Gpa1 (Figures 3.3 and 3.4). Deletion of four of these proteins disrupted trafficking of Gpa1 but not Ste2, indicating that the trafficking pathways for these proteins are largely distinct.

**Gpa1 is delivered to the plasma membrane in the absence of UBD proteins involved in endocytosis.** Having identified mutants that alter the cellular distribution of Gpa1, we next considered whether the defect was due to removal from, or delivery to, the plasma membrane. That is, Gpa1 mislocalization could be caused by impaired synthesis, maturation or delivery to the plasma membrane. To rule out this possibility we compared the localization of Gpa1 with that of Gpa1$^{\Delta UD}$, which in wild type cells is delivered to the plasma membrane but not the vacuole (Wang et al., 2005). For all the UBD mutants tested, we found that *gpa1*$^{\Delta UD}$-GFP was localized normally to the plasma membrane (Figure 3.5). These data indicate that the UBD-containing proteins identified in our screen are specifically required for trafficking of monoubiquitinated Gpa1 from the plasma membrane to the vacuole.

**Disruption of Gpa1 Trafficking Promotes Accumulation of Ubiquitinated Gpa1.** Post- translational modification by monoubiquitination and polyubiquitination are used to regulate the quantity of Gpa1 present at the plasma membrane. Whereas monoubiquitinated Gpa1 is delivered to the vacuole where it is eventually degraded, polyubiquinated Gpa1 is recruited to the proteasome where it is likewise degraded. We reasoned that disruption of Gpa1 trafficking might allow the monoubiquitinated protein to accumulate and perhaps undergo additional rounds of

Figure 3.5

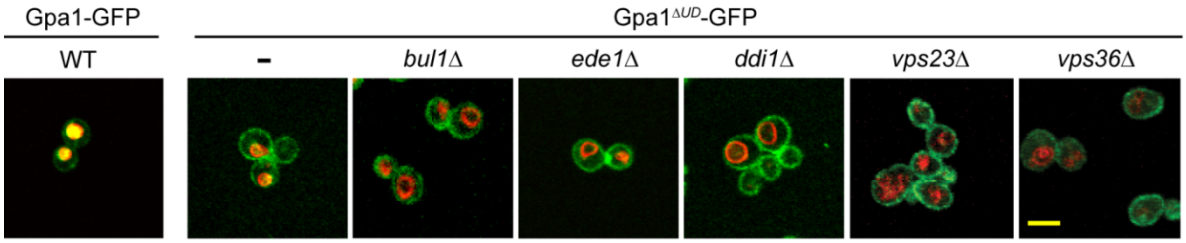


**Figure 3.5 Components of the Gpa1 trafficking machinery do not affect delivery of Gpa1 to the plasma membrane.**
Microscopy of full length Gpa1-GFP or Gpa1 lacking the ubiquitination domain (Gpa1$^{\Delta UD}$ – GFP) in the presence (WT) or absence (*bul1*Δ, *ede1*Δ, *ddi1*Δ, *vps36*Δ ,*vps23*Δ) of the indicated UBD proteins. Vacuoles are stained with FM4-64. Scale bar, 5μm. Despite repeated attempts, we were unable to delete *RUP1* in the *gpa1*$^{\Delta UD}$ background.

ubiquitination. To test our hypothesis we monitored the level of Gpa1 ubiquitination in the four UBD deletion mutants that exhibited trafficking defects for Gpa1 (but not Ste2). In order to visualize the rare monoubiquitinated species we overexpressed Gpa1 using a multi-copy plasmid (Torres et al., 2009). As expected we observed an increase of monoubiquitinated Gpa1 in three of the four UBD deletions (*ede1*Δ*, ddi1*Δ and *rup1*Δ). The increase was similar to that seen upon deletion of *PEP4* (Torres et al., 2009a) consistent with a defect in vacuolar degradation of Gpa1 (Figure 3.6). Additionally, we observed an increase in polyubiquitinated Gpa1, particularly upon deletion of *EDE1* (Figure 3.6). The increase in monoubiquitinated Gpa1 was not due to an overall increase in the amount of loaded substrate protein, as evident from shorter exposures of the blot. These data suggest that disruption of Gpa1 trafficking slows the clearance of monoubiquitinated Gpa1 and drives the system towards polyubiquitination (Torres et al., 2009).

**Retention of Gpa1$^{\Delta UD}$ at the plasma membrane inhibits proper morphogenesis and mating.** Previous studies revealed that persistent GTP-activation leads to an accumulation of Gpa1 at endosomes (Slessareva et al., 2006). Conversely, removal of the UD leads to an accumulation of Gpa1 at the plasma membrane (Wang et al., 2005). With the availability of the Gpa1$^{\Delta UD}$ mutant, as well as UBD mutants that disrupt translocation of the wild type protein, we have the ability to study the functional consequences of Gpa1 trafficking without the confounding effects of altered GTPase activity. Accordingly, we compared the pheromone response in wild type cells and mutants defective in Gpa1 trafficking, using MAPK activation and transcription reporter assays described previously

Figure 3.6

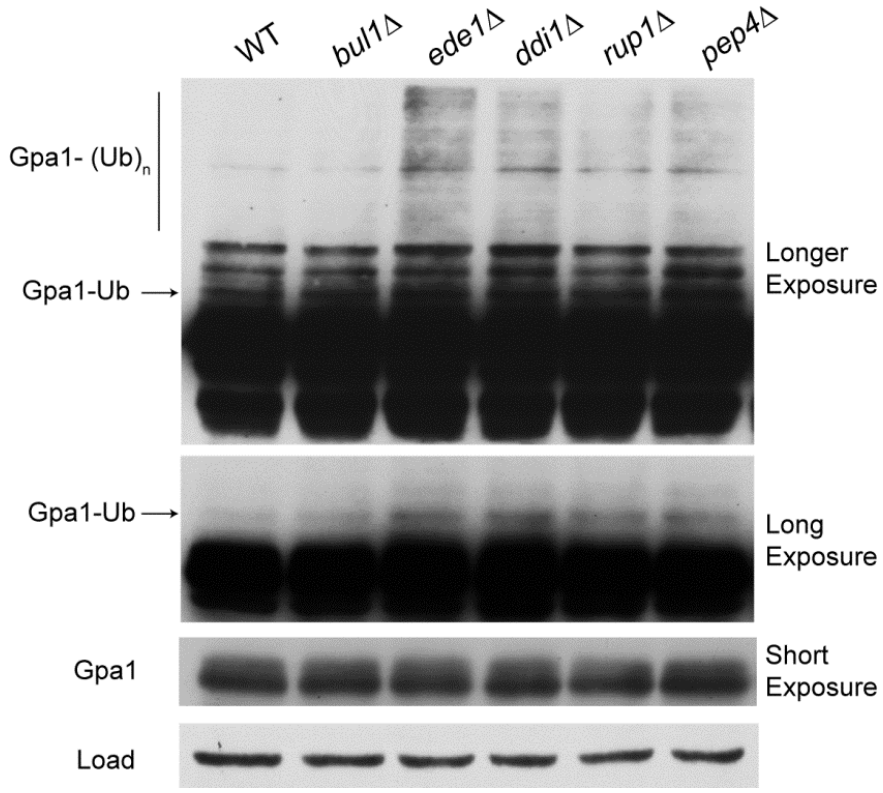


**Figure 3.6 Disruption of Gpa1 trafficking leads to accumulation of ubiquitinated Gpa1.** Gpa1 was overexpressed (pAD4M-GPA1) in the presence (WT) or absence (*bul1*Δ, *ede1*Δ, *ddi1*Δ, *rup1*Δ, and *pep4*Δ) of the indicated proteins and analyzed by immunoblotting with Gpa1 antibodies. Uppermost panels are identical except for exposure time. Bottom, immunoblotting with G6PDH antibodies (load) as a control.

(Clement et al., 2013). In the case of Gpa1$^{\Delta UD}$, we replaced the wild type gene with the UD mutant via PCR-mediated integration. This was done at the endogenous *GPA1* locus so as to maintain proper G protein expression and subunit stoichiometry. As shown in Figure 3.7 *A*, there was no significant change in MAPK activation in the UBD mutants (*bul1*Δ, *ede1*Δ*, ddi1*Δ and *rup1*Δ) when compared to wild type cells. Furthermore, we observed no significant differences when comparing the Gpa1$^{\Delta UD}$ mutant and wild type protein. Similarly, we observed only modest differences in the pheromone transcription response (Figure 3.7 *B*). Taken together, these data indicate that the MAPK branch of the pheromone pathway is unaffected by the trafficking-deficient mutants.

In addition to the MAPK and transcription response, the pheromone pathway has a second branch that activates the small G protein Cdc42. Active Cdc42 promotes polarization and morphogenesis to facilitate mating (Pruyne and Bretscher, 2000). We therefore asked whether defects in Gpa1 trafficking had any effect on cellular morphogenesis (shmoo formation). We monitored each mutant in a microfluidic chamber with constant pheromone stimulation, as previously described (Clement et al., 2013). At a saturating concentration of pheromone, wild type cells can form up to three mating projections. As shown in Figure 3.7 *C* there were no differences between wild type and *bul1*Δ*, ddi1*Δ or *rup1*Δ mutants. Cells lacking Ede1 did exhibit an increased number of projections, as compared to wild type, but this same phenotype was evident in an *ede1*Δ *gpa1*$^{\Delta UD}$ double mutant, indicatingF that the *ede1* phenotype is not the result of impaired Gpa1 trafficking (Figure 3.7 *C*). In contrast to all of the other strains tested, cells that express *gpa1*$^{\Delta UD}$ were able to

Figure 3.7

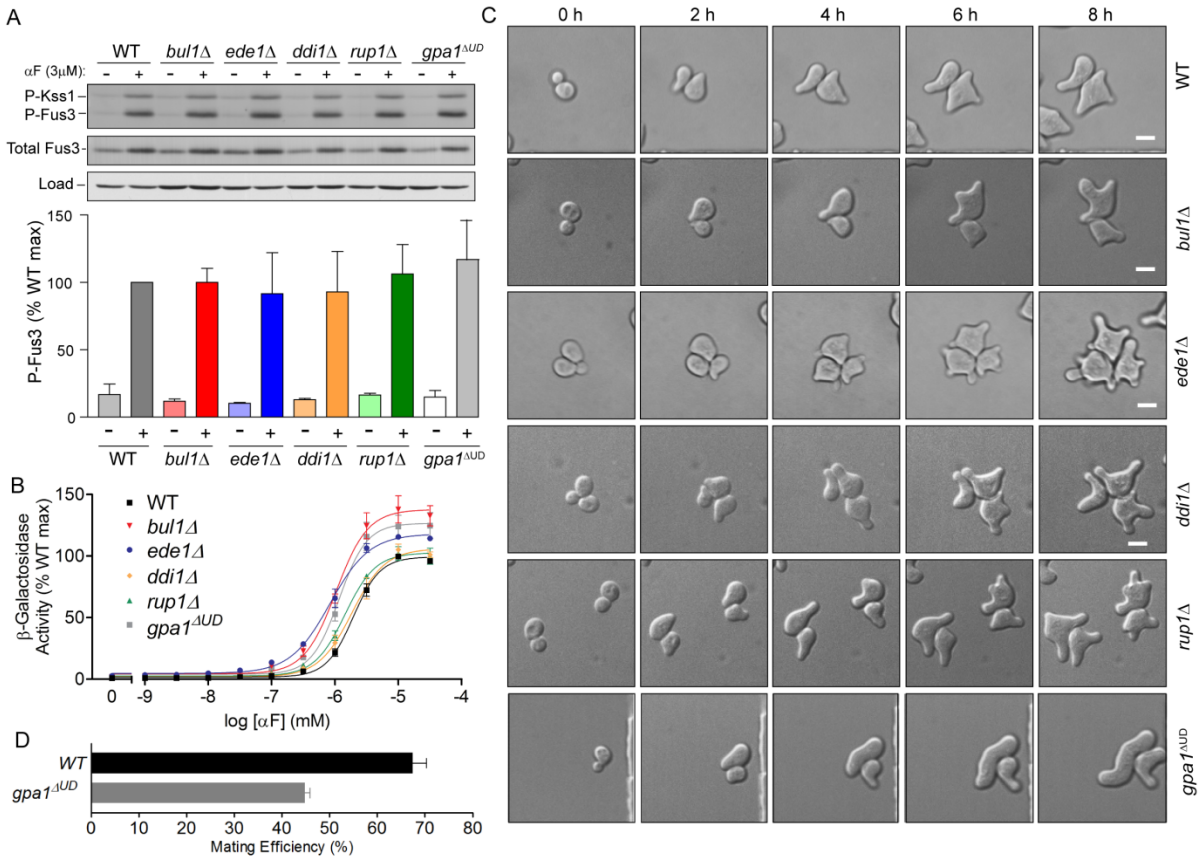


**Figure 3.7 Proper endocytosis of Gpa1 is required for sustained morphogenesis and efficient mating.**

(A) MAPK activation profiles. Wild type (WT) cells, *bul1*Δ, *ede1*Δ, *ddi1*Δ, *rup1*Δ and *gpa1*$^{\Delta UD}$ were either left untreated or treated with 3 μM α factor (αF) for 30 min. MAPK activation was determined by immunoblotting with phospho-MAPK p42/42 (P-Fus3, P-Kss1), Fus3 (Total Fus3) and G6PDH (load control) antibodies.

(B) Transcriptional activation (β-galactosidase activity) in response to α factor was measured spectrofluorometrically in wild-type, *bul1*Δ, *ede1*Δ, *ddi1*Δ, *rup1*Δ, and *gpa1*$^{\Delta UD}$ cells. Cells were transformed with a *FUS1-lacZ* reporter and treated with the indicated concentrations of α-factor (αF) for 90 min. Data for the individual mutants are normalized to WT. Results show mean ± SEM for three independent experiments, done in quadruplicate.

(C) Loss of ubiquitination domain of Gpa1 results in morphological abnormalities under prolonged pheromone stimulation. Wild type *bul1*Δ, *ede1*Δ, *ddi1*Δ, *rup1*Δ, and *gpa1*$^{\Delta UD}$ cells were stimulated with a constant saturating dose (300 nM) of α-factor in a microfluidic chamber. DIC images were taken every 5 min for 8 h to monitor changes in morphology.

(D) Mating efficiency assay. Separate cultures of wild type mating-type α cells (BY4742) and wild type or Gpa1$^{\Delta UD}$ mating-type **a** cells (BY4741) were used. Cells from each culture were mixed and incubated for 4 h. Results are the mean ± SEM from four replicates.

form just a single mating projection (Figure 3.7 *C*). These cells formed a shmoo and subsequently elongated. Taken together these results suggest that Gpa1 must be monoubiquitinated and endocytosed for proper morphogenesis to occur. Since the same morphological defect was not observed in the UBD deletion mutants, it is the first step of removing Gpa1 from the plasma membrane that is necessary for the formation of additional mating projections.

Finally, previous reports indicated that multiple projections are necessary for optimal mating efficiency (Tanaka and Yi, 2010). Accordingly, we observed a two-fold higher mating efficiency in wild type as compared to the *gpa1*$^{\Delta UD}$ mutant strain (Figure 3.7 *D*). Thus the cellular morphogenesis defects exhibited by ubiquitin-deficient *gpa1*$^{\Delta UD}$ mutants leads to reduced mating fitness. Because we have shown that removal of the UD does not alter Gpa1 enzymatic activity or MAPK signaling, we conclude that monoubiquitination and removal from the plasma membrane contributes to proper morphogenesis and mating.

**Discussion**

Here we have used biochemical, biophysical, genetic, and cell biological approaches to demonstrate a positive signaling role for Gα endocytosis. Taking advantage of the yeast system, we identified seven ubiquitin binding domain-containing proteins required for constitutive internalization of the G protein. Three of these proteins act on Ste2 as well as Gpa1. Four others act on Gpa1 alone, demonstrating that endocytosis of the G protein and receptor are distinct processes regulated by distinct binding partners. We show further that the Gpa1 ubiquitination

domain is targeted by the UBD proteins. In the absence of the ubiquitination domain, Gpa1 is retained at the plasma membrane and cellular morphogenesis is curtailed. A second effector pathway leading to MAPK activation is unaffected.

The proteins specifically required for Gpa1 trafficking (Rup1, Ddi1, Bul1 and Ede1) act at different stages of endocytosis (Figure 3.8). Rup1 binds to Rsp5 and stimulates Rsp5 autocatalysis and substrate ubiquitination (Lam and Emili, 2013). We suggest that Rup1 may promote Rsp5-mediated ubiquitination of particular membrane proteins. Bul1 is the ubiquitin binding component of the Rsp5 ubiquitin ligase (Yashiroda et al., 1996). Curiously, we find that Bul1, but not the closely related protein Bul2, promotes Gpa1 endocytosis. Even though Bul1 and Bul2 are closely related, they appear to have distinct functions within the cell. For example, Bul1 is a negative regulator of the tryptophan permease Tat2, but Bul2 is not (Abe and Lida, 2003; Hiraki and Abe, 2010). Ddi1 is a DNA damage inducible v-SNARE binding protein (Liu and Xiao, 1997), which was previously shown to be a negative regulator of the late secretory pathway, a function that is independent of the UBA domain of Ddi1 (Gabriely et al., 2008). Finally, Ede1 is a member of the epsin family of adapter proteins and a component of the early endocytic machinery (Abe and Lida, 2003; Gagny et al., 2000). Deletion of Ede1 but not other epsin proteins (Ent1, Ent2) leads to Ste2 mislocalization (Dores et al., 2010; Shih et al., 2002). Although Ede1 is implicated in Ste2 trafficking we did not observe Ste2 mislocalization in the absence of Ede1. Ste2 trafficking has previously been monitored in agonist-stimulated cells. In contrast we measured Gpa1 and Ste2 trafficking in unstimulated

Figure 3.8

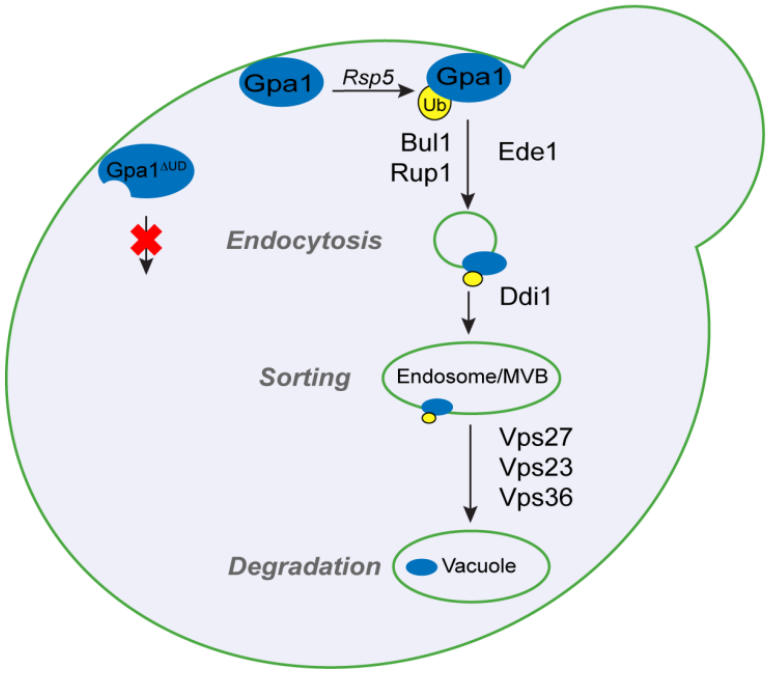


**Figure 3.8 Components required for proper endocytosis of Gpa1 following Rsp5-mediated monoubiquitination.**
The predicted order of action of UBD-containing proteins involved in the trafficking of monoubiquitinated (Ub) Gpa1. When Gpa1 cannot be ubiquitinated ($Gpa1^{\Delta UD}$), it remains at the plasma membrane.

cells. Thus it is possible that Ede1 is important for pheromone-dependent, but not basal, trafficking of Ste2.

It is of note that when endocytosis of Gpa1 is inhibited (*rup1Δ, ddi1Δ, ede1Δ)*, we could detect more of the monoubiquitinated protein and, in some cases, more polyubiquitinated Gpa1 as well. Differences in the levels of Gpa1 monoubiquitination and polyubiquitination likely reflect the roles of the UBD-containing proteins in the removal of monoubiquitinated substrates. When normal trafficking is abrogated the monoubiquitinated species accumulates, and may undergo additional ubiquitination steps resulting in the accumulation of polyubiquitinated substrate. Conversely, we observed no increase in the amount of ubiquitinated Gpa1 in the strain lacking *BUL1*, despite the trafficking defect in that mutant. Since Bul1 is a ubiquitin binding component of the ubiquitin ligase Rsp5, it is possible that the ligase is unable to act on Gpa1 when Bul1 is absent. Taken together these data suggest that the quantity of Gpa1 at the plasma membrane is finely tuned, and that if Gpa1 cannot be removed through monoubiquitination and delivery to the vacuole, it is instead removed through polyubiquitination and delivery to the proteasome.

Our second major finding is that the ubiquitination domain promotes Gpa1 trafficking without altering Gpa1 enzymatic activity *in vitro* or MAPK activation *in vivo*. These results are particularly striking given that (a) the ubiquitination domain is located near a key dynamic region of the α-helical domain, (b) the ubiquitination domain is essential for transport of Gpa1 to the vacuole, and (c) there are a number of Gpa1 binding partners that specifically target the ubiquitination domain. These binding partners include enzymes responsible for monoubiquitination (Rsp5) (Torres

et al., 2009), polyubiquitination (SCF/Cdc4) (Cappell et al., 2010), deubiquitination (Ubp12) (Wang et al., 2005), phosphorylation (Elm1, Tos1, Sak3) (Clement et al., 2013), and dephosphorylation (Reg1) (Clement et al., 2013), as well as the seven UBD proteins identified here. We conclude that the ubiquitination domain likely evolved to serve a unique trafficking function, and that this function is wholly separate from the regulation of G protein catalytic activity.

While the ubiquitination domain is unique to yeast Gα proteins, Gα trafficking is not. Trafficking of Gα has long been established in the visual system, where a redistribution of the protein serves to decrease signaling, allowing adaptation to bright light (Wedegaertner, 2012). Whereas the visual Gα acts directly to stimulate an effector enzyme, yeast Gpa1 acts indirectly to sequester Gβγ and prevent downstream signaling. Therefore, the final outcome of Gα endocytosis will be different in the visual and yeast signaling systems. Gα endocytosis attenuates signaling in the visual system but promotes signaling in the yeast mating pathway. On the other hand, Gα proteins have been shown to be activated at the endosomal membrane compartment, both in yeast and in mammalian cells (Irannejad et al., 2013; Slessareva et al., 2006). Prior to our analysis however, little was known about the proteins necessary for proper Gα trafficking.

Finally, our analysis of the UD may lead to insights regarding the function of unique inserts in other signaling proteins. For example, there are families of small GTPases that are known to contain inserts within the highly conserved Ras-like domains. Members of the Rho family of small GTPases have a unique insert, called the Rho insert, that is not present in other small GTPases (Rojas et al., 2012). The

presence or absence of the Rho insert does not alter the intrinsic activity of these small GTPases (Zong et al., 2001) . However, when the insert is absent Rho can bind, but no longer activate, its downstream effector Rho kinase (Zong et al., 2001). The Rho insert in the small GTPase Rac1 was recently shown to be monoubiquitinated (Visvikis et al., 2008). While no function has yet been assigned to monoubiquitination of Rac1, it is possible that this modification is involved in the mechanism by which Rho interacts with downstream effectors. Monoubiquitination of mammalian Ras proteins can lead to cell transformation (Sasaki et al., 2011), and does so by promoting nucleotide exchange or by impeding the binding of the GTPase activating protein (Baker et al., 2013a; Baker et al., 2013b).

In summary we have identified four UBD-containing proteins as specific regulators of G protein trafficking. When trafficking is abrogated, the morphogenesis branch of the pathway is attenuated. None of these UBD proteins affect the MAPK branch of the signaling pathway, and none affect trafficking of the receptor. Looking forward, our integrated approach should be broadly applicable as more ubiquitination substrates, ubiquitination domains and UBD-containing proteins are identified. Recently, dysregulation of NEDD4/Rsp5-mediated trafficking was shown to promote neurodegenerative disease (Tardiff et al., 2013). In view these findings, any components responsible for monoubiquitination and protein trafficking represent potential targets for future drug development efforts.

## Experimental Procedures

**Strains, Plasmids and Growth of Cultures.** Standard procedures were

followed for the growth, maintenance and transformation of yeast and bacteria. Proteins for biochemical studies were expressed in *E. coli* BL21 (DE3) RIPL cells (Stratagene: La Jolla, CA) grown at 18$^{o}$C overnight after induction with isopropyl β-D-1-thiogalactopyranoside. The yeast (*Saccharomyces cerevisiae*) strain used in this study was BY4741 (*MAT***a** *leu2Δ met15Δ his3-1 ura3Δ*) and its derivatives. Cells were grown at 30$^{o}$C in yeast extract peptone medium (YPD) or synthetic complete medium (SCD) containing 2% (w/v) dextrose. The gpa1$^{\Delta UD}$ mutant strain was generated by transformation of AflII digested pRS406-gpa1_trunc$^{\Delta UD}$ in wild type cells. In each case transformed cells were grown in SCD that lacked the appropriate nutrient or YPD with the appropriate drug.

**Plasmid Construction** Both the native (*sc*Gpa1) and codon optimized Gpa1 (*co*Gpa1) were cloned into the bacterial expression vector pQlinkH (Addgene), which contains an N-terminal Tobacco Etch Virus (TEV) protease-cleavable 6XHis tag, using the BamHI and NotI restriction sites. Efficient TEV protease cleavage required the use of Gpa1$^{\Delta N}$ lacking the first 38 amino acids, which are predicted to be unstructured based on alignment with G$\alpha_i$ (Coleman et al., 1994). The pRS406-STE2-GFP integrating vector was constructed by PCR amplification of approximately 900 base pairs from the 3' end of *STE2* in frame with GFP from the Yeast GFP strain collection (Invitrogen, Life technologies). Genomic DNA from the above strain was amplified with flanking KpnI and SacI sites for introduction to pRS406. The pRS406-gpa1_trunc$^{\Delta UD}$ integrating vector was constructed by PCR amplification of gpa1$^{\Delta UD}$ from pRS406-gpa1$^{\Delta UD}$-GFP minus the first 81 base pairs of Gpa1. The PCR product was flanked by XbaI and SacI sites for introduction to

pRS406. Site directed mutagenesis was used to introduce a silent mutation at bp 181 to generate an AflII site for integration. Construction of the pRS406-GPA1-GFP, pRS406-gpa1$^{\Delta UD}$-GFP, pRS423-FUS1-lacZ, and pADM4-GPA1 vectors have been described previously (Hoffman et al., 2002; Song et al., 1996; Wang et al., 2005).

**Bacterial protein expression and purification.** Generating the quantities of pure Gpa1 necessary to complete biophysical studies has been a barrier to progress, both because of low initial protein expression and impurities, necessitating additional purification steps. We optimized the process using small-scale batch purification and TEV protease-cleavage to release protein from the nickel beads. *E.coli* were lysed by homogenization (NanoDeBee) at 1000 psi in 25 mM potassium phosphate buffer pH 7.0 with 300 mM KCl and 250 μM tris(2-carboxyethyl)phosphine (TCEP). After clarification by centrifugation, the lysate from 500 ml of cell culture was bound to 1 ml Ni-NTA agarose bead slurry (Qiagen), pre-equilibrated in phosphate buffer, pH 7.0 for 20 min at 4$^{o}$C. The beads were washed three times at 4$^{o}$C with 25 mM phosphate buffer, pH 7.0 with 300 mM KCl, then three times with Gpa1 buffer (25 mM phosphate buffer, pH 7.0 and 100 mM KCl) with 100 μM GDP and 500 μM TCEP. Gpa1 was cleaved from the beads by incubation at 4$^{o}$C overnight with 500 ug TEV protease. The final product was judged > 95% pure by SDS–PAGE. Protein was stored at 4$^{o}$C (never frozen) and used within two days. While the use of TEV protease-cleavage to release Gpa1 decreased the yield from the first purification step (about half of the Gpa1 remains on the beads), this loss in efficiency is mitigated by the increase in purity (does not require further dialysis or purification steps). Furthermore, we found that 46% of the

codons in Gpa1 are rarely used in *E. coli*, which can significantly reduce the efficiency of expression (Clarke and Clark, 2008). A codon optimized Gpa1 yielded 18 mg/l, an increase of 11-fold over the original method.

**Circular Dichroism-** Circular Dichroism (CD) experiments were performed from 190 nm – 260 nm on a Chirascan plus CD spectrometer. Spectra of 5 μM protein were recorded in 25 mM Potassium Phosphate buffer, pH 7.0, 100 mM KCl, 50μM GDP, 50 μM $MgCl_2$, and 550 μM TCEP at 25$^{o}$C using a 1 mm quartz cell. Buffer background was subtracted from the spectra.

**Quantitative Mass Spectrometry of ABD-Labeled cysteines-** Gpa1$^{\Delta N}$ was diluted to 2 μM in 25 mM phosphate buffer, pH 7.0 and 100 mM KCl with 50 μM GDP or GTPγS. Protein sample was mixed with 4-fluoro-7-aminosulfonylbenzoflurazan (ABD–F, Anaspec) on ice (final concentration, 2 mM). 20 μL aliquots of the sample were reacted for three minutes at either 42$^{o}$C or 70$^{o}$C and then transferred to ice to quench ABD-F labeling. Samples were prepared for Mass Spectrometry and analyzed as described by Isom *et al.* (Isom et al., 2013). Data collected on a Nano-Acquity HPLC solvent delivery system (Waters Corp.) connected through an electrospray ionization source interfaced to an LTQ Orbitrap Velos ion trap mass spectrometer (Thermo Electron Corp.).

**Thermal Stability of Gpa1-** The fast quantitative cysteine reactivity (fQCR) method (Isom et al., 2011) was employed to measure changes in Gpa1 thermal stability. Briefly, 2 μM protein was incubated with 1 mM ABD-F at pH 7.0 in the presence of 20 μM GDP or GTPγS and 2 mM $MgCl_2$ at the desired temperature for three minutes. The reaction was quenched with HCl and ABD-F fluorescence was

measured on a PHERAstar plate reader (BMG Labtech, excitation at 400 nm and emission at 500 nm). The data were normalized and fit to determine the temperature at which half the protein was unfolded, representing the melting temperature ($T_m$). Results are the mean ± s.d. (n=4).

**MANT-Nucleotide Dissociation Assay-** Gpa1 was exchanged into 25 mM potassium phosphate buffer, pH 7.0, 100 mM KCl, 50 μM $MgCl_2$, and 100 μM GDP. To initiate association, 1 μM Mant-GDP was added to 1 μM protein. Gpa1 was determined to be fully loaded when the fluorescence intensity reaches a maximum at approximately 250 sec. Association was measured as a change in fluorescence intensity over time (excitation: 360 nm, emission: 440 nm) (LS50B Perkin–Elmer Luminescence Spectrometer). MANT-GDP dissociation was initiated by the addition of 500 μM unlabeled GDP. Fluorescence data were fit in GraphPad Prism (GraphPad Software; San Diego, CA) to a one–phase exponential association or decay curve. Results are the mean ± s.d. (n=4).

**Intrinsic GTP Binding and Hydrolysis-** Purified Gpa1 (200 nM) was equilibrated in a cuvette with 25 mM phosphate buffer, pH 7.0, 100 mM KCl, and 50 μM $MgCl_2$. GTP at a final concentration of 200 nM was added to the cuvette, and GTP binding and hydrolysis was monitored by the change in intrinsic fluorescence of Gpa1 that occurs upon rearrangement of the tryptophan near the nucleotide binding region (excitation at 284 nm and emission at 340 nm). Data was collected on a Perkin Elmer Luminescence Spectrometer and analyzed using GraphPad Prism (GraphPad Software; San Diego, CA). Results are the mean ± s.d. (n=3).

**Microscopy screen for Gpa1 and Ste2 trafficking-**BY4741-derived mutants

lacking specific ubiquitin binding domain containing proteins (disrupted using the KanMX G418-resistance marker, from Research Genetics, Huntsville, AL) were used for the screen. *PEP4* was disrupted in the deletion mutant strains by single-step gene replacement with *pep4*::*HIS3* (this work). Gpa1-GFP was introduced in each strains individually by transformation of pRS406 Gpa1 GFP after digestion with *HindIII* (Wang et al., 2005). Separately, Ste2-GFP was introduced in the deletion mutants by transformation of pRS406 Ste2 GFP (this study) after digestion with *AfeI*. Screen hits (deletion mutants that mislocalized Gpa1-GFP) were re-made in BY4741 and BY4641-derived strains by gene replacement with KanMX4 using pFA6KanMX as the template (Wach et al., 1994). All deletions were verified by PCR and nucleotide sequence analysis and analyzed for Gpa1-GFP localization.

**Transcriptional reporter assays -** Pheromone sensitivity was measured by a transcriptional reporter assay (Hoffman et al., 2002) as described earlier. Briefly cells transformed with pRS423Fus1-LacZ were stimulated with different doses of pheromone for 90 minutes and β-galactosidase activity was measured to generate dose-response curves.

**Protein Detection**- Briefly, cells either untreated or treated with 3 μM α-factor for 30 or 90 minutes were harvested in TCA (5% final concentration), washed with 10mM $NaN_3$ and pellets frozen at -80°C. Cell extracts were prepared by glass bead lysis in TCA as described before (Hao et al., 2007). Protein concentrations were determined by a colorimetric protein assay (Bio-Rad). To evaluate pheromone responses 25μg protein was loaded for each sample, whereas to evaluate Gpa1 ubiquitination 40μg protein was loaded for each sample. Proteins were resolved by

running on 10% SDS-PAGE, transferred to nitrocellulose and detected by immunoblotting with Phospho-p44/42 MAPK antibodies at 1:500 (9101L, Cell Signalling Technology), Fus3 antibodies at 1:500 (sc-6773, Santa Cruz Biotechnology, inc.) anti-G6PDH at 1:50,000 (A9521, Sigma-Aldrich) and anti-Gpa1 at 1:1,000 (Dohlman et al., 1993) . Immunoreactive species were visualized by chemiluminescent detection (PerkinElmer Life Sciences) of horseradish peroxidase-conjugated anti-rabbit (170-5046) or at anti-goat at 1:10,000. Blots were eithet scanned using Typhoon Trio+ (GE healthcare) or developed by film exposure on HyBlot Cl autoradiography film (Denville Scientific) and band intensity was quantified using Fiji (National Institute of Health).

**Time-lapse imaging in microfluidics chambers** A microfluidics device similar to the one described earlier was constructed (Hao et al., 2008). Early-mid log phase yeast cells were grown and loaded in the chamber and stimulated with the indicated dose of α-factor pheromone. DIC and/or GFP images were acquired every 5 minutes for 8 to 12 hours using a 60X PlanApo objective under oil immersion. Images were captured using an Olympus Spinning disc confocal microscope equipped with a motorized XYZ stage and photometrics EM CCD camera.

**Quantitative Mating Efficiency Assay-** The mating assay was performed as previously described (Sprague Jr, 1991). Equal amounts of early–log phase *MAT***a** cells (BY4741) and *MAT*α cells (BY4742, *leu2*Δ *his3*Δ *ura3*Δ *lys2*Δ *MET*$^+$) were mixed, sterile filtered onto nitrocellulose mebranes, and incubated on YPD plates at 30$^o$C for 4 hours. After incubation, cells were resuspened at an $OD_{600}$ measurement was used to calculate the dilution necessary to plate 100 – 300 colonies. The cells

were plated onto SCD and SD with only His, Ura, and Leu. Mating efficiency was calculated by dividing the number of diploid colonies by the total number of colonies on the SCD plate.

**Table 3.1: Strains used in Chapter III**

| Strains | Parent | Description |
|---|---|---|
| BY4741 | | MATa *leu2Δ met15Δ his3Δ ura3Δ* |
| *pep4Δ* | BY4741 | pep4Δ::HIS |
| *bul1Δ* | BY4741 | bul1::KanMx4 |
| *ede1Δ* | BY4741 | ede1::KanMx4 |
| *ddi1Δ* | BY4741 | ddi1::KanMx4 |
| *rup1Δ* | BY4741 | rup1::KanMx4 |
| gpa1$^{\Delta UD}$ | BY4741 | gpa1$^{\Delta UD}$::URA |
| *pep4Δ* Gpa1-GFP | BY4741 | pep4Δ::HIS3 GPA1-GFP::URA3 |
| *pep4Δ bul1Δ* Gpa1-GFP | BY4741 | pep4Δ::HIS3 bul1::KanMX4 Gpa1-GFP::URA3 |
| *pep4Δ ede1Δ* Gpa1-GFP | BY4741 | pep4Δ::HIS3 ede1::KanMX4 Gpa1-GFP::URA3 |
| *pep4Δ ddi1Δ* Gpa1-GFP | BY4741 | pep4Δ::HIS3 ddi1::KanMX4 Gpa1-GFP::URA3 |
| *pep4Δ rup1Δ* Gpa1-GFP | BY4741 | pep4Δ::HIS3 rup1::KanMX4 Gpa1-GFP::URA3 |
| *pep4Δ* gpa1$^{\Delta UD}$ -GFP | BY4741 | pep4Δ::KanMX4 gpa1$^{\Delta UD}$ -GFP::URA3 |
| *pep4Δ bul1Δ* gpa1$^{\Delta UD}$ – GFP | BY4741 | pep4Δ::KanMX4 bul1::HIS gpa1$^{\Delta UD}$ -GFP::URA3 |
| *pep4Δ ede1Δ* gpa1$^{\Delta UD}$ - GFP | BY4741 | pep4Δ::KanMX4 ede1::LEU2 gpa1$^{\Delta UD}$ -GFP::URA3 |
| *pep4Δ ddi1Δ* gpa1$^{\Delta UD}$ - GFP | BY4741 | pep4Δ::KanMX4 ddi1::LEU2 gpa1$^{\Delta UD}$ -GFP::URA3 |

**Table 3.2: Plasmids used in Chapter III**

| Name | Description | Source |
|---|---|---|
| pLicHis *sc*Gpa1 | $Amp^R$, TEV cleavable 6XHis | (Torres et al., 2009) |
| pLicHis *sc*Gpa1$^{\Delta N}$ | $Amp^R$, TEV cleavable 6XHis | This study |
| pQlinkH *co*Gpa1$^{\Delta N}$ | $Amp^R$, TEV cleavable 6XHis | This study |
| pRS406 Gpa1-GFP | YIp $Amp^R$ *URA3* GPA1-GFP | (Wang et al., 2005) |
| pRS406 gpa1$^{110\Delta}$-GFP | YIp $Amp^R$ *URA3* gpa1$^{110\Delta}$-GFP | (Wang et al., 2005) |
| pRS406 Ste2-GFP | YIp $Amp^R$ *URA3* STE2-GFP | This study |
| pRS423 FUS1-lacZ | 2 μm $Amp^R$ HIS3 FUS1-lacZ | (Hoffman et al., 2002) |
| pADM4 Gpa1 | 2 μm $Amp^R$ LEU2 $ADH1_p$/$ADH1_t$ | (Song et al., 1996) |

**Table 3.3: Oligonucleotide primer sequences used in chapter III**

| Name | Sequence 5'-3' |
|---|---|
| scGpa1ΔN_Fwd | GTAGTAGGGTCCAAGAATGAAATAAAACTGTTAC |
| scGpa1ΔN_Rev | TACGCGGCCGCATCATATAATACCAATTTTTTTAAGG |
| coGpa1ΔN_Fwd | GGAGGAGGATCCGATAAAAATGAAATTAAACTG |
| coGpa1_Rev | TACGCGGCCGCATCAGATAATACCGATTTTTTTTC |
| ddi1Δ KanMX(F) | CGCCCTGTAAATTCATCGCCACCGAAAAGATAATAATACCCGTACGCTGCAGGTCGAC |
| ddi1Δ KanMX(R) | CCTTATACTTATCTATTTGTGTTATGGGCTACATACGTAGAGGATCGATGAATTCGAGCTCG |
| ddi1 conf D(F) | CCTTTTTAGTTTCATTGAGACCAATCCCTC |
| ddi1 conf D(R) | GCATATTATATACTTAACAGAAGTACAATC |
| bul1Δ KanMX(F) | CCATCGGTGGATTGAACTTAAAACTGGCTTTAAATTGTTCTTTCCCGTACGCTGCAGGTCGAC |
| bul1Δ KanMX(R) | GGAATACAAAGGACGCGATAAATACCTTCATCTATAAGCAAACCATCGATGAATTCGAGCTCG |
| bul1 confD (F) | GCTTTGTTTATCGCCTCCTTGAATTGCAAC |
| KanB (R) | CTGCAGCGAGGAGCCGTAAT |
| rup1Δ KanMX(F) | CGGAAGTAAAAGATACTATTGTTGAAAGGTACTTCTCACTACAAGGCGTACGCTGCAGGTCGAC |
| rup1Δ KanMX(R) | CCTTAGAGTCTAATTTATGTCCGTAAATAGAAGTTTTCGGATTGCGATCGATGAATTCGAGCTCG |
| rup1 confD (F) | GTGGCGATGAAGGTTCACTATGTTCTTTTTTC |
| rup1 confD (R) | GAATTAAAATAGAAGGGGTATTGTTGCGGC |
| ede1Δ KanMX(F) | CGCGAAATAATATAGCGCGTTGAAACTAATAAATAGATTCGTGAAGCCGTACGCTGCAGGTCGAC |
| ede1Δ KanMX(R) | GGTAAATATGATTCAGCTTCGAGGAAGAAGTACAAAAAGAAGACGATCGATGAATTCGAGCTCG |
| ede1 conf D (F) | CGTCGAGCTCATAGCTTTTTATTGTGCTTTG |
| ede1 conf D (R) | GTAATACGCCCAAAGATTATGTGGTAGAGC |
| bul1D HIS (F) | CCATCGGTGGATTGAACTTAAAACTGGCTTTAAATTGTTCTTTCCAGATTGTACTGAGAGTGCAC |
| bul1D HIS (R) | GGAATACAAAGGACGCGATAAATACCTTCATCTATAAGCAAACCCTGTGCGGTATTTCACACCG |
| ede1D LEU (F) | CGCGAAATAATATAGCGCGTTGAAACTAATAAATAGATTCGTGAAGCAGATTGTACTGAGAGTGCAC |
| ede1D LEU (R) | GGTAAATATGATTCAGCTTCGAGGAAGAAGTACAAAAAGAAGACGCTGTGCGGTATTTCACACCG |
| ddi1D LEU (F) | CGCCCTGTAAATTCATCGCCACCGAAAAGATAATAATACAGATTGTACTGAGAGTGCAC |
| ddi1D LEU (R) | CCTTATACTTATCTATTTGTGTTATGGGCTACATACGTAGAGGCTGTGCGGTATTTCACACCG |
| Ste2_Fwd (F) | ATGCGGTACCCTTCTTGTGGCTTCTATTGAGACTTCACTGG |
| Ste2_Rev (R) | GCATGAGCTCCGACCTCATACTATACCTGAGAAAGCAACC |
| Bem1His (F) | TGTCTGAGGAAGAGTTAGAAA |
| Bem1His (R) | AGTATCTTTGGGCTGCGGTTA |
| Pep4 D (F) | GTGACCTAGTATTTAATCCAAATAAAATTCAAACAAAAACCAAAACTAACAGATTGTACTGAGAGTGCAC |
| Pep4 D (R) | CTCTCTAGATGGCAGAAAAGGATAGGGCGGAGAAGTAAGAAAAGTTTAGCCTGTGCGGTATTTCACACCG |
| Pep4 D conf(F) | CGTAACCTCTTATCAACTGGTTAAG |
| Pep4 D conf(F) | GATTTCAAATGTTTCTAGAGCGCAG |
| His3 seq (F) | GCGCCTTTGGATGAGGCACTTTCC |

* Red sequence binds pFA6-KanMX or a pRS40X series vector. Restriction enzyme sites are in bold font.

**Table 3.4: Optimization of Gpa1 purification**

| Construct | Induction | Purification | Purity | mg/l |
|---|---|---|---|---|
| *sc*Gpa1 | + | Column | < 25% | 1.6 |
| *sc*Gpa1 | + | Batch | ~ 50% | 10.4 |
| *sc*Gpa1 | + | Batch with TEV | *nd* | *nd* |
| *sc*Gpa1$^{\Delta N}$ | ++ | Batch with TEV | > 90% | 4.6 |
| *co*Gpa1$^{\Delta N}$ | ++++ | Batch with TEV | > 90% | 18 |

**Table 3.4 Optimization of Gpa1 purification.**
Construct describes the expression vector used. Induction, estimate of the quantity of Gpa1 produced in *E. coli.* Purification, method used for His purification. Purity, percent homogeneity after His column purification. Values are estimated from SDS-PAGE and Coomassie staining. Final yield given in the last column in mg/l.

# CHAPTER IV

## CONCLUSIONS AND GENERAL DISCUSSION*

G proteins and their associated receptors are among the most well studied signaling molecules. They mediate vital functions such as responses to hormones, neurotransmitters, and sensory inputs such as light, odors and taste, making them extremely important for human health and disease (Russ and Lampel, 2005; Thompson et al., 2008). While we have a good understanding of the basic architecture of G protein signaling systems, details of their regulation and dependence on factors such as cellular noise, protein posttranslational modification and trafficking are just beginning to be uncovered (Clement et al., 2013; Colman-Lerner et al., 2005; Irannejad et al., 2013). Consequently a better understanding of spatiotemporal regulation of signaling, particularly at the level of individual cells, will enable the development of more effective disease intervention strategies.

In this thesis, I demonstrate a novel role for the Regulator of G protein Signaling (RGS) protein in suppression of cell-to-cell variability. Using the yeast mating pathway as a model my co-contributors and I evaluated the ability of two activities of the RGS protein (Sst2) -GAP activity and receptor coupling to mediate signal suppression and noise suppression. Through biochemical assays and single

* Figures 4.1, 4.2, 4.3 and 4.5 contributed by Gauri Dixit. Figure 4.4 contributed by Joshua B. Kelley

cell analysis we found that both activities are equal contributors to signal suppression, but only GAP activity is responsible for noise suppression. Moreover, we found that the RGS-GAP activity limits variability in transcription as well as in morphogenesis. Suppression of variability in morphogenesis facilitates proper cell polarization and gradient tracking and thereby enables effective decision making in response to pheromone. Furthermore we were able to show for the first time that noise is dynamically regulated. We used mathematical modeling to understand the differences in noise dynamics in the presence and absence of Sst2, which points towards abundance/activity in pathway components upstream of the MAPK as a major source of variability in pathway output. However, the consequence of changes in noise in gene transcription is still not clear. Furthermore, the role of the receptor coupling function in Sst2 activity remains to be addressed.

In another project, my co-contributors and I found that G protein trafficking via endocytosis is required for appropriate pheromone stimulated morphogenesis. Through structural and biophysical studies we first determined that the ubiquitination domain of Gpa1 does not alter Gpa1 structure or function. Consequently by screening a panel of gene deletion mutants, each lacking a different ubiquitin-binding domain protein, we identified seven proteins needed to deliver Gpa1 to the vacuole compartment. Four of these proteins (Ede1, Bul1, Ddi1 and Rup1) were distinct from those needed for trafficking of the pheromone receptor Ste2. This work represents the first analysis of the consequences of Gα trafficking to the biology of the cell in a non-visual signaling system. Whether the newly identified G protein regulators bind indirectly or directly to Gpa1 is still under assessment.

Finally, through a collaborative effort we discovered that G proteins can act as points of cross talk between signaling pathways (presented in the Appendix). When yeast are nutritionally deprived, Gpa1 undergoes phosphorylation. Phosphorylated Gpa1 is associated with dampened mating response and delayed morphogenesis in response to pheromone. Overall, this work reveals three disparate instances where spatiotemporal modulation of G protein activity affects cellular morphogenesis. These add to the growing list of mechanisms that regulate signal transduction under different conditions. In this chapter, I discuss the implications of the work presented in this thesis, and speculate on the future direction of analysis of cell-to-cell variability and G protein trafficking in yeast.

**Noise regulation in yeast signaling**

Stochastic variation is intrinsic to biology. Signaling cascades are composed of a larger number of proteins, each of which may exhibit varying degrees of noise in activity or abundance (Newman et al., 2006). It is conceivable that noise in the expression of each gene will affect the final response. Therefore we postulated that noise suppression is encoded within signaling systems. We found that Sst2 is the main signal attenuator as well as a major noise suppressor in the yeast mating pathway. Our findings are consistent with theoretical predictions that negative feedback networks mediate noise suppression (Becskei and Serrano, 2000; Dublanche et al., 2006; Voliotis and Bowsher, 2012; Zhang and Chen, 2012).

As discussed in Chapter II, Sst2 acts early in the pathway at the level of the G protein and the receptor. Therefore any effects on noise were likely to be propagated

(amplified) to downstream events, adding substantially to the variability of the final readout. We demonstrated that in the absence of Sst2 there was approximately a 50% increase in noise (CV) in basal mating transcription (Chapter II, Figure 2.3 *D*). A similar increase in noise was seen in the GAP mutant (which abrogates G protein-RGS interaction) but not in the receptor uncoupling mutant (which abrogates RGS-receptor interaction), even though these two mutants were equally sensitive to pheromone (Chapter II, Figure 2.1). Using the same assay we saw an identical increase in the "benchmark" *dig1Δ* strain, reported previously to elevate CV in the absence of pheromone (McCullagh et al., 2010), suggesting that the increase in noise was significant and biologically relevant. As we predicted, cells lacking Sst2 or specifically Sst2-GAP activity displayed heterogeneous morphologies in response to pheromone, were unable to maintain directional polarization or track a pheromone gradient. Together the morphological variations resulted in a severe mating defect in the absence of GAP activity. Unexpectedly none of the morphological or polarization defects listed above were observed in the receptor uncoupled mutant, which was as sensitive to pheromone. Consequently, the receptor uncoupled mutant mated as efficiently as wild type cells.

The difference in mating response between two equally sensitive strains is surprising. For a long time researchers have postulated that initial super-sensitivity governs partner discrimination and that an increase in sensitivity is always accompanied by mating defects (Jackson and Hartwell, 1990). What our results have shown is that random stochastic changes in polarization (but not increased sensitivity) are responsible for mating defects.

To mediate the pheromone response, there are two effector systems downstream of the G protein: one that activates the MAP kinase cascade and the mating gene transcription and a second that triggers Cdc42-dependent morphological changes (Hao et al., 2007). Given that Sst2-GAP function acts at the top of the pathway, it is not surprising that it suppresses noise in the output of both effector systems. However this raises the question of whether noise in effector systems is insulated from each other or does noise in one system also directly induce noise in the other? We addressed this question using Dig 1 which is a transcriptional repressor and is involved in the mating transcription system but not in morphogenesis. In the absence of Dig1, there is an increase in transcriptional noise but no changes in morphogenesis or gradient tracking. We also tried using the opposite approach where we monitored transcriptional noise in three deletion mutants each lacking a Cdc42 GAP (*rga1*Δ*, rga2*Δ and *bem3*Δ*)* to ascertain whether disruptions in the morphogenesis branch has any effect on transcriptional noise. As shown in Figure 4.1, loss of Cdc42 GAPs does not affect basal noise. Furthermore there are no significant differences in pheromone-induced noise dynamics when comparing the GAP mutants to wild type cells. Although these data are preliminary, they suggest that disruptions in one effector system may not obligatorily lead to noise in the other.

Gene expression is the most well studied measure of noise, but other cellular processes such as protein localization and cytoskeletal changes may also contribute to generating variability. The work presented here highlights the importance of measuring multiple network nodes in single cells over time (McCullagh et al., 2009;

Figure 4.1

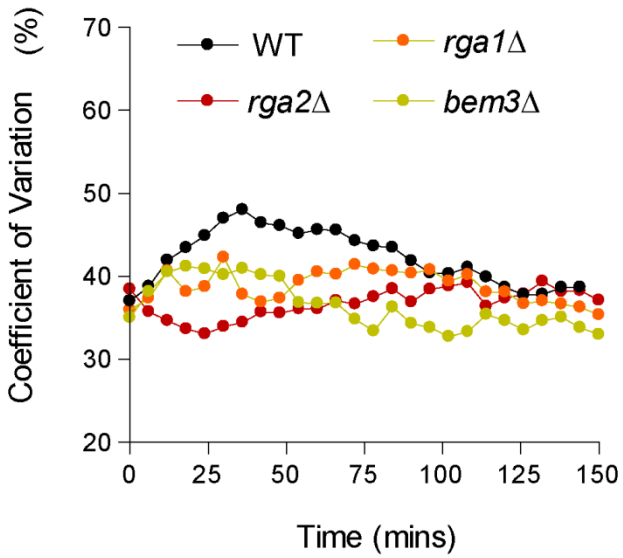


**Figure 4.1 Cdc42-GAPs do not affect noise in gene expression in the pheromone pathway**. Pheromone pathway specific reporter *FUS1*-GFP was integrated at the *FUS1* promoter; reference reporter *ADH1*-mCherry was integrated at the *ADH1* promoter in wild type cells and mutant strains lacking one Cdc42-GAP each (*rga1*Δ, *rga2*Δ and *bem3*Δ). Cells were treated with150 nM α-factor and fluorescence and CV measurements were made every 6 min. There was no significant difference in the basal CV of wild type cells and Cdc42 GAP deletion mutants. Minor changes were observed in pheromone induced transient changes in noise.

Purvis and Lahav, 2013). Accordingly, we employed gene expression and morphogenesis as our read-outs for noise. In the future, coupling gene expression measurements with simultaneous phenotypic analysis of morphology will provide an even clearer understanding of Sst2 mediated noise suppression and how it affects cell fate decisions.

Measuring noise in other events upstream of gene transcription will be informative in determining which particular processes within the pathway are most susceptible to perturbations. In the context of yeast mating, Yu et al. monitored the output of two processes before gene transcription. These included activation-induced G protein dissociation and recruitment of the scaffold Ste5 to the membrane (Yu et al., 2008). The authors were able to show that both these events occurred within a minute after stimulation, pointing to the feasibility of such early measurements. Accordingly we are developing a triple GFP tagged Ste5 reporter as a marker for Ste5 membrane recruitment and Gβ activation (Winters et al., 2005). The Ste5XGFP$_3$ reporter is expressed from the endogenous *STE5* gene locus. Ste5 is expressed at only a few hundred molecules per cell and is difficult to image (Thomson et al., 2011). Thus a triple GFP tag enables easier visualization without any change in pathway sensitivity (Figure 4.2). Preliminary analysis shows that there is an overall increase in Ste5 membrane localization upon pheromone treatment. Initially there is rapid stochastic wandering over the entire membrane and eventually Ste5 accumulates at the site of polarization. Unexpectedly we find that the intensity of polarized Ste5 in individual cells becomes more variable over time, while the intensity of total membrane localized Ste5 is not as variable (Figure 4.3) (This initial

Figure 4.2

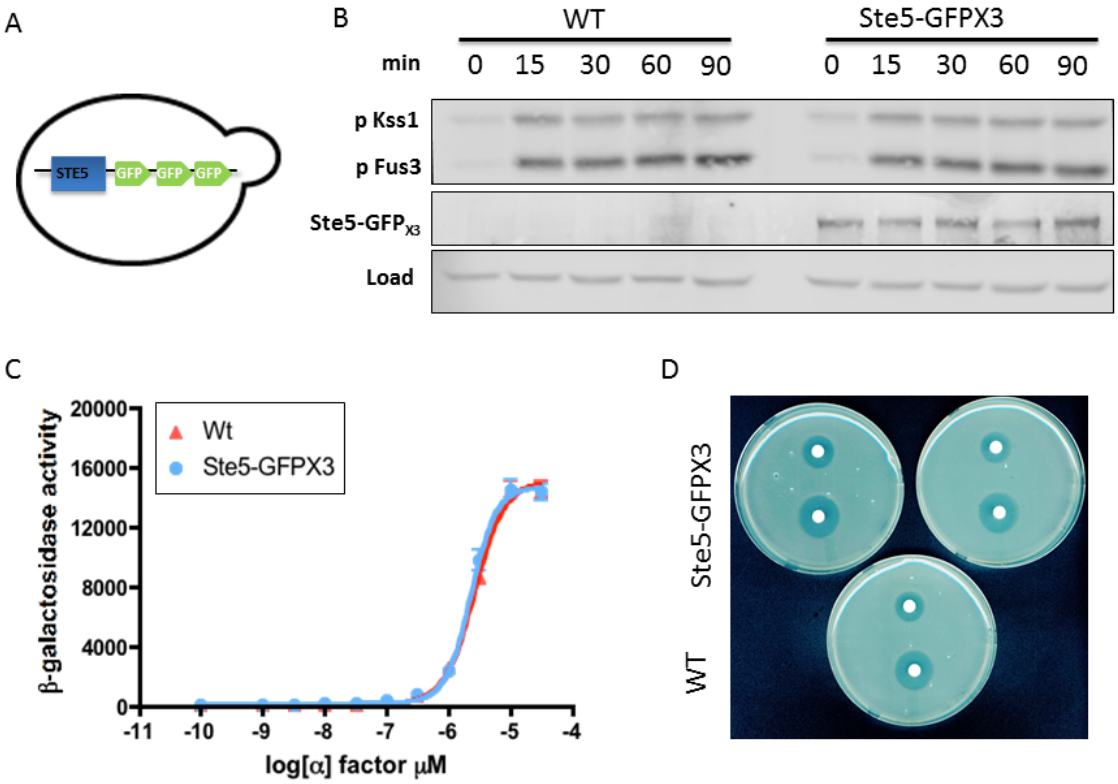


**Figure 4.2 Ste5-GFPX3: a new reporter of the pheromone pathway**. In order to better visualize Ste5, we introduced a tandem repeat encoding three GFP molecules downstream 3' ORF of Ste5. The cloning was based on a pFA6KanMx integrating plasmid that eliminated the stop codon of Ste5. Ste5 is a scaffold with many binding partners (including Ste2, Ste11, Ste7 and Fus3). Therefore we first tested whether having a bulky group attached to the C terminal disrupted any of its activities by monitoring pathway activation in the tagged strain versus a wild type untagged strain. (A) Ste5 with three tandem GFP molecules expressed from its endogenous locus. (B) Time course of MAPK activation. Wild type and Ste5-GFPX3 cells were stimulated with 3μM α factor and samples collected at the indicated times and probed by immunoblotting with p44/42 (P-Fus3, P-Kss1), Fus3 and G6PDH (load control) antibodies. (C) Transcriptional activation (β-Galactosidase activity) was measured spectrofluorometrically in both strains. Cells expressing *FUS1-lacZ* were exposed to the indicated concentrations of α factor for 90 min. (D) Halo Assay to measure pheromone induced growth arrest in two Ste5-GFPX3 clones and one wild type colony. Disks were spotted with 15 and 75 μg α factor.

analysis was done in collaboration with Meng Jin, a former graduate student in Dr. Tim Elston's lab). Analysis of Ste5 dynamics in single cells remains an area of investigation in the lab. One of the immediate questions being addressed is how the dynamics and variability in Ste5 recruitment are affected by Sst2. To summarize, a good understanding of the various time scales of pathway output is necessary to fully understand the causes and consequences of noise regulation. Reaching this goal will require further advancements in our ability to monitor multiple parameters such as transcription, protein subcellular localization, cellular growth rates and morphologies among others.

Investigations on the regulation of noise in gene expression in yeast have suggested that noise in gene expression may be a negative trait. Accordingly yeast have evolved mechanisms to minimize noise. (Fraser et al., 2004). Our results support the idea of noise suppression in yeast signaling networks. Other processes, such as cell cycle progression can be intrinsically noisy. In yeast it has been shown that Cln2 is the only G1 cyclin that reduces noise in the transition from G1 to START(Bean et al., 2006). Cln2 maintains cell cycle regularity by promoting coherence of events such as gene expression and bud morphogenesis at START (Bean et al., 2006; Di Talia et al., 2007). It will be interesting to see how other cellular processes cope with variability, and to what extent this variability is adaptive. However there is also evidence showing that yeast have evolved mechanisms to maintain variability in certain processes. An example is variability seen in the expression of stress response genes (Newman et al., 2006). Recently it was shown that slow-growing yeast cells resist stress better than fast-growing cells, thanks in

Figure 4.3

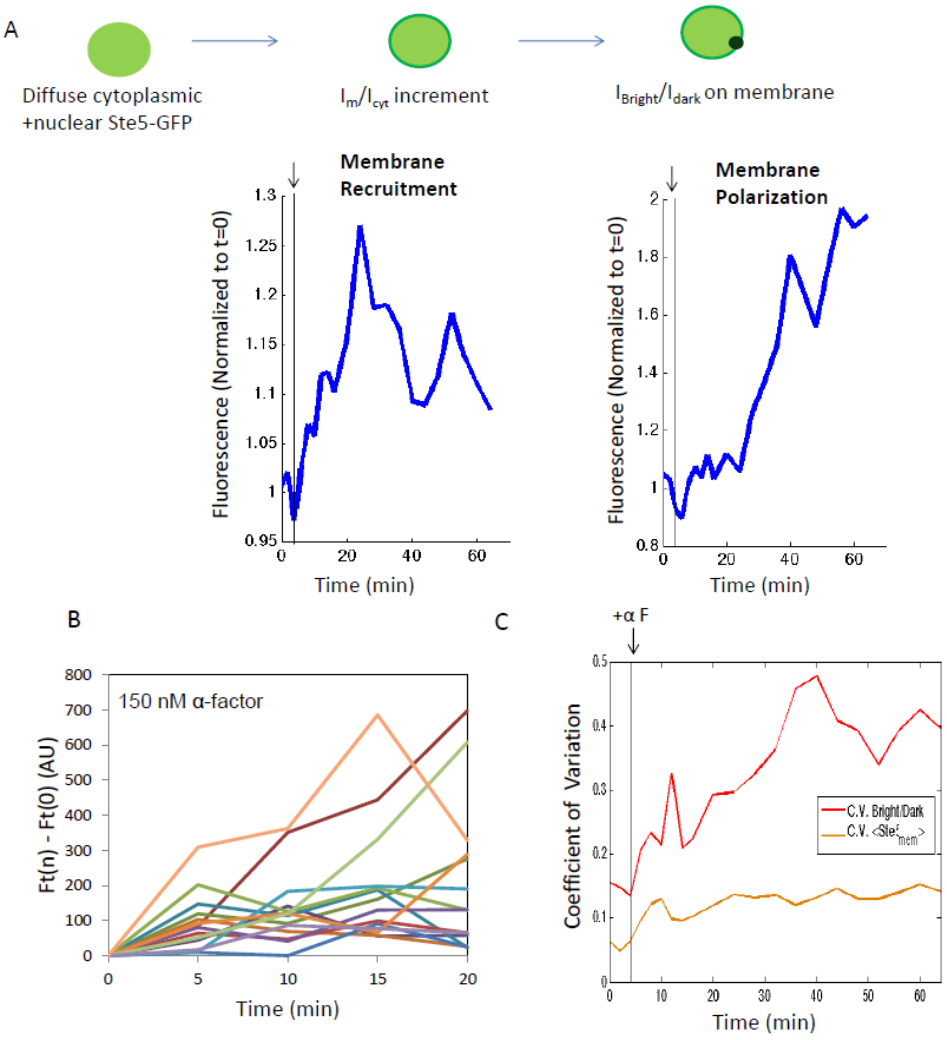


**Figure 4.3 Increased recruitment and variable polarization of Ste5 at the membrane in response to pheromone.** (A) Initially Ste5-GFP fluorescence is nuclear and/or diffuse cytoplasmic. Pheromone stimulation promotes exit of Ste5 from the nucleus and recruitment at the membrane. Cells were treated with 150nM α factor (downward arrow). For the first few minutes Ste5 wanders at sites all over the membrane and eventually it accumulates at the presumptive site of polarization. Bottom left, plot showing mean increase in Ste5 total membrane intensity (membrane recruitment), calculated as $I_m$ / $I_{cyt}$ ($I_m$= Intensity at membrane; $I_{cyt}$=Intensity in the cytoplasm). Bottom right, plot showing mean increase in polarization of Ste5 at the membrane over time calculated as $I_{bright}/I_{dark}$. ($I_{bright}$=Intensity of the brightest spot with a fixed size; $I_{dark}$= Intensity of Ste5 along the rest of the membrane). (B) Increased recruitment of Ste5 membrane recruitment in the presence of pheromone in single cells. (C) Over time the noise (CV) in total Ste5 membrane recruitment stays the same. However noise in Ste5 polarization increases over time.

part to higher levels of a stress-related protein (Tsl1) (Levy et al., 2012). It is important to understand how yeast are able to switch between slow and fast states. Doing so will enable better understanding of bet hedging in malignant cells where cells switch between many states and are therefore resistant to chemotherapeutics (Brock et al., 2009).

**Emerging roles for Sst2 and their implication for human RGS proteins**

Sst2 is the founding member of the RGS family. It was identified as a mutant that was supersensitive to pheromone.(Chan and Otte, 1982a; Chan and Otte, 1982b; Dohlman et al., 1996). Although traditionally thought to be a signal attenuator causing pathway deactivation, mounting evidence in the last decade suggests more roles for Sst2 than originally proposed. Additional functions attributed to Sst2 are (i) promoting pheromone-dependent membrane recruitment of Ste5, (ii) conferring the ability to track a pheromone gradient and (iii) binding to the Ste2 receptor (Ballon et al., 2006; Segall, 1993; Yu et al., 2008). Therefore Sst2 is a kinetic regulator that fine tunes signal activation. Previous work by Seikhaus *et al* surmised that loss of Sst2 results in spontaneous G protein activation in a subset of the population. This work was based on measurements done with plasmid borne reporters (Siekhaus and Drubin, 2003). The work presented here conclusively adds noise suppression as yet another function of Sst2. Our measurements using chromosomally expressed reporters, microfluidics and time lapse single cell microscopy demonstrate for the first time that Sst2 regulates dynamic changes in transcriptional noise and morphogenesis in the presence of pheromone.

The mechanism by which Sst2 restricts noise in mating gene transcription is readily explained by our stochastic model of pathway activation. Our model predicts that Sst2-GAP activity normally ensures that basal MAPK activity is minimal. Therefore, variability due to fluctuations in upstream pathway components (both activity and abundance) is not propagated through the pathway. Going ahead, it will be important to test this prediction by precisely measuring noise in expression of early pathway components. Available data from high-throughput analysis suggests that the MAPKKK Ste11, the MAPKK Ste7 and the MAPK scaffold Ste5 are highly variably expressed (Newman et al., 2006).

However there are two important questions that this work raises: (1) **At the molecular level how does Sst2-GAP activity limit variability in morphogenesis and promote efficient gradient tracking?** and (2) **what is the role of Sst2-receptor coupling in the cell**? In collaboration with the Elston lab at UNC we have begun addressing both of these questions.

In the absence of Sst2-GAP activity, cells show stochastic changes in orientation during elongated growth. Additionally these mutants display an increased mobility of their polar patch, suggesting the loss of a boundary that restricts polar cap movement. Septins are cytoskeletal scaffolds that form a boundary between mother and daughter during mitosis (Caudron and Barral, 2009; Gladfelter et al., 2005). Upon tracking Sst2-GFP in pheromone stimulated cells, we saw Sst2 localized to presumptive areas of septin deposition at particular times (chapter II, Figure 2.4 *E*). Therefore we hypothesize that Sst2-GAP is necessary for establishment of a septin boundary to limit movement of the Cdc42 polarity patch.

So far our results monitoring septin and Cdc42 localization are consistent with this hypothesis. In wild type cells, we found that septins form structures at the periphery of the cell during elongated growth, but were excluded from the polar patch. However, in the absence of Sst2 (GAP activity), septins display significant colocalization with the polar patch and are not incorporated into normal structures at the cell periphery (Figure 4.4). Formation of proper septin structures is an interplay of endocytosis and exocytosis (Okada et al., 2013). We are now examining which of these two are regulated by Sst2-GAP activity to ensure proper septin boundary formation. Our preliminary results examining the distribution of an array of endocytic and exocytic markers in wild type and mutant cells suggests that GAP activity is required for separation of septins from sites of endocytosis.

Addressing the role of Sst2-receptor coupling, we believe that Sst2 regulates receptor dynamics at the plasma membrane. It is known that in the absence of pheromone the receptor is uniformly distributed along the membrane. Upon stimulation Ste2 is phosphorylated by Yck1/2 and subsequently ubiquitinated, endocytosed and degraded (Hicke et al., 1998; Jenness and Spatrick, 1986; Schandel and Jenness, 1994). Over time new gene transcription promotes recovery of the receptor at the membrane in the form of a polarized crescent. We monitored Ste2 membrane distribution over time in the presence and absence of Sst2. We found that Sst2 normally blocks Ste2 endocytosis. By blocking receptor endocytosis Sst2 helps to convert a weak initial polarization of Ste2 to complete receptor polarization. The above data suggests that Sst2-receptor binding has not just evolved for positioning the receptor and G protein in close proximity as thought

Figure 4.4

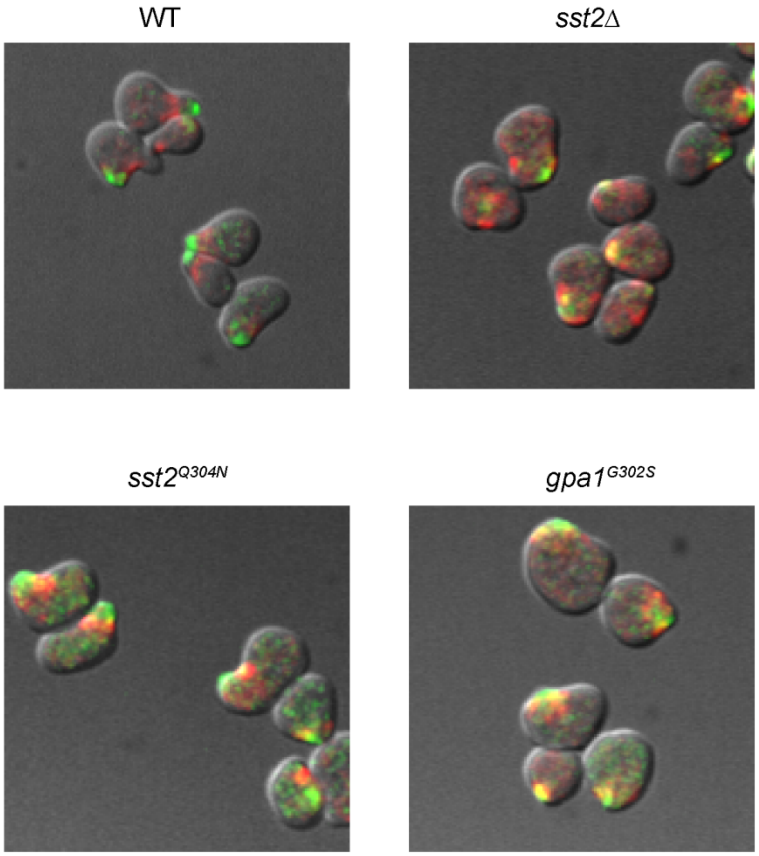


**Figure 4.4 Sst2 GAP activity promotes separation of septins from the polar cap.** Merged DIC and fluorescence images with Bem1-GFP (polar cap) and Cdc3-mCherry (septin). Cells were treated with 300nM pheromone in a microfluidic chamber and imaged 3 hours after treatment. Greater co-localization of septins and Bem1 GFP is seen *sst2*Δ and *gpa1*$^{G302S}$.

before (Ballon et al., 2006). Instead Sst2 also regulates receptor endocytosis and steady state levels in response to pheromone.

RGS proteins have been found to be important in plants, fungi, worms and mammalian cells. Across species they possess a conserved region called the RGS domain, wherein resides their ability to act as GTPase accelerating proteins (GAPs) (Berman et al., 1996; Koelle and Horvitz, 1996; Popov et al., 1997; Siderovski et al., 1996; Watson et al., 1996). As we learn more about their structures and functions, we are beginning to realize that RGS proteins play roles beyond G protein turn off. For instance there are over 30 members in the mammalian RGS family which are classified into several subclasses based on sequence and diverse functional domains (Willars, 2006). In addition to acting as GAPs, RGS proteins have been shown to bind other cellular components such as receptors, calmodulin and tubulin to mediate such effects as cytoskeletal rearrangement and activation of small G proteins (Bansal et al., 2007). Unsurprisingly RGS proteins have been implicated in many diseases including brain disorders like parkinsons and schizophrenia, cancers and retinitis pigmentosa among others (Bansal et al., 2007; Hurst and Hooks, 2009). Accordingly RGS proteins are prime drug targets (Neubig, 2002; Riddle et al., 2005; Sjogren, 2011; Zhong and Neubig, 2001). Sst2 mediated noise suppression may represent a general activity for all RGS proteins- and might be important in understanding human physiology and pharmacology. Suppression of cell-to-cell variability relies only on the GAP activity, which is the common thread among all RGS proteins. Furthermore it is significant that the morphological defects seen in the absence of GAP activity are due to defects in septin organization as septins are also

important in human physiology. Improper septin assembly has been implicated in several diseases including cancer, bacterial infections and neurodegenerative diseases (Saarikangas and Barral, 2011; Spiliotis and Nelson, 2006).

Studying cell-to-cell variation has practical implications for the development of new drugs (Cohen et al., 2008; Spencer et al., 2009). For example, if a cancer drug enhances the sensitivity of cells for a proliferation blocker, but in doing so also changes the variability, it may result in a few cells that are not sensitive enough to the blocker and continue proliferation. Clearly manipulating the level or activity of RGS proteins can have diverse and variable consequences. Given that any drug should confer a predictable response, the potential of RGS proteins as drug targets should be carefully considered.

**Emerging questions for the field of noise**

While several studies have focused on the causes and consequences of noise, one area that has been relatively unexplored is how cell-to-cell variability contributes to aging and vice-versa (Somel et al., 2006). Convincing evidence for the link between aging and variability comes from a study where it was shown that the cell-to cell variability in expression of several housekeeping genes increased in the hearts of older mice (Bahar et al., 2006). The authors demonstrated that treating young cardiac cells with hydrogen peroxide (causing genomic damage) increased gene expression variability. Conversely, it is also possible that variability determines aging. For example a study in *C. elegans* found that the expression of a heat shock reporter was highly stochastic between organisms and predictive of the life span of

the organism (Rea et al., 2005). The question of whether aging determines variability or variability causes aging is still an open ended one. Furthermore it remains to be addressed whether certain genes that control aging (such as Sirtuins in yeast) are susceptible to noise or causative of noise.

Recent advances in technology allowing the separation of mother-daughter pairs have enabled answering some of these questions related to aging and variability and non-genetic heritability in yeast (Lee et al., 2012; Zhang et al., 2012). One group has attempted to apply measure pheromone response in mother-daughter pairs and tried to address whether related cells correlate better in terms of signal output compared to unrelated cells (Falconnet et al., 2011; Ricicova et al., 2013). They were successful at developing a platform to efficiently assign cell lineages and show that mother-daughter responses correlate to a certain extent. However their results were uninterpretable with respect to the control of signaling as a function of age. We are now in a position to use the single cell assays we have developed and test whether aging affects signaling. Using calcofluor or FITC- WGA staining of the bud scars that form with each round of replication (Powell et al., 2003) we can sort yeast by flow cytometry into young and old cells. We can load these sorted populations in microfluidic chambers separately and observe the transcriptional output in the two populations. When compared with unsorted cells, this approach will ascertain whether or not age is a source of variability in signaling. Alternatively we can allow cells to replicate a few times in a microfluidic device, stimulate them with pheromone and monitor differences in gene expression in mother, daughter and grand-daughter cells. Additionally through this set up and the

use of a short-lived GFP reporter made by attaching a PEST degradation sequence (Mateus and Avery, 2000) (Figure 4.5 *A*) we can address addition questions about cellular memory. When cells are stimulated with the same signal repeatedly, does memory of the past response module subsequent responses? Is there a difference in the memories of mother-daughter or young/old cells? Preliminary data looking at two pulses of pheromone indicate that the average pheromone response of daughters may be a little higher than mother cells. When allowed a period of recovery between two pheromone pulses, daughter cells recovery faster compared to mother cells. Similarly, daughters mount a response to the second pulse of pheromone faster than mother cells (Figure 4.5 *B*). However, so far the problem with this approach has been overcrowding of the cells in the chamber as we allow them to undergo at least two divisions before stimulation. To circumvent this problem, we might have to revise the design of our microfluidic chamber.

Another area where tools have been limiting is the assessment of the consequence of noise under diverse stress situations. Our data have shown that there are dynamic changes in noise when cells respond to pheromone (Figure 2.3 *E* and *F*). What happens if we were to perturb the system during high or low noise states, with a second signal, say for instance salt induced osmostress? Will a high noise state lead to better survival, as seen in other cases of bet hedging? With the tools we have built, we have a platform where we can test how robust systems are to environmental changes and how perturbing noise affects the final outcomes. We are in a position where we can test whether increased variability allows better survival in stresses like salt, acid and peroxide.

Figure 4.5

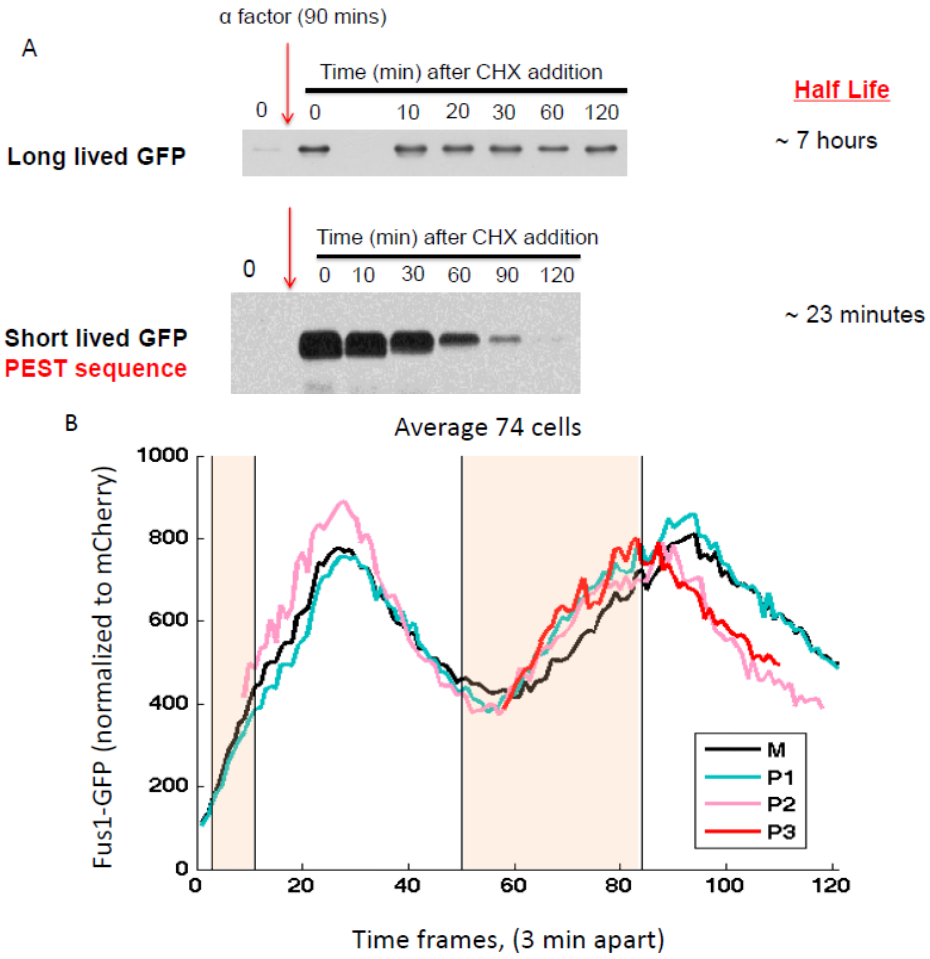


**Figure 4.5 Analysis of pheromone responses in single cells as a function of age and memory** (A) Generating a short lived GFP reporter for the pheromone pathway. GFP was tagged with a PEST rich 178 amino acid sequence (as described by *Mateus and Avery*, 2000). Either regular (long lived) GFP or (short lived) GFP-PEST were chromosomally integrated under the control of the FUS1 promoter. Cells were treated with α factor for 90 minutes to initiate transcription from the FUS1 locus. Subsequently cyclohexamide (CHX) was added to inhibit any further protein synthesis and samples taken for probing with GFP antibody at the indicated times. Regular GFP has an approximate half-life of 7 hours while GFP PEST was found to have a half-life of ~ 23 minutes. (B) Pheromone reporter *FUS1*-GFP-*PEST* was integrated at the *FUS1* promoter; reference reporter *ADH1*-mCherry was integrated at the *ADH1* promoter. Cells in a microfluidic chamber were subject to a short (30 minute) pulse of 150 nM pheromone, followed by a 90 minute recovery period and re-stimulation with pheromone for 90 minutes. The pheromone responses (normalized to mCherry) were measured in mother and daughter cells for each pulse. (M- mother, P1, 2 and 3 –first, second and third generation daughters respectively). Pink rectangles- period of pheromone treatment.

Furthermore, it will address the question of cross-talk and signal prioritization in single cells simultaneously responding to different stimuli (Nagiec and Dohlman, 2012).

**G protein trafficking**

Although G proteins are primarily localized to the plasma membrane, evidence in multiple systems suggests that G proteins move between compartments in constitutive and activation-dependent ways (Wedegaertner, 2012). The most information about trafficking of the Gα and its consequences comes from the visual system. In the visual system Gα is trafficked from the rod outer segments to the inner compartments in a light dependent manner. Activation causes G protein dissociation which promotes internalization of the Gα and Gβγ (Slepak and Hurley, 2008). Other examples of activation induced G protein trafficking come from drosophila visual system ($G\alpha_q$) (Frechter et al., 2007) and from a mammalian non-visual system ($G\alpha_s$) (Wedegaertner et al., 1996). For each of the cases presented above there is strong evidence for a trafficking model whereby activated Gα translocates independently of the GPCR.

In addition to activation induced trafficking, evidence for constitutive G protein trafficking is fast emerging. Most information for constitutive trafficking comes from non-visual systems. $G\alpha_o$ has been shown to shuttle between the plasma membrane and golgi endomembranes (Chisari et al., 2007). Despite the wealth of available literature, it is still not clear how trafficking of the G protein is mediated. The only mechanistic insight into trafficking suggests that palmitoylation - depalmitoylation

cycles determine localization of the G protein. However, the exact trafficking pathway for G proteins after movement off of the PM remains obscure. Major unanswered questions in the field include (A) Do both Gα and Gβγ translocate? (B) Is translocation mediated by diffusion or vesicle-mediate active transport? Our analysis for trafficking of the yeast Gα Gpa1 presented in Chapter III is the first study to show the trafficking machinery for constitutive Gα trafficking. Our results provide strong evidence in support of vesicle mediated transport. While we were able to show that Gpa1 and the receptor have shared and distinct signaling components, we have yet to determine whether Gpa1 and Gβγ are internalized together. Furthermore we would like to conduct more imaging studies to further resolve the exact subcellular locations through which the G proteins traffic.

**Gpa1 monoubiquitination and trafficking**

There is a growing body of literature highlighting the importance of ubiquitination in several intracellular processes such as trafficking and regulation of signaling (Cappell et al., 2010; Hammond-Martel et al., 2012; Hurst and Dohlman, 2013; Liu and Chen, 2011). Despite all the information available on ubiquitination, not many studies have explored the consequences of trafficking to proper signaling. Yeast Gpa1 has a 109 amino acid loop in the helical domain that we term the ubiquitination domain (UD). In Chapter III we presented data showing that the UD does not alter Gpa1 structure or activity. Removing the entire UD did not disrupt the secondary structure nor did it change GTP loading or hydrolysis. However, Gpa1 UD is important for mediating vacuolar trafficking of the G protein from the

membrane via endocytosis (Wang et al., 2005). Since removal of the UD affected only trafficking but not Gpa1 form or function, it presented us with an opportunity to test the effects of trafficking on signaling outcomes, without any confounding effects on Gpa1 function. For the first time we were able to identify components of the trafficking machinery for Gpa1 and demonstrated that trafficking is important for prolonged pathway activation. In the absence of Gpa1 trafficking ($gpa1^{\Delta UD}$) cells are unable to form multiple shmoos and mate half as well as wild type cells. While we have shown that there is no change in the activity of Gpa1 when the ubiquitination domain is removed, we don't still know if ubiquitination itself alters the biochemical activity of Gpa1. Answering this question requires purification of large quantities of monoubiquitinated Gpa1. Since the percentage of monoubiquitinated species in vivo is quite low, we may have to try to purify Gpa1 and chemically modify it in vitro (Baker et al., 2013). Another question that our results pose is why do we not observe multiple shmoos in the absence of Gpa1 trafficking? Clearly it is not due to pathway insensitivity as the MAPK activation and transcriptional response in $gpa1^{\Delta UD}$ mutant were unaltered. We propose that presence of Gpa1 at the membrane might be inhibitory to some protein involved in polarization. It is certainly possible that by being present at the membrane all the time, Gpa1 might engage Gβγ, Sst2 which may be required for morphogenesis.

The trafficking pathway components identified through our microscopy screen (Bul1, Ede1, Ddi1, Rup1) represent potential G protein binding proteins. To test whether these proteins indeed bind to Gpa1 we will have to tag these proteins individually in a strain containing a tagged form of Gpa1 and to perform immune-

precipitations to test binding. As a control we will have to do a similar analysis in a Gpa1 mutant lacking the UD. Alternatively we could do a mass spectrometry screen of proteins that pull down with Gpa1 compared to Gpa1 without the ubiquitination domain. Since most of these trafficking components have human homologues, the work done in yeast may shed some light on how trafficking might be mediated in more complex systems.

The identification of components mediating G protein trafficking is just the beginning of an effort to understand the regulation of signaling by trafficking. The work presented here is part of an ongoing effort to identify novel G protein regulators. The list of known UBDs has grown since the work presented here was conducted (Winget and Mayor, 2010). Therefore, we need to screen the newly identified UBDs to determine their involvement in Gpa1 and Ste2 trafficking. The ultimate goal in this regard is to map out the entire trafficking pathway for Gpa1 and determine to what extent our findings apply to human systems. Identifying novel G protein regulators like those involved in trafficking may eventually lead to identification of novel therapeutics that may allow selective intracellular regulation of the G protein without perturbing other signaling functions.

**Conclusions**

Better understanding of the spatio-temporal regulation of G proteins is important in order to identify new drug targets and design more effective drugs. The work in this thesis evaluates a new function for a known regulator of signaling (noise suppression by RGS proteins); and identifies a new class of previously unknown G

protein regulators (UBD containing proteins) that mediate G protein trafficking. Both RGS and UBD proteins regulate cellular morphogenesis. The conserved GAP activity of the Regulator of G protein Signaling (RGS) was found to reduce cell-to-cell variability in transcriptional and morphological responses. Given the importance of RGS proteins in diseases and as potential drug targets this research points towards an important aspect of RGS function that will have to be considered in future studies of mammalian RGS proteins. Furthermore this work identifies new potential G protein binding proteins that facilitate intracellular trafficking. We present the first example of the consequences of Gα trafficking to the biology of the cell in a non-visual signaling system. If the trafficking pathways delineated in yeast are found to function similarly in humans, they present exciting new avenues of targeted intracellular regulation of G protein signaling.

# APPENDIX

## REGULATION OF YEAST G PROTEIN SIGNALING BY THE KINASES THAT ACTIVATE THE AMPK HOMOLOG SNF1[*,◦]

Extracellular signals such as nutrients and hormones cue intracellular pathways to produce adaptive responses. Often, there are multiple input signals and cells must coordinate these signals to produce an appropriate outcome. Here we show that components of a glucose-sensing pathway act on components of a G protein-mediated pathway in yeast *Saccharomyces cerevisiae*. We demonstrate that the G protein α subunit Gpa1 is phosphorylated in response to low glucose conditions, and that this phosphorylation contributes to a reduction in pheromone-dependent MAPK activation, gene transcription, cell morphogenesis and mating efficiency. The Snf1/AMP-activated protein kinase (AMPK) kinases, Elm1, Sak1, and Tos3 phosphorylate Gpa1 and contribute to diminished mating. Conversely, the Snf1 phosphatase Reg1 is needed to reverse phosphorylation of Gpa1 and to restore the mating response. Thus the same kinases and phosphatase that regulate AMPK/Snf1

[*] Elements of the work referenced in this appendix have been published in: Clement ST, Dixit G, and Dohlman HG. (2013). Regulation of Yeast G Protein Signaling by the Kinases That Activate the AMPK Homolog Snf1. *Science Signaling* 6 (291) ra78.

[◦] I am including a portion of this work in my thesis as I am a co-author on this publication. I performed the microscopy experiments and cell biology analysis for this paper. Sarah T. Clement conducted the rest of the experiments included in this paper and wrote the majority of the paper, with input from all authors. Figures A1A, A1B, A1C and A1D contributed by Sarah T. Clement. Figures A2B, A2C, A2D contributed by Gauri Dixit

also regulate Gpa1. More broadly, these results indicate that the glucose-sensing and mating response pathways communicate directly to coordinate cell behaviors.

## Introduction

Gpa1 has been shown to be undergo several post-translational modifications that regulate its activity and ability to transmit a signal. Examples of some of these modifications include myristoylation, palmitoylation, ubiquitination and most prominently, phosphorylation (Song and Dohlman, 1996; Stone et al., 1991; Torres et al., 2011). Previously in the lab, it was demonstrated that the kinase Elm1 phosphorylates Gpa1. Under nutrient-rich conditions, Elm1 is present predominantly during the G2-M phase, and this leads to concomitant, cell cycle‐dependent phosphorylation of Gpa1(Torres et al., 2011). Elm1 is also one of the three kinases that phosphorylate and activate Snf1, the founding member of the adenosine monophosphate‐activated protein kinase (AMPK) family under conditions of limited glucose availability (Sutherland et al., 2003). In turn Snf1 promotes transcription of genes that help maintain energy homeostasis (Hardie et al., 1998). Given that Snf1 and Gpa1 share a kinase, we hypothesized that just like Snf1, Gpa1 would be phosphorylated under conditions of limited glucose availability. Additionally we aimed to assess the consequence of this modification on Gpa1 on overall pheromone signaling. We found that not only is Gpa1 phosphorylated by the same kinases that phosphorylate Snf1 under low glucose, but is also dephosphosohorylated by the same phosphatase. Under conditions that promoted the phosphorylation of Gpa1, cells exhibited a diminished response to pheromone, a delay in mating morphogenesis, and a reduction in mating efficiency. These findings

established a previously uncharacterized link between the nutrient sensing (AMPK) and G protein signaling pathways. More broadly, they reveal how metabolic and GPCR signaling pathways coordinate their actions in response to competing stimuli.

## Results

**Gpa1 is phosphorylated in response to reduced glucose availability:** We tested the extent of Gpa1 phosphorylation in the presence of typical or high (2%) glucose compared to low (0.05%) glucose by western blotting using Gpa1 antibodies. We were able to distinguish the phosphorylated and unphosphorylated species based on the migration differences between the two. Indeed, we found that Gpa1 was phosphorylated (Figure A1 *A*), and that phosphorylation was rapid and sustained in cells cultured in medium with lower glucose concentration (Figure A1 *B*); however, Gpa1 was still phosphorylated in cells deficient in Elm1 (elm1D mutant cells). Because two other kinases, Sak1 and Tos3, are also capable of phosphorylating Snf1 (Sutherland et al., 2003), we examined whether these kinases, alone or in combination, contributed to the phosphorylation of Gpa1 under conditions of limited glucose availability. Of the single kinase deletion mutants, sak1D cells exhibited the smallest increase in Gpa1 phosphorylation because of glucose limitation (Figure A1 *C*). Deletion of all three kinases was needed to eliminate Gpa1 phosphorylation at early time points (Figures A1 *B* and *D*). Having shown that the kinases that phosphorylate Snf1 also phosphorylated Gpa1, we asked whether the phosphatase for Snf1, which consists of the subunits Glc7 and Reg1(Ludin et al., 1998), was capable of dephosphorylating phosphorylated Gpa1. Reg1 is the

**Figure A1**

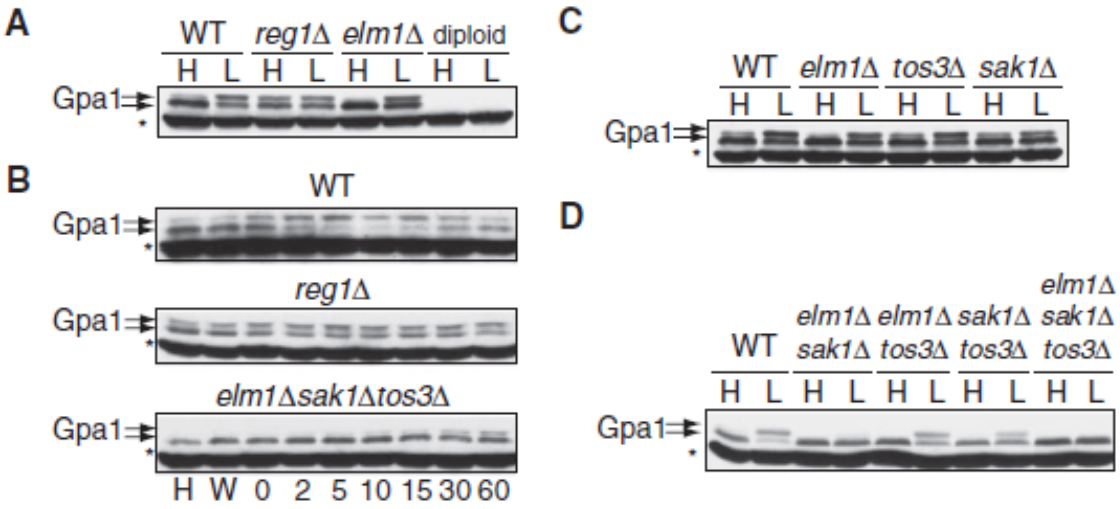


**Figure A1 Gpa1 is phosphorylated in cells cultured under conditions of low glucose availability**. **(A)** Wild-type (WT), reg1D, elm1D, and diploid yeast strains expressing endogenous GPA1 were grown in yeast extract, peptone, and dextrose (YPD) containing 2% [high (H)] or 0.05% [low (L)] glucose and analyzed by blotting with an anti-Gpa1 antibody. Treatment with 0.05% glucose was performed for 5 min after cells had undergone log-phase growth in YPD containing 2% glucose. Diploid cells lack Gpa1 and thus were used as a negative control. Gpa1 was detected in two bands; the upper band corresponds to the phosphorylated protein. The asterisk denotes a nonspecific band. **(B)** Time-course analysis of Gpa1 phosphorylation. WT, reg1D, and elm1Dsak1Dtos3D strains were grown in 2% glucose (H), were washed in 0.05% glucose (W), or were grown in 0.05% glucose for the indicated times (in minutes). Cell lysates were analyzed by Western blotting with an anti-Gpa1 antibody. **(C)** Analysis of Gpa1 phosphorylation in yeast strains singly deficient in kinases that phosphorylate Snf1. WT cells and the indicated strains were treated as described in (A) and were analyzed by Western blotting with anti-Gpa1 antibody. **(D)** Left: Analysis of Gpa1 phosphorylation in WT cells and in the indicated double and triple kinase–deficient strains treated as described in (A).

for yeast survival, we tested reg1D mutant cells. Indeed, we found that the abundance of phosphorylated Gpa1 was increased in reg1D compared to that in wild-type cells, and that Gpa1 remained phosphorylated even under conditions of abundant glucose concentration (Figures A1 *A* and *B*). Together, these data suggest that the kinases and phosphatase that act on Snf1 are capable of acting on Gpa1 as well.

**Limited glucose availability dampens the mating response pathway:** The Snf1 complex and its human counterparts, the AMPKs, serve as molecular switches to turn on catabolic pathways while suppressing anabolic pathways when cells are under energy-poor or other stressful conditions (Hardie et al., 2012). Gpa1, we found is phosphorylated under low glucose conditions. In light of these findings, we postulated that Gpa1 might serve as a point of crosstalk to delay mating during periods of glucose limitation. To test this model, we investigated how a decrease in extracellular glucose concentration might alter MAPK activation and mating-specific gene expression, as well as the consequent changes in cell morphology and mating efficiency. We monitored MAPK activation when cells were treated with low and high pheromone and found a dampened MAPK activation under low glucose conditions. These changes in the extent of MAPK activation were mirrored in the transcriptional reporter assay (Clement et al., 2013). Thus, we found that low glucose induced phosphorylation of Gpa1 appeared to dampen signaling immediately after stimulation of cells with pheromone.

Ultimately, a stress-dependent reduction of pheromone responses should

lead to impaired mating. we observed a nearly threefold reduction in mating efficiency in cells grown in 0.05% glucose compared to that in cells grown in 2% glucose (Figure A2 *A*). We then monitored pheromone-induced morphological changes in cells, including polarized cell expansion ( “shmoo” formation), which produces the eventual site of haploid cell fusion (Ydenberg and Rose, 2008). The use of a microfluidic chamber enabled us to maintain fixed concentrations of glucose and pheromone over time. For cells cultured in medium containing 2% glucose, the addition of α-factor pheromone resulted in shmoo formation after ~120 min. For cells cultured in medium containing 0.05% glucose, the addition of a-factor resulted in shmoo formation after 180 min (Figure A2 *B*). Moreover, whereas pheromone-treated cells normally arrest in the first G1 phase, we found that cells grown in 0.05% glucose divided once and did not arrest until the second G1 phase (Figures A2 *B* and *C*). In contrast, we observed no differences in the rate of cell division (budding) whenpheromone was absent (Figure A2 *D*). These observations suggest that general cellular and cell cycle functions are not substantially dysregulated under conditions of low glucose concentration, at least for the first 4 hours. We conclude that suppression of the mating pathway and delayed morphogenesis are sufficient to reduce mating efficiency when glucose is limiting. More broadly,these findings demonstrate a degree of coordination that serves to prioritize signaling events during conditions of metabolic stress.

**Figure A2**

A

Quantitative mating

| Glucose | Mating efficiency (%) |
|---|---|
| 2% | 77 ± 4 |
| 0.05% | 28 ± 3 |

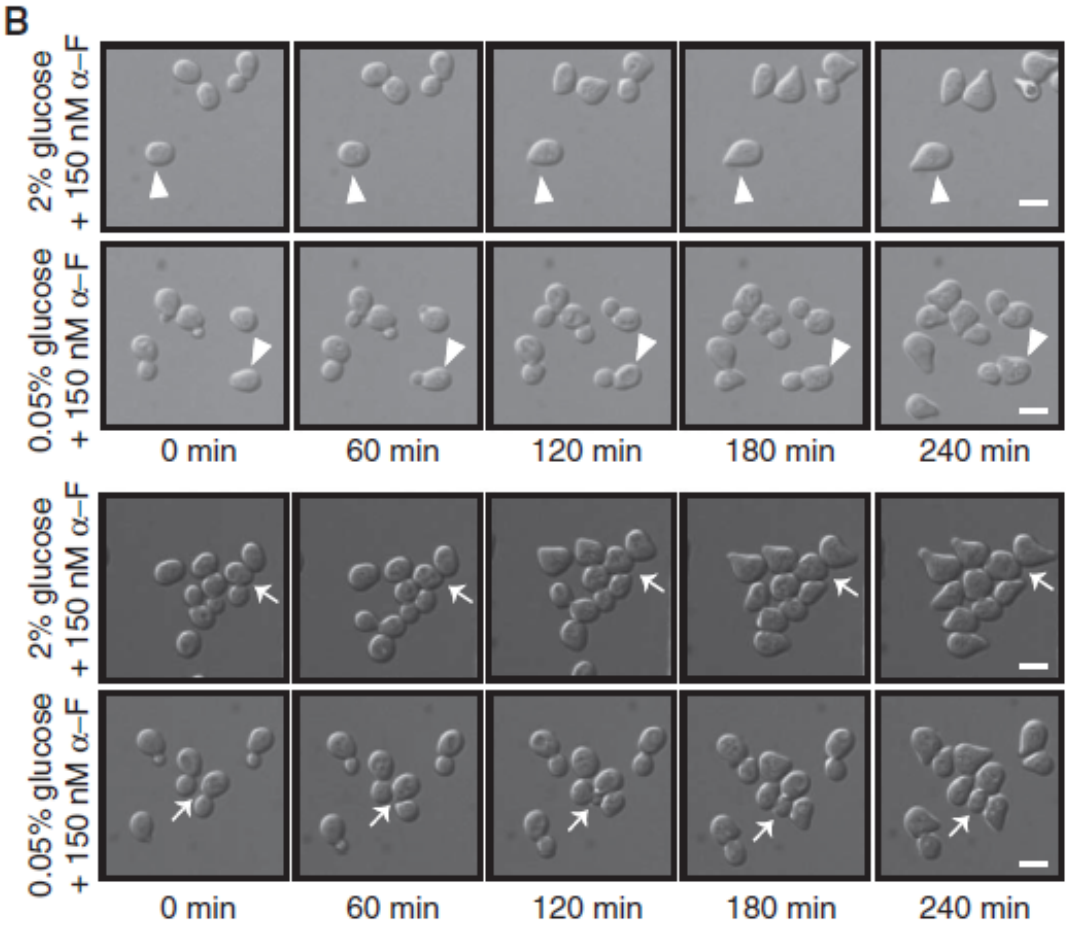


**Figure A2 Shmoo formation and mating are impaired under conditions of limited glucose availability**. **(A)** Mating efficiency assay. WT mating-type a cells (BY4741) and WT mating-type α cells (BY4742) were grown in medium containing 2% glucose. Cells from each culture were mixed, filtered onto a nitrocellulose membrane, and incubated on a YPD plate containing either 2 or 0.05% glucose for 4 hours. Data are means ± SEM from three independent experiments. **(B)** WT cells treated for the indicated times with 150 nM α-F in SCD medium containing 2 or 0.05% glucose were visualized by differential interference contrast microscopy in a microfluidic chamber. The appearance of shmoo projections was monitored after the addition of α-F. Top two rows: Arrowheads indicate cells in G1 phase at the beginning of α-F addition. Bottom two rows: Arrows indicate budding cells at the beginning of α-F addition. Scale bars, 5 μm.

**Figure A2 (contd.)**

**C**

| Time (min) | 2% glucose + 150 nM α-F | | 0.05% glucose + 150 nM α-F | |
|---|---|---|---|---|
| | Total cells | Shmooing cells | Total cells | Shmooing cells |
| 0 | 100 | 0 | 57 | 0 |
| 60 | 108 | 2 | 65 | 0 |
| 120 | 111 | 91 | 80 | 6 |
| 180 | 118 | 114 | 89 | 51 |
| 240 | 118 | 115 | 93 | 87 |

**D**

Budding rate

| Glucose | Rate (min) | *n* |
|---|---|---|
| 2% | 122 ± 2 | 51 |
| 0.05% | 118 ± 2 | 54 |

**Figure A2 Shmoo formation and mating are impaired under conditions of limited glucose availability. (C)** Analysis of cell counts for the experiments shown in (A) and (B). **(D)** Budding rate was determined by measuring the average time for successive buds to emerge in WT cells in a microfluidic chamber in SCD medium containing 2 or 0.05% glucose.

## Experimental Procedures

**Strains, Plasmids and Growth of Cultures.** Standard methods for growth, maintenance, and transformation of yeast and bacteria were used throughout. Strains used in this study were BY4741 (*MAT***a** *leu2*Δ *met15*Δ *his3*Δ *ura3*Δ and BY4741-derived mutants constructed by use of the KanMX4 G418-resistance marker (Yeast Deletion Clones, Invitrogen; originally purchased from Research Genetics). Double gene deletion and triple gene deletion strains were made using PCR-mediated gene disruption cassettes from pRS400 series vectors (Brachmann et al., 1998). Cells were grown in yeast extract peptone medium (YPD) or synthetic complete medium (SCD) containing 2% (w/v) D-glucose. Low glucose treatment was conducted by growth in 2% glucose media to early-log phase, then cells were centrifuged and washed with 0.05% glucose media before being resuspended in 0.05% glucose media for 5 min. Cells were then collected for immunoblotting or further treated with α-factor pheromone.

**Protein Detection.** Unless otherwise noted, cell pellets were harvested by addition of 100% trichloroacetic acid (5% final concentration), centrifuged at 3000 x g for 2 min, washed with 1 mL of 10 mM $NaN_3$, and stored as a frozen cell pellet at ---20 °C. Protein extracts were generated by glass bead lysis in trichloroacetic acid as described previously(Lee and Dohlman, 2008). For immunoblotting, nitrocellulose membranes were probed with anti-Gpa1 at 1:1,000 (Dohlman et al., 1993).

**Quantitative mating assay and microscopy.** mating assays were conducted as described previously (Sprague, 1991). Briefly, equal amounts of early-log phase *MAT***a** cells (BY4741) and *MAT*α cells (BY4742, *leu2*Δ *his3*Δ *ura3*Δ *lys*Δ

*MET*$^{+}$) were mixed, filtered onto nitrocellulose membranes and incubated on YPD plates containing 2% or 0.05% glucose. After 4 hours of incubation, cells were resuspended and plated onto SCD or SD +Leu/His/Ura plates. Mating efficiency was calculated by dividing the number of diploid colonies by total number of cells on SCD plate. To perform the microscopy experiments, microfluidic devices were constructed similar to those previously described (Hao et al., 2008). Cells were imaged every 5 min for 12 hours. Image acquisition was performed with an Olympus spinning disc confocal microscope, and image processing and analysis were performed with ImageJ software.

**References for Appendix**

Brachmann, C. B., Davies, A., Cost, G. J., Caputo, E., Li, J., Hieter, P., and Boeke, J. D. (1998). Designer deletion strains derived from Saccharomyces cerevisiae S288C: a useful set of strains and plasmids for PCR-mediated gene disruption and other applications. Yeast *14*, 115-132.

Clement, S. T., Dixit, G., and Dohlman, H. G. (2013). Regulation of yeast G protein signaling by the kinases that activate the AMPK homolog Snf1. Science signaling *6*, ra78.

Dohlman, H. G., Goldsmith, P., Spiegel, A. M., and Thorner, J. (1993). Pheromone action regulates G-protein alpha-subunit myristoylation in the yeast Saccharomyces cerevisiae. Proceedings of the National Academy of Sciences of the United States of America *90*, 9688-9692.

Hao, N., Nayak, S., Behar, M., Shanks, R. H., Nagiec, M. J., Errede, B., Hasty, J., Elston, T. C., and Dohlman, H. G. (2008). Regulation of cell signaling dynamics by the protein kinase-scaffold Ste5. Molecular cell *30*, 649-656.

Hardie, D. G., Carling, D., and Carlson, M. (1998). The AMP-activated/SNF1 protein kinase subfamily: metabolic sensors of the eukaryotic cell? Annual review of biochemistry *67*, 821-855.

Hardie, D. G., Ross, F. A., and Hawley, S. A. (2012). AMPK: a nutrient and energy sensor that maintains energy homeostasis. Nature reviews Molecular cell biology *13*, 251-262.

Lee, M. J., and Dohlman, H. G. (2008). Coactivation of G protein signaling by cell-surface receptors and an intracellular exchange factor. Current biology : CB *18*, 211-215.

Ludin, K., Jiang, R., and Carlson, M. (1998). Glucose-regulated interaction of a regulatory subunit of protein phosphatase 1 with the Snf1 protein kinase in Saccharomyces cerevisiae. Proceedings of the National Academy of Sciences of the United States of America *95*, 6245-6250.

Song, J., and Dohlman, H. G. (1996). Partial constitutive activation of pheromone responses by a palmitoylation-site mutant of a G protein alpha subunit in yeast. Biochemistry *35*, 14806-14817.

Sprague, G. F., Jr. (1991). Assay of yeast mating reaction. Methods in enzymology *194*, 77-93.

Stone, D. E., Cole, G. M., de Barros Lopes, M., Goebl, M., and Reed, S. I. (1991). N-myristoylation is required for function of the pheromone-responsive G alpha protein of yeast: conditional activation of the pheromone response by a temperature-sensitive N-myristoyl transferase. Genes & development *5*, 1969-1981.

Sutherland, C. M., Hawley, S. A., McCartney, R. R., Leech, A., Stark, M. J., Schmidt, M. C., and Hardie, D. G. (2003). Elm1p is one of three upstream kinases for the Saccharomyces cerevisiae SNF1 complex. Current biology : CB *13*, 1299-1305.

Torres, M. P., Clement, S. T., Cappell, S. D., and Dohlman, H. G. (2011). Cell cycle-dependent phosphorylation and ubiquitination of a G protein alpha subunit. The Journal of biological chemistry *286*, 20208-20216.

Ydenberg, C. A., and Rose, M. D. (2008). Yeast mating: a model system for studying cell and nuclear fusion. Methods in molecular biology *475*, 3-20.

## REFERENCES


Abe, F., and Iida, H. (2003). Pressure-Induced Differential Regulation of the Two Tryptophan Permeases Tat1 and Tat2 by Ubiquitin Ligase Rsp5 and Its Binding Proteins, Bul1 and Bul2. Molecular and cellular biology *23*, 7566-7584.

Acar, M., Becskei, A., and van Oudenaarden, A. (2005). Enhancement of cellular memory by reducing stochastic transitions. Nature *435*, 228-232.

Acar, M., Mettetal, J. T., and van Oudenaarden, A. (2008). Stochastic switching as a survival strategy in fluctuating environments. Nature genetics *40*, 471-475.

Adalsteinsson, D., McMillen, D., and Elston, T. C. (2004). Biochemical Network Stochastic Simulator (BioNetS): software for stochastic modeling of biochemical networks. BMC Bioinformatics *5*, 24.

Ali, N., Milligan, G., and Evans, W. H. (1989). Distribution of G-proteins in rat liver plasma-membrane domains and endocytotic pathways. Biochemical Journal *261*, 905-912.

Apanovitch, D. M., Iiri, T., Karasawa, T., Bourne, H. R., and Dohlman, H. G. (1998). Second site suppressor mutations of a GTPase-deficient G-protein alpha-subunit. Selective inhibition of Gbeta gamma-mediated signaling. The Journal of biological chemistry *273*, 28597-28602.

Arkin, A., Ross, J., and McAdams, H. H. (1998). Stochastic kinetic analysis of developmental pathway bifurcation in phage lambda-infected Escherichia coli cells. Genetics *149*, 1633-1648.

Arshavsky, V. Y., Lamb, T. D., and Pugh, E. N., Jr. (2002). G proteins and phototransduction. Annual review of physiology *64*, 153-187.

Audigier, Y., Nigam, S. K., and Blobel, G. (1988). Identification of a G protein in rough endoplasmic reticulum of canine pancreas. Journal of Biological Chemistry *263*, 16352-16357.

Avery, S. V. (2006). Microbial cell individuality and the underlying sources of heterogeneity. Nature reviews Microbiology *4*, 577-587.

Backer, J. M. (2008). The regulation and function of Class III PI3Ks: novel roles for Vps34. Biochemical Journal *410*, 1-17.

Bahar, R., Hartmann, C. H., Rodriguez, K. A., Denny, A. D., Busuttil, R. A., Dolle, M. E., Calder, R. B., Chisholm, G. B., Pollock, B. H., Klein, C. A., and Vijg, J. (2006).

Increased cell-to-cell variation in gene expression in ageing mouse heart. Nature *441*, 1011-1014.

Baker, R., Lewis, S. M., Sasaki, A. T., Wilkerson, E. M., Locasale, J. W., Cantley, L. C., Kuhlman, B., Dohlman, H. G., and Campbell, S. L. (2013). Site-specific monoubiquitination activates Ras by impeding GTPase-activating protein function. Nature structural & molecular biology *20*, 46-52.

Baker, R., Wilkerson, E. M., Sumita, K., Isom, D. G., Sasaki, A. T., Dohlman, H. G., and Campbell, S. L. (2013b). Differences in the regulation of K-Ras and H-Ras isoforms by monoubiquitination. The Journal of biological chemistry *288*, 36856-36862.

Balaban, N. Q., Merrin, J., Chait, R., Kowalik, L., and Leibler, S. (2004). Bacterial persistence as a phenotypic switch. Science *305*, 1622-1625.

Balazsi, G., van Oudenaarden, A., and Collins, J. J. (2011). Cellular decision making and biological noise: from microbes to mammals. Cell *144*, 910-925.

Ballon, D. R., Flanary, P. L., Gladue, D. P., Konopka, J. B., Dohlman, H. G., and Thorner, J. (2006). DEP-domain-mediated regulation of GPCR signaling responses. Cell *126*, 1079-1093.

Bansal, G., Druey, K. M., and Xie, Z. (2007). R4 RGS proteins: regulation of G-protein signaling and beyond. Pharmacology & therapeutics *116*, 473-495.

Bar-Even, A., Paulsson, J., Maheshri, N., Carmi, M., O'Shea, E., Pilpel, Y., and Barkai, N. (2006). Noise in protein expression scales with natural protein abundance. Nature genetics *38*, 636-643.

Bardwell, L. (2005). A walk-through of the yeast mating pheromone response pathway. Peptides *26*, 339-350.

Bean, J. M., Siggia, E. D., and Cross, F. R. (2006). Coherence and timing of cell cycle start examined at single-cell resolution. Molecular cell *21*, 3-14.

Becskei, A., Kaufmann, B. B., and van Oudenaarden, A. (2005). Contributions of low molecule number and chromosomal positioning to stochastic gene expression. Nat Genet *37*, 937-944.

Becskei, A., Seraphin, B., and Serrano, L. (2001). Positive feedback in eukaryotic gene networks: cell differentiation by graded to binary response conversion. EMBO J *20*, 2528-2535.

Becskei, A., and Serrano, L. (2000). Engineering stability in gene networks by autoregulation. Nature *405*, 590-593.

Berman, D. M., Kozasa, T., and Gilman, A. G. (1996a). The GTPase-activating Protein RGS4 Stabilizes the Transition State for Nucleotide Hydrolysis. Journal of Biological Chemistry *271*, 27209-27212.

Berman, D. M., Wilkie, T. M., and Gilman, A. G. (1996b). GAIP and RGS4 are GTPase-activating proteins for the Gi subfamily of G protein alpha subunits. Cell *86*, 445-452.

Betz, W. J., Mao, F., and Smith, C. B. (1996). Imaging exocytosis and endocytosis. Current opinion in neurobiology *6*, 365-371.

Biggar, S. R., and Crabtree, G. R. (2001). Cell signaling can direct either binary or graded transcriptional responses. The EMBO journal *20*, 3167-3176.

Bjarnadottir, T. K., Gloriam, D. E., Hellstrand, S. H., Kristiansson, H., Fredriksson, R., and Schioth, H. B. (2006). Comprehensive repertoire and phylogenetic analysis of the G protein-coupled receptors in human and mouse. Genomics *88*, 263-273.

Blake, W. J., Balazsi, G., Kohanski, M. A., Isaacs, F. J., Murphy, K. F., Kuang, Y., Cantor, C. R., Walt, D. R., and Collins, J. J. (2006). Phenotypic consequences of promoter-mediated transcriptional noise. Mol Cell *24*, 853-865.

Blake, W. J., M, K. A., Cantor, C. R., and Collins, J. J. (2003). Noise in eukaryotic gene expression. Nature *422*, 633-637.

Bourne, H. R., Landis, C. A., and Masters, S. B. (1989). Hydrolysis of GTP by the alpha-chain of Gs and other GTP binding proteins. Proteins *6*, 222-230.

Boyer, J. L., Graber, S. G., Waldo, G. L., Harden, T. K., and Garrison, J. C. (1994). Selective activation of phospholipase C by recombinant G-protein alpha- and beta gamma-subunits. The Journal of biological chemistry *269*, 2814-2819.

Brachmann, C. B., Davies, A., Cost, G. J., Caputo, E., Li, J., Hieter, P., and Boeke, J. D. (1998). Designer deletion strains derived from Saccharomyces cerevisiae S288C: a useful set of strains and plasmids for PCR-mediated gene disruption and other applications. Yeast *14*, 115-132.

Brandman, O., and Meyer, T. (2008). Feedback loops shape cellular signals in space and time. Science *322*, 390-395.

Brock, A., Chang, H., and Huang, S. (2009). Non-genetic heterogeneity--a mutation-independent driving force for the somatic evolution of tumours. Nature reviews Genetics *10*, 336-342.

Buck, L., and Axel, R. (1991). A novel multigene family may encode odorant receptors: a molecular basis for odor recognition. Cell *65*, 175-187.

Cai, L., Friedman, N., and Xie, X. S. (2006). Stochastic protein expression in individual cells at the single molecule level. Nature *440*, 358-362.

Calvert, M. E., Lannigan, J. A., and Pemberton, L. F. (2008). Optimization of yeast cell cycle analysis and morphological characterization by multispectral imaging flow cytometry. Cytometry A *73*, 825-833.

Cappell, S. D., Baker, R., Skowyra, D., and Dohlman, H. G. (2010). Systematic analysis of essential genes reveals important regulators of G protein signaling. Molecular cell *38*, 746-757.

Caudron, F., and Barral, Y. (2009). Septins and the lateral compartmentalization of eukaryotic membranes. Developmental cell *16*, 493-506.

Chaleff, D. T., and Tatchell, K. (1985). Molecular cloning and characterization of the STE7 and STE11 genes of Saccharomyces cerevisiae. Molecular and cellular biology *5*, 1878-1886.

Chan, R. K., and Otte, C. A. (1982a). Isolation and genetic analysis of Saccharomyces cerevisiae mutants supersensitive to G1 arrest by a factor and alpha factor pheromones. Molecular and cellular biology *2*, 11-20.

Chan, R. K., and Otte, C. A. (1982b). Physiological characterization of Saccharomyces cerevisiae mutants supersensitive to G1 arrest by a factor and alpha factor pheromones. Molecular and cellular biology *2*, 21-29.

Chandrashekar, J., Hoon, M. A., Ryba, N. J., and Zuker, C. S. (2006). The receptors and cells for mammalian taste. Nature *444*, 288-294.

Chang, F., and Herskowitz, I. (1990). Identification of a gene necessary for cell cycle arrest by a negative growth factor of yeast: FAR1 is an inhibitor of a G1 cyclin, CLN2. Cell *63*, 999-1011.

Chang, H. H., Hemberg, M., Barahona, M., Ingber, D. E., and Huang, S. (2008). Transcriptome-wide noise controls lineage choice in mammalian progenitor cells. Nature *453*, 544-547.

Chasse, S. A., Flanary, P., Parnell, S. C., Hao, N., Cha, J. Y., Siderovski, D. P., and Dohlman, H. G. (2006). Genome-scale analysis reveals Sst2 as the principal regulator of mating pheromone signaling in the yeast Saccharomyces cerevisiae. Eukaryotic cell *5*, 330-346.

Chau, V., Tobias, J. W., Bachmair, A., Marriott, D., Ecker, D. J., Gonda, D. K., and Varshavsky, A. (1989). A multiubiquitin chain is confined to specific lysine in a targeted short-lived protein. Science *243*, 1576-1583.

Chen, C. A., and Manning, D. R. (2001). Regulation of G proteins by covalent modification. Oncogene *20*, 1643-1652.

Chen, J. Y., Lin, J. R., Cimprich, K. A., and Meyer, T. (2012). A two-dimensional ERK-AKT signaling code for an NGF-triggered cell-fate decision. Molecular cell *45*, 196-209.

Chen, R. E., and Thorner, J. (2007). Function and regulation in MAPK signaling pathways: lessons learned from the yeast Saccharomyces cerevisiae. Biochimica et biophysica acta *1773*, 1311-1340.

Chess, A., Simon, I., Cedar, H., and Axel, R. (1994). Allelic inactivation regulates olfactory receptor gene expression. Cell *78*, 823-834.

Chisari, M., Saini, D. K., Kalyanaraman, V., and Gautam, N. (2007). Shuttling of G Protein Subunits between the Plasma Membrane and Intracellular Membranes. Journal of Biological Chemistry *282*, 24092-24098.

Cho, H., Harrison, K., and Kehrl, J. H. (2004). Regulators of G protein signaling: potential drug targets for controlling cardiovascular and immune function. Current drug targets Immune, endocrine and metabolic disorders *4*, 107-118.

Choi, P. J., Cai, L., Frieda, K., and Xie, X. S. (2008). A stochastic single-molecule event triggers phenotype switching of a bacterial cell. Science *322*, 442-446.

Clarke, T. F. I. V., and Clark, P. L. (2008). Rare Codons Cluster. PLoS One *3*, e3412.

Clement, S. T., Dixit, G., and Dohlman, H. G. (2013). Regulation of yeast G protein signaling by the kinases that activate the AMPK homolog Snf1. Science signaling *6*, ra78.

Cohen, A. A., Geva-Zatorsky, N., Eden, E., Frenkel-Morgenstern, M., Issaeva, I., Sigal, A., Milo, R., Cohen-Saidon, C., Liron, Y., Kam, Z.*, et al.* (2008). Dynamic proteomics of individual cancer cells in response to a drug. Science *322*, 1511-1516.

Coleman, D. E., Berghuis, A. M., Lee, E., Linder, M., Gilman, A. G., and Sprang, S. (1994). Structures of active conformations of Gi alpha 1 and the mechanism of GTP hydrolysis. Science *265*, 1405-1412.

Colman-Lerner, A., Gordon, A., Serra, E., Chin, T., Resnekov, O., Endy, D., Pesce, C. G., and Brent, R. (2005). Regulated cell-to-cell variation in a cell-fate decision system. Nature *437*, 699-706.

Cook, D. L., Gerber, A. N., and Tapscott, S. J. (1998). Modeling stochastic gene expression: implications for haploinsufficiency. Proc Natl Acad Sci U S A *95*, 15641-15646.

Cotari, J. W., Voisinne, G., and Altan-Bonnet, G. (2013a). Diversity training for signal transduction: leveraging cell-to-cell variability to dissect cellular signaling, differentiation and death. Current opinion in biotechnology *24*, 760-766.

Cotari, J. W., Voisinne, G., Dar, O. E., Karabacak, V., and Altan-Bonnet, G. (2013b). Cell-to-cell variability analysis dissects the plasticity of signaling of common gamma chain cytokines in T cells. Science signaling *6*, ra17.

Crouch, M. F., Davy, D. A., Willard, F. S., and Berven, L. A. (2000). Insulin induces epidermal growth factor (EGF) receptor clustering and potentiates EGF-stimulated DNA synthesis in Swiss 3T3 cells: A mechanism for costimulation in mitogenic synergy. Immunological Cell Biology *78*, 408-414.

das Neves, R. P., Jones, N. S., Andreu, L., Gupta, R., Enver, T., and Iborra, F. J. (2010). Connecting variability in global transcription rate to mitochondrial variability. PLoS biology *8*, e1000560.

Delbruck, M. (1945). The Burst Size Distribution in the Growth of Bacterial Viruses (Bacteriophages). J Bacteriol *50*, 131-135.

Deutschbauer, A. M., Jaramillo, D. F., Proctor, M., Kumm, J., Hillenmeyer, M. E., Davis, R. W., Nislow, C., and Giaever, G. (2005). Mechanisms of haploinsufficiency revealed by genome-wide profiling in yeast. Genetics *169*, 1915-1925.

Dhar, N., and McKinney, J. D. (2007). Microbial phenotypic heterogeneity and antibiotic tolerance. Current opinion in microbiology *10*, 30-38.

Di Talia, S., Skotheim, J. M., Bean, J. M., Siggia, E. D., and Cross, F. R. (2007). The effects of molecular noise and size control on variability in the budding yeast cell cycle. Nature *448*, 947-951.

DiBello, P. R., Garrison, T. R., Apanovitch, D. M., Hoffman, G., Shuey, D. J., Mason, K., Cockett, M. I., and Dohlman, H. G. (1998). Selective uncoupling of RGS action by a single point mutation in the G protein alpha-subunit. The Journal of biological chemistry *273*, 5780-5784.

Dikic, I., Wakatsuki, S., and Walters, K. J. (2009a). Ubiquitin-binding domains - from structures to functions. Nature reviews Molecular cell biology *10*, 659-671.

Dikic, I., Wakatsuki, S., and Walters, K. J. (2009b). Ubiquitin-binding domains [mdash] from structures to functions. Nature Reviews Molecular Cell Biology *10*, 659-671.

Dohlman, H. G. (2002). G proteins and pheromone signaling. Annual review of physiology *64*, 129-152.

Dohlman, H. G., Apaniesk, D., Chen, Y., Song, J., and Nusskern, D. (1995). Inhibition of G-protein signaling by dominant gain-of-function mutations in Sst2p, a pheromone desensitization factor in Saccharomyces cerevisiae. Molecular and cellular biology *15*, 3635-3643.

Dohlman, H. G., Goldsmith, P., Spiegel, A. M., and Thorner, J. (1993). Pheromone action regulates G-protein alpha-subunit myristoylation in the yeast Saccharomyces cerevisiae. Proceedings of the National Academy of Sciences of the United States of America *90*, 9688-9692.

Dohlman, H. G., and Jones, J. C. (2012). Signal Activation and Inactivation by the G{alpha} Helical Domain: A Long-Neglected Partner in G Protein Signaling. Science Signalling *5*.

Dohlman, H. G., Song, J., Ma, D., Courchesne, W. E., and Thorner, J. (1996). Sst2, a negative regulator of pheromone signaling in the yeast Saccharomyces cerevisiae: expression, localization, and genetic interaction and physical association with Gpa1 (the G-protein alpha subunit). Molecular and cellular biology *16*, 5194-5209.

Dohlman, H. G., and Thorner, J. (2001a). Regulation of G Protein Initiated Signal Transduction in Yeast: Paradigms and Principles. Annual Review of Biochemistry *70*, 703-754.

Dohlman, H. G., and Thorner, J. W. (2001b). Regulation of G protein-initiated signal transduction in yeast: paradigms and principles. Annu Rev Biochem *70*, 703-754.

Dolan, J. W., Kirkman, C., and Fields, S. (1989). The yeast STE12 protein binds to the DNA sequence mediating pheromone induction. Proceedings of the National Academy of Sciences of the United States of America *86*, 5703-5707.

Donaldson, K. M., Yin, H., Gekakis, N., Supek, F., and Joazeiro, C. A. (2003). Ubiquitin signals protein trafficking via interaction with a novel ubiquitin binding domain in the membrane fusion regulator, Vps9p. Current biology : CB *13*, 258-262.

Doncic, A., Falleur-Fettig, M., and Skotheim, J. M. (2011). Distinct interactions select and maintain a specific cell fate. Molecular cell *43*, 528-539.

Dores, M. R., Schnell, J. D., Maldonado-Baez, L., Wendland, B., and Hicke, L. (2010). The function of yeast epsin and Ede1 ubiquitin-binding domains during receptor internalization. Traffic *11*, 151-160.

Drews, J. (2000). Drug discovery: a historical perspective. Science *287*, 1960-1964.

Dublanche, Y., Michalodimitrakis, K., Kummerer, N., Foglierini, M., and Serrano, L. (2006). Noise in transcription negative feedback loops: simulation and experimental analysis. Molecular systems biology *2*, 41.

Dunn, R., and Hicke, L. (2001). Domains of the Rsp5 ubiquitin-protein ligase required for receptor-mediated and fluid-phase endocytosis. Molecular biology of the cell *12*, 421-435.

Elf, J., Li, G. W., and Xie, X. S. (2007). Probing transcription factor dynamics at the single-molecule level in a living cell. Science *316*, 1191-1194.

Elion, E. A., Grisafi, P. L., and Fink, G. R. (1990). FUS3 encodes a cdc2+/CDC28-related kinase required for the transition from mitosis into conjugation. Cell *60*, 649-664.

Elion, E. A., Satterberg, B., and Kranz, J. E. (1993). FUS3 phosphorylates multiple components of the mating signal transduction cascade: evidence for STE12 and FAR1. Molecular biology of the cell *4*, 495-510.

Elowitz, M. B., Levine, A. J., Siggia, E. D., and Swain, P. S. (2002). Stochastic gene expression in a single cell. Science *297*, 1183-1186.

Emmert-Buck, M. R., Bonner, R. F., Smith, P. D., Chuaqui, R. F., Zhuang, Z., Goldstein, S. R., Weiss, R. A., and Liotta, L. A. (1996). Laser capture microdissection. Science *274*, 998-1001.

Ercolani, L., Stow, J. L., Boyle, J. F., Holtzman, E. J., Lin, H., Grove, J. R., and Ausiello, D. A. (1990).
Membrane localization of the pertussis toxin-sensitive G-protein subunits alpha i-2 and alpha i-3 and expression of a metallothionein-alpha i-2 fusion gene in LLC-PK1 cells. Proceedings of the National Academy of Sciences *87*, 4635-4639.

Erdman, S., Lin, L., Malczynski, M., and Snyder, M. (1998). Pheromone-regulated genes required for yeast mating differentiation. The Journal of cell biology *140*, 461-483.

Errede, B., and Ammerer, G. (1989). STE12, a protein involved in cell-type-specific transcription and signal transduction in yeast, is part of protein-DNA complexes. Genes & development *3*, 1349-1361.

Errede, B., and Levin, D. E. (1993). A conserved kinase cascade for MAP kinase activation in yeast. Current opinion in cell biology *5*, 254-260.

Falconnet, D., Niemisto, A., Taylor, R. J., Ricicova, M., Galitski, T., Shmulevich, I., and Hansen, C. L. (2011). High-throughput tracking of single yeast cells in a microfluidic imaging matrix. Lab on a chip *11*, 466-473.

Farfel, Z., Bourne, H. R., and Iiri, T. (1999). The expanding spectrum of G protein diseases. The New England journal of medicine *340*, 1012-1020.

Feinerman, O., Veiga, J., Dorfman, J. R., Germain, R. N., and Altan-Bonnet, G. (2008). Variability and robustness in T cell activation from regulated heterogeneity in protein levels. Science *321*, 1081-1084.

Feng, Y., Song, L. Y., Kincaid, E., Mahanty, S. K., and Elion, E. A. (1998). Functional binding between Gbeta and the LIM domain of Ste5 is required to activate the MEKK Ste11. Current biology : CB *8*, 267-278.

Ferrell, J. E., Jr., and Machleder, E. M. (1998). The biochemical basis of an all-or-none cell fate switch in Xenopus oocytes. Science *280*, 895-898.

Fiedler, D., Braberg, H., Mehta, M., Chechik, G., Cagney, G., Mukherjee, P., Silva, A. C., Shales, M., Collins, S. R., van Wageningen, S.*, et al.* (2009). Functional organization of the S. cerevisiae phosphorylation network. Cell *136*, 952-963.

Fields, S., and Herskowitz, I. (1985). The yeast STE12 product is required for expression of two sets of cell-type specific genes. Cell *42*, 923-930.

Fields, S., and Herskowitz, I. (1987). Regulation by the yeast mating-type locus of STE12, a gene required for cell-type-specific expression. Molecular and cellular biology *7*, 3818-3821.

Fischer, T., De Vries, L., Meerloo, T., and Farquhar, M. G. (2003). Promotion of G alpha i3 subunit down-regulation by GIPN, a putative E3 ubiquitin ligase that interacts with RGS-GAIP. Proceedings of the National Academy of Sciences of the United States of America *100*, 8270-8275.

Fraser, H. B., Hirsh, A. E., Giaever, G., Kumm, J., and Eisen, M. B. (2004). Noise minimization in eukaryotic gene expression. PLoS biology *2*, e137.

Frechter, S., Elia, N., Tzarfaty, V., Selinger, Z., and Minke, B. (2007a). Translocation of Gq alpha mediates long-term adaptation in Drosophila photoreceptors. The Journal of neuroscience : the official journal of the Society for Neuroscience *27*, 5571-5583.

Freed, N. E., Silander, O. K., Stecher, B., Bohm, A., Hardt, W. D., and Ackermann, M. (2008). A simple screen to identify promoters conferring high levels of phenotypic noise. PLoS genetics *4*, e1000307.

Gabriely, G., Kama, R., Gelin-Licht, R., and Gerst, J. E. (2008). Different Domains of the UBL-UBA Ubiquitin Receptor, Ddi1/Vsm1, Are Involved in Its Multiple Cellular Roles. Molecular Biology of the Cell *19*, 3625-3637.

Gagny, B., Wiederkehr, A., Dumoulin, P., Winsor, B., Riezman, H., and Haguenauer-Tsapis, R. (2000). A novel EH domain protein of Saccharomyces cerevisiae, Ede1p, involved in endocytosis. Journal of cell science *113 ( Pt 18)*, 3309-3319.

Gainetdinov, R. R., Premont, R. T., Bohn, L. M., Lefkowitz, R. J., and Caron, M. G. (2004). Desensitization of G protein-coupled receptors and neuronal functions. Annual review of neuroscience *27*, 107-144.

Garcia-Marcos, M., Ghosh, P., and Farquhar, M. G. (2009). GIV is a nonreceptor GEF for G alpha i with a unique motif that regulates Akt signaling. Proceedings of the National Academy of Sciences of the United States of America *106*, 3178-3183.

Gascoigne, K. E., and Taylor, S. S. (2008). Cancer cells display profound intra- and interline variation following prolonged exposure to antimitotic drugs. Cancer Cell *14*, 111-122.

Ghaemmaghami, S., Huh, W. K., Bower, K., Howson, R. W., Belle, A., Dephoure, N., O'Shea, E. K., and Weissman, J. S. (2003). Global analysis of protein expression in yeast. Nature *425*, 737-741.

Giaever, G., Chu, A. M., Ni, L., Connelly, C., Riles, L., Veronneau, S., Dow, S., Lucau-Danila, A., Anderson, K., Andre, B.*, et al.* (2002). Functional profiling of the Saccharomyces cerevisiae genome. Nature *418*, 387-391.

Gilman, A. G. (1987). G proteins: transducers of receptor-generated signals. Annual review of biochemistry *56*, 615-649.

Gladfelter, A. S., Kozubowski, L., Zyla, T. R., and Lew, D. J. (2005). Interplay between septin organization, cell cycle and cell shape in yeast. Journal of cell science *118*, 1617-1628.

Goffeau, A., Barrell, B. G., Bussey, H., Davis, R. W., Dujon, B., Feldmann, H., Galibert, F., Hoheisel, J. D., Jacq, C., Johnston, M.*, et al.* (1996). Life with 6000 genes. Science *274*, 546, 563-547.

Golding, I., Paulsson, J., Zawilski, S. M., and Cox, E. C. (2005). Real-time kinetics of gene activity in individual bacteria. Cell *123*, 1025-1036.

Goley, E. D., Rodenbusch, S. E., Martin, A. C., and Welch, M. D. (2004). Critical conformational changes in the Arp2/3 complex are induced by nucleotide and nucleation promoting factor. Molecular cell *16*, 269-279.

Gordon, A., Colman-Lerner, A., Chin, T. E., Benjamin, K. R., Yu, R. C., and Brent, R. (2007). Single-cell quantification of molecules and rates using open-source microscope-based cytometry. Nat Methods *4*, 175-181.

Gregor, T., Fujimoto, K., Masaki, N., and Sawai, S. (2010). The onset of collective behavior in social amoebae. Science *328*, 1021-1025.

Gu, Z., Jiang, Q., and Yan, Z. (2007). RGS4 modulates serotonin signaling in prefrontal cortex and links to serotonin dysfunction in a rat model of schizophrenia. Molecular pharmacology *71*, 1030-1039.

Guptasarma, P. (1995). Does replication-induced transcription regulate synthesis of the myriad low copy number proteins of Escherichia coli? BioEssays : news and reviews in molecular, cellular and developmental biology *17*, 987-997.

Gustin, M. C., Albertyn, J., Alexander, M., and Davenport, K. (1998). MAP kinase pathways in the yeast Saccharomyces cerevisiae. Microbiology and molecular biology reviews : MMBR *62*, 1264-1300.

Hagopian, M. (1970). Intercellular attachments of cockroach nymph epidermal cells. Journal of ultrastructure research *33*, 233-244.

Hammond-Martel, I., Yu, H., and Affar el, B. (2012). Roles of ubiquitin signaling in transcription regulation. Cellular signalling *24*, 410-421.

Hao, N., Behar, M., Elston, T. C., and Dohlman, H. G. (2007a). Systems biology analysis of G protein and MAP kinase signaling in yeast. Oncogene *26*, 3254-3266.

Hao, N., Behar, M., Parnell, S. C., Torres, M. P., Borchers, C. H., Elston, T. C., and Dohlman, H. G. (2007b). A systems-biology analysis of feedback inhibition in the Sho1 osmotic-stress-response pathway. Curr Biol *17*, 659-667.

Hao, N., Nayak, S., Behar, M., Shanks, R. H., Nagiec, M. J., Errede, B., Hasty, J., Elston, T. C., and Dohlman, H. G. (2008). Regulation of cell signaling dynamics by the protein kinase-scaffold Ste5. Mol Cell *30*, 649-656.

Hartwell, L. H., Culotti, J., and Reid, B. (1970). Genetic control of the cell-division cycle in yeast. I. Detection of mutants. Proceedings of the National Academy of Sciences of the United States of America *66*, 352-359.

Hartwell, L. H., Mortimer, R. K., Culotti, J., and Culotti, M. (1973). Genetic Control of the Cell Division Cycle in Yeast: V. Genetic Analysis of cdc Mutants. Genetics *74*, 267-286.

Harvey, C. D., Ehrhardt, A. G., Cellurale, C., Zhong, H., Yasuda, R., Davis, R. J., and Svoboda, K. (2008). A genetically encoded fluorescent sensor of ERK activity. Proceedings of the National Academy of Sciences of the United States of America *105*, 19264-19269.

Hershko, A., Heller, H., Elias, S., and Ciechanover, A. (1983). Components of ubiquitin-protein ligase system. Resolution, affinity purification, and role in protein breakdown. The Journal of biological chemistry *258*, 8206-8214.

Hershko, A., Heller, H., Eytan, E., and Reiss, Y. (1986). The protein substrate binding site of the ubiquitin-protein ligase system. The Journal of biological chemistry *261*, 11992-11999.

Hicke, L. (1999). Gettin' down with ubiquitin: turning off cell-surface receptors, transporters and channels. Trends in Cell Biology *9*, 107.

Hicke, L. (2001). Protein regulation by monoubiquitin. Nature reviews Molecular cell biology *2*, 195-201.

Hicke, L., and Riezman, H. (1996). Ubiquitination of a yeast plasma membrane receptor signals its ligand-stimulated endocytosis. Cell *84*, 277-287.

Hicke, L., Schubert, H. L., and Hill, C. P. (2005). Ubiquitin-binding domains. Nature reviews Molecular cell biology *6*, 610-621.

Hicke, L., Zanolari, B., and Riezman, H. (1998). Cytoplasmic tail phosphorylation of the alpha-factor receptor is required for its ubiquitination and internalization. The Journal of cell biology *141*, 349-358.

Hicks, J. B., and Herskowitz, I. (1976). Evidence for a new diffusible element of mating pheromones in yeast. Nature *260*, 246-248.

Higashijima, T., Ferguson, K. M., Sternweis, P. C., Ross, E. M., Smigel, M. D., and Gilman, A. G. (1987). The effect of activating ligands on the intrinsic fluorescence of guanine nucleotide-binding regulatory proteins. Journal of Biological Chemistry *262*, 752-756.

Hildebrandt, J. D. (1997). Role of subunit diversity in signaling by heterotrimeric G proteins. Biochemical pharmacology *54*, 325-339.

Hiraki, T., and Abe, F. (2010). Overexpression of Sna3 stabilizes tryptophan permease Tat2, potentially competing for the WW domain of Rsp5 ubiquitin ligase with its binding protein Bul1. FEBS Letters *584*, 55-60.

Hislop, J. N., and von Zastrow, M. (2011). Role of ubiquitination in endocytic trafficking of G-protein-coupled receptors. Traffic *12*, 137-148.

Hoang, T. (2004). The origin of hematopoietic cell type diversity. Oncogene *23*, 7188-7198.

Hoffman, G. A., Garrison, T. R., and Dohlman, H. G. (2000). Endoproteolytic processing of Sst2, a multidomain regulator of G protein signaling in yeast. J Biol Chem *275*, 37533-37541.

Hoffman, G. A., Garrison, T. R., and Dohlman, H. G. (2002). Analysis of RGS proteins in Saccharomyces cerevisiae. Methods Enzymol *344*, 617-631.

Hooshangi, S., Thiberge, S., and Weiss, R. (2005). Ultrasensitivity and noise propagation in a synthetic transcriptional cascade. Proceedings of the National Academy of Sciences of the United States of America *102*, 3581-3586.

Hooshangi, S., and Weiss, R. (2006). The effect of negative feedback on noise propagation in transcriptional gene networks. Chaos *16*, 026108.

Hornung, G., and Barkai, N. (2008). Noise propagation and signaling sensitivity in biological networks: a role for positive feedback. PLoS Comput Biol *4*, e8.

Houser, J. R., Ford, E., Nagiec, M. J., Errede, B., and Elston, T. C. (2012). Positive roles for negative regulators in the mating response of yeast. Molecular systems biology *8*, 586.

Hu, J., Nudelman, G., Shimoni, Y., Kumar, M., Ding, Y., Lopez, C., Hayot, F., Wetmur, J. G., and Sealfon, S. C. (2011). Role of cell-to-cell variability in activating a positive feedback antiviral response in human dendritic cells. PLoS One *6*, e16614.

Huh, W. K., Falvo, J. V., Gerke, L. C., Carroll, A. S., Howson, R. W., Weissman, J. S., and O'Shea, E. K. (2003). Global analysis of protein localization in budding yeast. Nature *425*, 686-691.

Hur, E.-M., and Kim, K.-T. (2002). G protein-coupled receptor signalling and cross-talk: Achieving rapidity and specificity. Cellular Signalling *14*, 397-405.

Hurley, J., Lee, S., and Prag, G. (2006a). Ubiquitin-Binding Domains. Biochemistry Journal *399*, 361-372.

Hurley, J. H. (2010). The ESCRT complexes. Critical reviews in biochemistry and molecular biology *45*, 463-487.

Hurley, J. H., Lee, S., and Prag, G. (2006b). Ubiquitin-binding domains. The Biochemical journal *399*, 361-372.

Hurley, J. H., and Stenmark, H. (2011). Molecular mechanisms of ubiquitin-dependent membrane traffic. Annual review of biophysics *40*, 119-142.

Hurowitz, E. H., Melnyk, J. M., Chen, Y. J., Kouros-Mehr, H., Simon, M. I., and Shizuya, H. (2000). Genomic characterization of the human heterotrimeric G protein alpha, beta, and gamma subunit genes. DNA research : an international journal for rapid publication of reports on genes and genomes *7*, 111-120.

Hurst, J. H., and Dohlman, H. G. (2013). Dynamic ubiquitination of the mitogen-activated protein kinase kinase (MAPKK) Ste7 determines mitogen-activated protein kinase (MAPK) specificity. The Journal of biological chemistry *288*, 18660-18671.

Hurst, J. H., and Hooks, S. B. (2009). Regulator of G-protein signaling (RGS) proteins in cancer biology. Biochemical pharmacology *78*, 1289-1297.

Husnjak, K., and Dikic, I. (2012). Ubiquitin-Binding Proteins: Decoders of Ubiquitin-Mediated Cellular Functions. Annual Review of Biochemistry *81*, 291-322.

Inouye, C., Dhillon, N., and Thorner, J. (1997). Ste5 RING-H2 domain: role in Ste4-promoted oligomerization for yeast pheromone signaling. Science *278*, 103-106.

Irannejad, R., Tomshine, J. C., Tomshine, J. R., Chevalier, M., Mahoney, J. P., Steyaert, J., Rasmussen, S. G., Sunahara, R. K., El-Samad, H., Huang, B., and von Zastrow, M. (2013a). Conformational biosensors reveal GPCR signalling from endosomes. Nature *495*, 534-538.

Irannejad, R., Tomshine, J. C., Tomshine, J. R., Chevalier, M., Mahoney, J. P., Steyaert, J., Rasmussen, S. G. F., Sunahara, R. K., El-Samad, H., Huang, B., and von Zastrow, M. (2013b). Conformational biosensors reveal GPCR signalling from endosomes. Nature *495*, 534-538.

Isaacs, F. J., Hasty, J., Cantor, C. R., and Collins, J. J. (2003). Prediction and measurement of an autoregulatory genetic module. Proc Natl Acad Sci U S A *100*, 7714-7719.

Isom, D. G., Marguet, P. R., Oas, T. G., and Hellinga, H. W. (2011). A miniaturized technique for assessing protein thermodynamics and function using fast determination of quantitative cysteine reactivity. Proteins: Struct, Funct, and Bioinf *79*, 1034-1047.

Isom, Daniel G., Sridharan, V., Baker, R., Clement, Sarah T., Smalley, David M., and Dohlman, Henrik G. (2013). Protons as Second Messenger Regulators of G Protein Signaling. Molecular Cell *51*, 531-538.

Jackson, C. L., and Hartwell, L. H. (1990). Courtship in S. cerevisiae: both cell types choose mating partners by responding to the strongest pheromone signal. Cell *63*, 1039-1051.

Jahng, K. Y., Ferguson, J., and Reed, S. I. (1988). Mutations in a gene encoding the alpha subunit of a Saccharomyces cerevisiae G protein indicate a role in mating pheromone signaling. Molecular and cellular biology *8*, 2484-2493.

Jan, Y. N., and Jan, L. Y. (1995). Maggot's hair and bug's eye: role of cell interactions and intrinsic factors in cell fate specification. Neuron *14*, 1-5.

Jenness, D. D., and Spatrick, P. (1986). Down regulation of the alpha-factor pheromone receptor in S. cerevisiae. Cell *46*, 345-353.

Jeschke, M., Baumgartner, S., and Legewie, S. (2013). Determinants of cell-to-cell variability in protein kinase signaling. PLoS computational biology *9*, e1003357.

Johnson, D. I. (1999). Cdc42: An essential Rho-type GTPase controlling eukaryotic cell polarity. Microbiology and molecular biology reviews : MMBR *63*, 54-105.

Johnston, I. G., Gaal, B., Neves, R. P., Enver, T., Iborra, F. J., and Jones, N. S. (2012). Mitochondrial variability as a source of extrinsic cellular noise. PLoS computational biology *8*, e1002416.

Johnston, R. J., Jr., and Desplan, C. (2010). Stochastic mechanisms of cell fate specification that yield random or robust outcomes. Annual review of cell and developmental biology *26*, 689-719.

Jones, J. C., Jones, A. M., Temple, B. R. S., and Dohlman, H. G. (2012). Differences in intradomain and interdomain motion confer distinct activation properties to structurally similar Gα proteins. Proceedings of the National Academy of Sciences *109*, 7275-7279.

Jones, T. R., Carpenter, A. E., Lamprecht, M. R., Moffat, J., Silver, S. J., Grenier, J. K., Castoreno, A. B., Eggert, U. S., Root, D. E., Golland, P., and Sabatini, D. M. (2009). Scoring diverse cellular morphologies in image-based screens with iterative feedback and machine learning. Proceedings of the National Academy of Sciences of the United States of America *106*, 1826-1831.

Kaern, M., Elston, T. C., Blake, W. J., and Collins, J. J. (2005). Stochasticity in gene expression: from theories to phenotypes. Nat Rev Genet *6*, 451-464.

Kalita, M. K., Sargsyan, K., Tian, B., Paulucci-Holthauzen, A., Najm, H. N., Debusschere, B. J., and Brasier, A. R. (2011). Sources of cell-to-cell variability in canonical nuclear factor-kappaB (NF-kappaB) signaling pathway inferred from single cell dynamic images. The Journal of biological chemistry *286*, 37741-37757.

Katritch, V., Cherezov, V., and Stevens, R. C. (2013). Structure-function of the G protein-coupled receptor superfamily. Annual review of pharmacology and toxicology *53*, 531-556.

Kaufmann, B. B., and van Oudenaarden, A. (2007). Stochastic gene expression: from single molecules to the proteome. Current opinion in genetics & development *17*, 107-112.

Kee, Y., Lyon, N., and Huibregtse, J. M. (2005). The Rsp5 ubiquitin ligase is coupled to and antagonized by the Ubp2 deubiquitinating enzyme. The EMBO Journal *24*, 2414-2424.

Kelly, C. D., and Rahn, O. (1932). The Growth Rate of Individual Bacterial Cells. Journal of bacteriology *23*, 147-153.

Kennedy, B. K., Austriaco, N. R., Jr., Zhang, J., and Guarente, L. (1995). Mutation in the silencing gene SIR4 can delay aging in S. cerevisiae. Cell *80*, 485-496.

Kepler, T. B., and Elston, T. C. (2001). Stochasticity in transcriptional regulation: origins, consequences, and mathematical representations. Biophysical journal *81*, 3116-3136.

Keren, I., Shah, D., Spoering, A., Kaldalu, N., and Lewis, K. (2004). Specialized persister cells and the mechanism of multidrug tolerance in Escherichia coli. Journal of bacteriology *186*, 8172-8180.

Kleuss, C., Raw, A. S., Lee, E., Sprang, S. R., and Gilman, A. G. (1994). Mechanism of GTP hydrolysis by G-protein alpha subunits. Proceedings of the National Academy of Sciences *91*, 9828-9831.

Ko, M. S. (1991). A stochastic model for gene induction. J Theor Biol *153*, 181-194.

Koelle, M. R., and Horvitz, H. R. (1996). EGL-10 regulates G protein signaling in the C. elegans nervous system and shares a conserved domain with many mammalian proteins. Cell *84*, 115-125.

Kolitz, S. E., and Lauffenburger, D. A. (2012). Measurement and modeling of signaling at the single-cell level. Biochemistry *51*, 7433-7443.

Kosako, H., Nishida, E., and Gotoh, Y. (1993). cDNA cloning of MAP kinase kinase reveals kinase cascade pathways in yeasts to vertebrates. The EMBO journal *12*, 787-794.

Kussell, E., Kishony, R., Balaban, N. Q., and Leibler, S. (2005). Bacterial persistence: a model of survival in changing environments. Genetics *169*, 1807-1814.

Kussell, E., and Leibler, S. (2005). Phenotypic diversity, population growth, and information in fluctuating environments. Science *309*, 2075-2078.

Lam, M., Urban-Grimal, D., Bugnicourt, A., Greenblatt, J., Haguenauer-Tsapis, R., and Emili, A. (2009). Interaction of the Deubiquitinating Enzyme Ubp2 and the E3 Ligase Rsp5 Is Required for Transporter/Receptor Sorting in the Multivesicular Body Pathway. PLoS One.

Lambert, N. A., Johnston, C. A., Cappell, S. D., Kuravi, S., Kimple, A. J., Willard, F. S., and Siderovski, D. P. Regulators of G-protein signaling accelerate GPCR signaling kinetics and govern sensitivity solely by accelerating GTPase activity. Proc Natl Acad Sci U S A *107*, 7066-7071.

Lan, K. L., Sarvazyan, N. A., Taussig, R., Mackenzie, R. G., DiBello, P. R., Dohlman, H. G., and Neubig, R. R. (1998). A point mutation in Galphao and Galphai1 blocks interaction with regulator of G protein signaling proteins. The Journal of biological chemistry *273*, 12794-12797.

Le, T. T., Harlepp, S., Guet, C. C., Dittmar, K., Emonet, T., Pan, T., and Cluzel, P. (2005). Real-time RNA profiling within a single bacterium. Proceedings of the National Academy of Sciences of the United States of America *102*, 9160-9164.

Leberer, E., Dignard, D., Harcus, D., Thomas, D. Y., and Whiteway, M. (1992). The protein kinase homologue Ste20p is required to link the yeast pheromone response G-protein beta gamma subunits to downstream signalling components. The EMBO journal *11*, 4815-4824.

Lee, M. J., and Dohlman, H. G. (2008). Coactivation of G protein signaling by cell-surface receptors and an intracellular exchange factor. Current biology : CB *18*, 211-215.

Lee, S. S., Avalos Vizcarra, I., Huberts, D. H., Lee, L. P., and Heinemann, M. (2012). Whole lifespan microscopic observation of budding yeast aging through a microfluidic dissection platform. Proceedings of the National Academy of Sciences of the United States of America *109*, 4916-4920.

Levsky, J. M., and Singer, R. H. (2003). Gene expression and the myth of the average cell. Trends in cell biology *13*, 4-6.

Levy, S. F., Ziv, N., and Siegal, M. L. (2012). Bet hedging in yeast by heterogeneous, age-correlated expression of a stress protectant. PLoS biology *10*, e1001325.

Lewis, K. (2007). Persister cells, dormancy and infectious disease. Nature reviews Microbiology *5*, 48-56.

Li, X., Gerber, S. A., Rudner, A. D., Beausoleil, S. A., Haas, W., Villén, J., Elias, J. E., and Gygi, S. P. (2007). Large-Scale Phosphorylation Analysis of α-Factor-Arrested Saccharomyces cerevisiae. Journal of Proteome Research *6*, 1190-1197.

Lidstrom, M. E., and Konopka, M. C. (2010). The role of physiological heterogeneity in microbial population behavior. Nature chemical biology *6*, 705-712.

Lidstrom, M. E., and Meldrum, D. R. (2003). Life-on-a-chip. Nature reviews Microbiology *1*, 158-164.

Lipson, D., Raz, T., Kieu, A., Jones, D. R., Giladi, E., Thayer, E., Thompson, J. F., Letovsky, S., Milos, P., and Causey, M. (2009). Quantification of the yeast transcriptome by single-molecule sequencing. Nature biotechnology *27*, 652-658.

Liu, S., and Chen, Z. J. (2011). Expanding role of ubiquitination in NF-kappaB signaling. Cell research *21*, 6-21.

Liu, W., Kim, H. J., Lucchetta, E. M., Du, W., and Ismagilov, R. F. (2009). Isolation, incubation, and parallel functional testing and identification by FISH of rare microbial single-copy cells from multi-species mixtures using the combination of chemistrode and stochastic confinement. Lab on a chip *9*, 2153-2162.

Liu, Y., and Xiao, W. (1997). Bidirectional regulation of two DNA-damage-inducible genes, MAG1 and DDI1, from Saccharomyces cerevisiae. Molecular microbiology *23*, 777-789.

Lobner-Olesen, A. (1999). Distribution of minichromosomes in individual Escherichia coli cells: implications for replication control. The EMBO journal *18*, 1712-1721.

Longo, D., and Hasty, J. (2006). Dynamics of single-cell gene expression. Molecular systems biology *2*, 64.

Losick, R., and Desplan, C. (2008). Stochasticity and cell fate. Science *320*, 65-68.

Luttrell, L. M. (2008). Reviews in molecular biology and biotechnology: transmembrane signaling by G protein-coupled receptors. Molecular biotechnology *39*, 239-264.

Maamar, H., and Dubnau, D. (2005). Bistability in the Bacillus subtilis K-state (competence) system requires a positive feedback loop. Molecular microbiology *56*, 615-624.

Maamar, H., Raj, A., and Dubnau, D. (2007). Noise in gene expression determines cell fate in Bacillus subtilis. Science *317*, 526-529.

MacGurn, J. A., Hsu, P.-C., and Emr, S. D. (2012). Ubiquitin and Membrane Protein Turnover: From Cradle to Grave. Annual Review of Biochemistry *81*, 231-259.

Madden, K., and Snyder, M. (1998). Cell polarity and morphogenesis in budding yeast. Annual review of microbiology *52*, 687-744.

Madura, K., and Varshavsky, A. (1994). Degradation of G alpha by the N-end rule pathway. Science *265*, 1454-1458.

Magee, J. A., Abdulkadir, S. A., and Milbrandt, J. (2003). Haploinsufficiency at the Nkx3.1 locus. A paradigm for stochastic, dosage-sensitive gene regulation during tumor initiation. Cancer Cell *3*, 273-283.

Maheshri, N., and O'Shea, E. K. (2007). Living with noisy genes: how cells function reliably with inherent variability in gene expression. Annual review of biophysics and biomolecular structure *36*, 413-434.

Maloney, P. C., and Rotman, B. (1973). Distribution of suboptimally induces -D-galactosidase in Escherichia coli. The enzyme content of individual cells. Journal of molecular biology *73*, 77-91.

Marchese, A., and Trejo, J. (2013). Ubiquitin-dependent regulation of G protein-coupled receptor trafficking and signaling. Cellular signalling *25*, 707-716.

Marcus, J. S., Anderson, W. F., and Quake, S. R. (2006). Microfluidic single-cell mRNA isolation and analysis. Analytical chemistry *78*, 3084-3089.

Marotti, L. A., Jr., Newitt, R., Wang, Y., Aebersold, R., and Dohlman, H. G. (2002). Direct identification of a G protein ubiquitination site by mass spectrometry. Biochemistry *41*, 5067-5074.

Mateus, C., and Avery, S. V. (2000). Destabilized green fluorescent protein for monitoring dynamic changes in yeast gene expression with flow cytometry. Yeast *16*, 1313-1323.

McAdams, H. H., and Arkin, A. (1997). Stochastic mechanisms in gene expression. Proc Natl Acad Sci U S A *94*, 814-819.

McAdams, H. H., and Arkin, A. (1999). It's a noisy business! Genetic regulation at the nanomolar scale. Trends in genetics : TIG *15*, 65-69.

McCullagh, E., Farlow, J., Fuller, C., Girard, J., Lipinski-Kruszka, J., Lu, D., Noriega, T., Rollins, G., Spitzer, R., Todhunter, M., and El-Samad, H. (2009). Not all quiet on the noise front. Nature chemical biology *5*, 699-704.

McCullagh, E., Seshan, A., El-Samad, H., and Madhani, H. D. (2010). Coordinate control of gene expression noise and interchromosomal interactions in a MAP kinase pathway. Nature cell biology *12*, 954-962.

Megason, S. G., and Fraser, S. E. (2007). Imaging in systems biology. Cell *130*, 784-795.

Mixon, M. B., Lee, E., Coleman, D. E., Berghuis, A. M., Gilman, A. G., and Sprang, S. R. (1995). Tertiary and Quaternary Structural Changes in Gialpha Induced by GTP Hydrolysis. Science *270*, 954-960.

Miyajima, I., Nakafuku, M., Nakayama, N., Brenner, C., Miyajima, A., Kaibuchi, K., Arai, K., Kaziro, Y., and Matsumoto, K. (1987). GPA1, a haploid-specific essential gene, encodes a yeast homolog of mammalian G protein which may be involved in mating factor signal transduction. Cell *50*, 1011-1019.

Mnaimneh, S., Davierwala, A. P., Haynes, J., Moffat, J., Peng, W. T., Zhang, W., Yang, X., Pootoolal, J., Chua, G., Lopez, A.*, et al.* (2004). Exploration of essential gene functions via titratable promoter alleles. Cell *118*, 31-44.

Mombaerts, P. (2004). Odorant receptor gene choice in olfactory sensory neurons: the one receptor-one neuron hypothesis revisited. Current opinion in neurobiology *14*, 31-36.

Moore, T. I., Chou, C. S., Nie, Q., Jeon, N. L., and Yi, T. M. (2008). Robust spatial sensing of mating pheromone gradients by yeast cells. PLoS One *3*, e3865.

Moskow, J. J., Gladfelter, A. S., Lamson, R. E., Pryciak, P. M., and Lew, D. J. (2000). Role of Cdc42p in pheromone-stimulated signal transduction in Saccharomyces cerevisiae. Molecular and cellular biology *20*, 7559-7571.

Munsky, B., Neuert, G., and van Oudenaarden, A. (2012). Using gene expression noise to understand gene regulation. Science *336*, 183-187.

Murphy, J. E., Padilla, B. E., Hasdemir, B., Cottrell, G. S., and Bunnett, N. W. (2009). Endosomes: A legitimate platform for the signaling train. Proceedings of the National Academy of Sciences *106*, 17615-17622.

Murphy, K. F., Balazsi, G., and Collins, J. J. (2007). Combinatorial promoter design for engineering noisy gene expression. Proceedings of the National Academy of Sciences of the United States of America *104*, 12726-12731.

Nagai, Y., Nishimura, A., Tago, K., Mizuno, N., and Itoh, H. (2010). Ric-8B stabilizes the alpha subunit of stimulatory G protein by inhibiting its ubiquitination. The Journal of biological chemistry *285*, 11114-11120.

Nagalakshmi, U., Wang, Z., Waern, K., Shou, C., Raha, D., Gerstein, M., and Snyder, M. (2008). The transcriptional landscape of the yeast genome defined by RNA sequencing. Science *320*, 1344-1349.

Nagiec, M. J., and Dohlman, H. G. (2012). Checkpoints in a yeast differentiation pathway coordinate signaling during hyperosmotic stress. PLoS genetics *8*, e1002437.

Nakafuku, M., Itoh, H., Nakamura, S., and Kaziro, Y. (1987). Occurrence in Saccharomyces cerevisiae of a gene homologous to the cDNA coding for the alpha subunit of mammalian G proteins. Proceedings of the National Academy of Sciences of the United States of America *84*, 2140-2144.

Nathans, J. (1999). The evolution and physiology of human color vision: insights from molecular genetic studies of visual pigments. Neuron *24*, 299-312.

Neubig, R. R. (2002). Regulators of G protein signaling (RGS proteins): novel central nervous system drug targets. The journal of peptide research : official journal of the American Peptide Society *60*, 312-316.

Neves, S. R., Ram, P. T., and Iyengar, R. (2002). G protein pathways. Science *296*, 1636-1639.

Newman, J. R., Ghaemmaghami, S., Ihmels, J., Breslow, D. K., Noble, M., DeRisi, J. L., and Weissman, J. S. (2006). Single-cell proteomic analysis of S. cerevisiae reveals the architecture of biological noise. Nature *441*, 840-846.

Niepel, M., Spencer, S. L., and Sorger, P. K. (2009). Non-genetic cell-to-cell variability and the consequences for pharmacology. Current opinion in chemical biology *13*, 556-561.

Novick, P., Field, C., and Schekman, R. (1980). Identification of 23 complementation groups required for post-translational events in the yeast secretory pathway. Cell *21*, 205-215.

Obin, M. S., Jahngen-Hodge, J., Nowell, T., and Taylor, A. (1996). Ubiquitinylation and ubiquitin-dependent proteolysis in vertebrate photoreceptors (rod outer

segments). Evidence for ubiquitinylation of Gt and rhodopsin. The Journal of biological chemistry *271*, 14473-14484.

Oehlen, L. J., and Cross, F. R. (1998). The role of Cdc42 in signal transduction and mating of the budding yeast Saccharomyces cerevisiae. The Journal of biological chemistry *273*, 8556-8559.

Okada, S., Leda, M., Hanna, J., Savage, N. S., Bi, E., and Goryachev, A. B. (2013). Daughter cell identity emerges from the interplay of Cdc42, septins, and exocytosis. Developmental cell *26*, 148-161.

Orth, J. D., Tang, Y., Shi, J., Loy, C. T., Amendt, C., Wilm, C., Zenke, F. T., and Mitchison, T. J. (2008). Quantitative live imaging of cancer and normal cells treated with Kinesin-5 inhibitors indicates significant differences in phenotypic responses and cell fate. Molecular cancer therapeutics *7*, 3480-3489.

Overton, M. C., and Blumer, K. J. (2000). G-protein-coupled receptors function as oligomers in vivo. Current biology : CB *10*, 341-344.

Ozbudak, E. M., Thattai, M., Kurtser, I., Grossman, A. D., and van Oudenaarden, A. (2002). Regulation of noise in the expression of a single gene. Nat Genet *31*, 69-73.

Paliwal, S., Iglesias, P. A., Campbell, K., Hilioti, Z., Groisman, A., and Levchenko, A. (2007). MAPK-mediated bimodal gene expression and adaptive gradient sensing in yeast. Nature *446*, 46-51.

Parnell, S. C., Marotti, L. A., Jr., Kiang, L., Torres, M. P., Borchers, C. H., and Dohlman, H. G. (2005). Phosphorylation of the RGS protein Sst2 by the MAP kinase Fus3 and use of Sst2 as a model to analyze determinants of substrate sequence specificity. Biochemistry *44*, 8159-8166.

Parsa, H., Upadhyay, R., and Sia, S. K. (2011). Uncovering the behaviors of individual cells within a multicellular microvascular community. Proceedings of the National Academy of Sciences of the United States of America *108*, 5133-5138.

Pedraza, J. M., and van Oudenaarden, A. (2005). Noise propagation in gene networks. Science *307*, 1965-1969.

Pelet, S., Dechant, R., Lee, S. S., van Drogen, F., and Peter, M. (2012). An integrated image analysis platform to quantify signal transduction in single cells. Integrative biology : quantitative biosciences from nano to macro *4*, 1274-1282.

Pickart, C. M., and Eddins, M. J. (2004). Ubiquitin: structures, functions, mechanisms. Biochimica et biophysica acta *1695*, 55-72.

Pierce, K. L., Premont, R. T., and Lefkowitz, R. J. (2002). Seven-transmembrane receptors. Nature reviews Molecular cell biology *3*, 639-650.

Pincus, Z., and Theriot, J. A. (2007). Comparison of quantitative methods for cell-shape analysis. Journal of microscopy *227*, 140-156.

Popov, S., Yu, K., Kozasa, T., and Wilkie, T. M. (1997). The regulators of G protein signaling (RGS) domains of RGS4, RGS10, and GAIP retain GTPase activating protein activity in vitro. Proceedings of the National Academy of Sciences of the United States of America *94*, 7216-7220.

Powell, C. D., Quain, D. E., and Smart, K. A. (2003). Chitin scar breaks in aged Saccharomyces cerevisiae. Microbiology *149*, 3129-3137.

Powell, E. O. (1956). Growth rate and generation time of bacteria, with special reference to continuous culture. Journal of general microbiology *15*, 492-511.

Predrag, R., Vladimir, V., Chad, H., Ross, R. C., Amrita, M., Joshua, W. H., Mark, G. G., and Lilia, M. I. (2010). Identification, analysis, and prediction of protein ubiquitination sites. Proteins: Structure, Function, and Bioinformatics *78*, 365-380.

Premont, R. T., Inglese, J., and Lefkowitz, R. J. (1995). Protein kinases that phosphorylate activated G protein-coupled receptors. FASEB journal : official publication of the Federation of American Societies for Experimental Biology *9*, 175-182.

Pruyne, D., and Bretscher, A. (2000). Polarization of cell growth in yeast. I. Establishment and maintenance of polarity states. Journal of cell science *113 ( Pt 3)*, 365-375.

Ptacek, J., Devgan, G., Michaud, G., Zhu, H., Zhu, X., Fasolo, J., Guo, H., Jona, G., Breitkreutz, A., Sopko, R.*, et al.* (2005). Global analysis of protein phosphorylation in yeast. Nature *438*, 679-684.

Purvis, J. E., and Lahav, G. (2013). Encoding and decoding cellular information through signaling dynamics. Cell *152*, 945-956.

Raj, A., Peskin, C. S., Tranchina, D., Vargas, D. Y., and Tyagi, S. (2006). Stochastic mRNA synthesis in mammalian cells. PLoS biology *4*, e309.

Raj, A., van den Bogaard, P., Rifkin, S. A., van Oudenaarden, A., and Tyagi, S. (2008). Imaging individual mRNA molecules using multiple singly labeled probes. Nature methods *5*, 877-879.

Raj, A., and van Oudenaarden, A. (2008). Nature, nurture, or chance: stochastic gene expression and its consequences. Cell *135*, 216-226.

Rajala, T., Hakkinen, A., Healy, S., Yli-Harja, O., and Ribeiro, A. S. (2010). Effects of transcriptional pausing on gene expression dynamics. PLoS computational biology *6*, e1000704.

Raser, J. M., and O'Shea, E. K. (2004). Control of stochasticity in eukaryotic gene expression. Science *304*, 1811-1814.

Raser, J. M., and O'Shea, E. K. (2005). Noise in gene expression: origins, consequences, and control. Science *309*, 2010-2013.

Rea, S. L., Wu, D., Cypser, J. R., Vaupel, J. W., and Johnson, T. E. (2005). A stress-sensitive reporter predicts longevity in isogenic populations of Caenorhabditis elegans. Nature genetics *37*, 894-898.

Rhodes, N., Connell, L., and Errede, B. (1990). STE11 is a protein kinase required for cell-type-specific transcription and signal transduction in yeast. Genes & development *4*, 1862-1874.

Ricicova, M., Hamidi, M., Quiring, A., Niemisto, A., Emberly, E., and Hansen, C. L. (2013). Dissecting genealogy and cell cycle as sources of cell-to-cell variability in MAPK signaling using high-throughput lineage tracking. Proceedings of the National Academy of Sciences of the United States of America *110*, 11403-11408.

Riddle, E. L., Schwartzman, R. A., Bond, M., and Insel, P. A. (2005). Multi-tasking RGS proteins in the heart: the next therapeutic target? Circulation research *96*, 401-411.

Rinott, R., Jaimovich, A., and Friedman, N. (2011). Exploring transcription regulation through cell-to-cell variability. Proceedings of the National Academy of Sciences of the United States of America *108*, 6329-6334.

Roberts, C. J., Nelson, B., Marton, M. J., Stoughton, R., Meyer, M. R., Bennett, H. A., He, Y. D., Dai, H., Walker, W. L., Hughes, T. R.*, et al.* (2000). Signaling and circuitry of multiple MAPK pathways revealed by a matrix of global gene expression profiles. Science *287*, 873-880.

Rohrer, J., Benedetti, H., Zanolari, B., and Riezman, H. (1993). Identification of a Novel Sequence Mediating Regulated Endocytosis of the G Protein-Coupled Alpha-Pheromone Receptor in Yeast. Molecular Biology of the Cell *4*, 511-521.

Rojas, A. M., Fuentes, G., Rausell, A., and Valencia, A. (2012). The Ras protein superfamily: Evolutionary tree and role of conserved amino acids. The Journal of Cell Biology *196*, 545.

Roman, D. L., Talbot, J. N., Roof, R. A., Sunahara, R. K., Traynor, J. R., and Neubig, R. R. (2007). Identification of small-molecule inhibitors of RGS4 using a high-throughput flow cytometry protein interaction assay. Molecular pharmacology *71*, 169-175.

Rosenfeld, N., Young, J. W., Alon, U., Swain, P. S., and Elowitz, M. B. (2005). Gene regulation at the single-cell level. Science *307*, 1962-1965.

Ross, E. M., and Wilkie, T. M. (2000). GTPase-Activating Proteins for Heterotrimeric G Proteins: Regulators of G Protein Signaling (RGS) and RGS-Like Proteins. Annual Review of Biochemistry *69*, 795-827.

Russ, A. P., and Lampel, S. (2005). The druggable genome: an update. Drug discovery today *10*, 1607-1610.

Saarikangas, J., and Barral, Y. (2011). The emerging functions of septins in metazoans. EMBO reports *12*, 1118-1126.

Sako, Y. (2006). Imaging single molecules in living cells for systems biology. Molecular systems biology *2*, 56.

Sanchez, A., and Golding, I. (2013). Genetic determinants and cellular constraints in noisy gene expression. Science *342*, 1188-1193.

Sasaki, A. T., Carracedo, A., Locasale, J. W., Anastasiou, D., Takeuchi, K., Kahoud, E. R., Haviv, S., Asara, J. M., Pandolfi, P. P., and Cantley, L. C. (2011).

Schandel, K. A., and Jenness, D. D. (1994). Direct evidence for ligand-induced internalization of the yeast alpha-factor pheromone receptor. Molecular and cellular biology *14*, 7245-7255.

Segall, J. E. (1993). Polarization of yeast cells in spatial gradients of alpha mating factor. Proceedings of the National Academy of Sciences of the United States of America *90*, 8332-8336.

Shalek, A. K., Satija, R., Adiconis, X., Gertner, R. S., Gaublomme, J. T., Raychowdhury, R., Schwartz, S., Yosef, N., Malboeuf, C., Lu, D.*, et al.* (2013). Single-cell transcriptomics reveals bimodality in expression and splicing in immune cells. Nature *498*, 236-240.

Shaw, J. D., Cummings, K. B., Huyer, G., Michaelis, S., and Wendland, B. (2001). Yeast as a Model System for Studying Endocytosis. Experimental Cell Research *271*, 1-9.

Shih, S. C., Katzmann, D. J., Schnell, J. D., Sutanto, M., Emr, S. D., and Hicke, L. (2002). Epsins and Vps27p/Hrs contain ubiquitin-binding domains that function in receptor endocytosis. Nature cell biology *4*, 389-393.

Shih, S. C., Sloper-Mould, K. E., and Hicke, L. (2000). Monoubiquitin carries a novel internalization signal that is appended to activated receptors. The EMBO Journal *19*, 187-198.

Siderovski, D. P., Hessel, A., Chung, S., Mak, T. W., and Tyers, M. (1996). A new family of regulators of G-protein-coupled receptors? Current biology : CB *6*, 211-212.

Siderovski, D. P., and Willard, F. S. (2005). The GAPs, GEFs, and GDIs of heterotrimeric G-protein alpha subunits. International journal of biological sciences *1*, 51-66.

Siderovski, D. P. a. W., F. S. (2005). The GAPs, GEFs, and GDIs of heterotrimeric G-protein alpha subunits. International Journal of Biological Sciences, 51-66.

Siekhaus, D. E., and Drubin, D. G. (2003). Spontaneous receptor-independent heterotrimeric G-protein signalling in an RGS mutant. Nat Cell Biol *5*, 231-235.

Sierra, D. A., Popov, S., and Wilkie, T. M. (2000). Regulators of G-protein signaling in receptor complexes. Trends in cardiovascular medicine *10*, 263-268.

Simon, M. N., De Virgilio, C., Souza, B., Pringle, J. R., Abo, A., and Reed, S. I. (1995). Role for the Rho-family GTPase Cdc42 in yeast mating-pheromone signal pathway. Nature *376*, 702-705.

Sjogren, B. (2011). Regulator of G protein signaling proteins as drug targets: current state and future possibilities. Advances in pharmacology *62*, 315-347.

Slepak, V. Z., and Hurley, J. B. (2008). Mechanism of light-induced translocation of arrestin and transducin in photoreceptors: Interaction-restricted diffusion. IUBMB Life *60*, 2-9.

Slessareva, J. E., and Dohlman, H. G. (2006). G Protein Signaling in Yeast: New Components, New Connections, New Compartments. Science *314*, 1412-1413.

Slessareva, J. E., Routt, S. M., Temple, B., Bankaitis, V. A., and Dohlman, H. G. (2006). Activation of the phosphatidylinositol 3-kinase Vps34 by a G protein alpha subunit at the endosome. Cell *126*, 191-203.

Sloper-Mould, K. E., Jemc, J. C., Pickart, C. M., and Hicke, L. (2001). Distinct Functional Surface Regions on Ubiquitin. Journal of Biological Chemistry *276*, 30483-30489.

Smits, W. K., Kuipers, O. P., and Veening, J. W. (2006). Phenotypic variation in bacteria: the role of feedback regulation. Nature reviews Microbiology *4*, 259-271.

Somel, M., Khaitovich, P., Bahn, S., Paabo, S., and Lachmann, M. (2006). Gene expression becomes heterogeneous with age. Current biology : CB *16*, R359-360.

Song, D., Dolan, J. W., Yuan, Y. L., and Fields, S. (1991). Pheromone-dependent phosphorylation of the yeast STE12 protein correlates with transcriptional activation. Genes & development *5*, 741-750.

Song, J., Hirschman, J., Gunn, K., and Dohlman, H. G. (1996). Regulation of membrane and subunit interactions by N-myristoylation of a G protein alpha subunit in yeast. The Journal of biological chemistry *271*, 20273-20283.

Spencer, S. L., Gaudet, S., Albeck, J. G., Burke, J. M., and Sorger, P. K. (2009). Non-genetic origins of cell-to-cell variability in TRAIL-induced apoptosis. Nature *459*, 428-432.

Spiegel, A. M., and Weinstein, L. S. (2004). Inherited diseases involving g proteins and g protein-coupled receptors. Annual review of medicine *55*, 27-39.

Spiliotis, E. T., and Nelson, W. J. (2006). Here come the septins: novel polymers that coordinate intracellular functions and organization. Journal of cell science *119*, 4-10.

Sprague, G. F., Jr. (1991). Assay of yeast mating reaction. Methods Enzymol *194*, 77-93.

Sprang, S. R. (1997). G protein mechanisms: insights from structural analysis. Annual review of biochemistry *66*, 639-678.

Spudich, J. L., and Koshland, D. E., Jr. (1976). Non-genetic individuality: chance in the single cell. Nature *262*, 467-471.

Staub, O., and Rotin, D. (2006). Role of ubiquitylation in cellular membrane transport. Physiological reviews *86*, 669-707.

Sternberg, P. W., and Horvitz, H. R. (1986). Pattern formation during vulval development in C. elegans. Cell *44*, 761-772.

Stewart-Ornstein, J., Weissman, J. S., and El-Samad, H. (2012). Cellular noise regulons underlie fluctuations in Saccharomyces cerevisiae. Molecular cell *45*, 483-493.

Stow, J. L., de Almeida, J. B., Narula, N., Holtzman, E. J., Ercolani, L., and Ausiello, D. A. (1991). A heterotrimeric G protein, G alpha i-3, on Golgi membranes regulates

the secretion of a heparan sulfate proteoglycan in LLC-PK1 epithelial cells. The Journal of Cell Biology *114*, 1113-1124.

Suel, G. M., Garcia-Ojalvo, J., Liberman, L. M., and Elowitz, M. B. (2006). An excitable gene regulatory circuit induces transient cellular differentiation. Nature *440*, 545-550.

Suel, G. M., Kulkarni, R. P., Dworkin, J., Garcia-Ojalvo, J., and Elowitz, M. B. (2007). Tunability and noise dependence in differentiation dynamics. Science *315*, 1716-1719.

Sureka, K., Ghosh, B., Dasgupta, A., Basu, J., Kundu, M., and Bose, I. (2008). Positive feedback and noise activate the stringent response regulator rel in mycobacteria. PLoS One *3*, e1771.

Swain, P. S., Elowitz, M. B., and Siggia, E. D. (2002). Intrinsic and extrinsic contributions to stochasticity in gene expression. Proc Natl Acad Sci U S A *99*, 12795-12800.

Takahashi, S., and Pryciak, P. M. (2008). Membrane localization of scaffold proteins promotes graded signaling in the yeast MAP kinase cascade. Curr Biol *18*, 1184-1191.

Tanabe, S., Kreutz, B., Suzuki, N., and Kozasa, T. (2004). Regulation of RGS-RhoGEFs by Galpha12 and Galpha13 proteins. Methods in enzymology *390*, 285-294.

Tanaka, H., and Yi, T.-M. (2010). The Effects of Replacing Sst2 with the Heterologous RGS4 on Polarization and Mating in Yeast. Biophysical Journal *99*, 1007-1017.

Taniguchi, Y., Choi, P. J., Li, G. W., Chen, H., Babu, M., Hearn, J., Emili, A., and Xie, X. S. (2010). Quantifying E. coli proteome and transcriptome with single-molecule sensitivity in single cells. Science *329*, 533-538.

Tardiff, D. F., Jui, N. T., Khurana, V., Tambe, M. A., Thompson, M. L., Chung, C. Y., Kamadurai, H. B., Kim, H. T., Lancaster, A. K., Caldwell, K. A.*, et al.* (2013). Yeast Reveal a “Druggable” Rsp5/Nedd4 Network that Ameliorates α-Synuclein Toxicity in Neurons. Science *342*, 979-983.

Tawfik, D. S. (2010). Messy biology and the origins of evolutionary innovations. Nature chemical biology *6*, 692-696.

Taylor, R. J., Falconnet, D., Niemisto, A., Ramsey, S. A., Prinz, S., Shmulevich, I., Galitski, T., and

Hansen, C. L. (2009). Dynamic analysis of MAPK signaling using a high-throughput microfluidic single-cell imaging platform. Proc Natl Acad Sci U S A *106*, 3758-3763.

Teague, M. A., Chaleff, D. T., and Errede, B. (1986). Nucleotide sequence of the yeast regulatory gene STE7 predicts a protein homologous to protein kinases. Proceedings of the National Academy of Sciences of the United States of America *83*, 7371-7375.

Thattai, M., and van Oudenaarden, A. (2001). Intrinsic noise in gene regulatory networks. Proc Natl Acad Sci U S A *98*, 8614-8619.

Thattai, M., and van Oudenaarden, A. (2002). Attenuation of noise in ultrasensitive signaling cascades. Biophysical journal *82*, 2943-2950.

Thattai, M., and van Oudenaarden, A. (2004). Stochastic gene expression in fluctuating environments. Genetics *167*, 523-530.

Thompson, M. D., Cole, D. E., and Jose, P. A. (2008). Pharmacogenomics of G protein-coupled receptor signaling: insights from health and disease. Methods in molecular biology *448*, 77-107.

Thomson, T. M., Benjamin, K. R., Bush, A., Love, T., Pincus, D., Resnekov, O., Yu, R. C., Gordon, A., Colman-Lerner, A., Endy, D., and Brent, R. (2011). Scaffold number in yeast signaling system sets tradeoff between system output and dynamic range. Proceedings of the National Academy of Sciences of the United States of America *108*, 20265-20270.

Torres, M. P., Clement, S. T., Cappell, S. D., and Dohlman, H. G. (2011). Cell cycle-dependent phosphorylation and ubiquitination of a G protein alpha subunit. The Journal of biological chemistry *286*, 20208-20216.

Torres, M. P., Lee, M. J., Ding, F., Purbeck, C., Kuhlman, B., Dokholyan, N. V., and Dohlman, H. G. (2009). G Protein Mono-ubiquitination by the Rsp5 Ubiquitin Ligase. The Journal of biological chemistry *284*, 8940-8950.

Toutant, M., Aunis, D., Bockaert, J., Homburger, V., and Rouot, B. (1987). Presence of three pertussis toxin substrates and Goα immunoreactivity in both plasma and granule membranes of chromaffin cells. FEBS Letters *215*, 339-344.

Unger, T., Jacobovitch, Y., Dantes, A., Bernheim, R., and Peleg, Y. (2010). Applications of the Restriction Free (RF) cloning procedure for molecular manipulations and protein expression. Journal of structural biology *172*, 34-44.

Van Eps, N., Preininger, A. M., Alexander, N., Kaya, A. I., Meier, S., Meiler, J., Hamm, H. E., and Hubbell, W. L. (2011). Interaction of a G protein with an activated

receptor opens the interdomain interface in the alpha subunit. Proceedings of the National Academy of Sciences *108*, 9420-9424.

Veening, J. W., Hamoen, L. W., and Kuipers, O. P. (2005). Phosphatases modulate the bistable sporulation gene expression pattern in Bacillus subtilis. Molecular microbiology *56*, 1481-1494.

Veening, J. W., Stewart, E. J., Berngruber, T. W., Taddei, F., Kuipers, O. P., and Hamoen, L. W. (2008). Bet-hedging and epigenetic inheritance in bacterial cell development. Proceedings of the National Academy of Sciences of the United States of America *105*, 4393-4398.

Vieira, A. V., Lamaze, C., and Schmid, S. L. (1996). Control of EGF Receptor Signaling by Clathrin-Mediated Endocytosis. Science *274*, 2086-2089.

Visvikis, O., Lorès, P., Boyer, L., Chardin, P., Lemichez, E., and Gacon, G. (2008). Activated Rac1, but not the tumorigenic variant Rac1b, is ubiquitinated on Lys 147 through a JNK-regulated process. FEBS Journal *275*, 386-396.

Volfson, D., Marciniak, J., Blake, W. J., Ostroff, N., Tsimring, L. S., and Hasty, J. (2006). Origins of extrinsic variability in eukaryotic gene expression. Nature *439*, 861-864.

Voliotis, M., and Bowsher, C. G. (2012). The magnitude and colour of noise in genetic negative feedback systems. Nucleic acids research *40*, 7084-7095.

Wach, A., Brachat, A., Pohlmann, R., and Philippsen, P. (1994). New heterologous modules for classical or PCR-based gene disruptions in Saccharomyces cerevisiae. Yeast *10*, 1793-1808.

Wang, D., and Bodovitz, S. (2010). Single cell analysis: the new frontier in 'omics'. Trends in biotechnology *28*, 281-290.

Wang, Y., and Dohlman, H. G. (2006). Regulation of G protein and mitogen-activated protein kinase signaling by ubiquitination: insights from model organisms. Circulation research *99*, 1305-1314.

Wang, Y., Marotti, L. A., Jr., Lee, M. J., and Dohlman, H. G. (2005). Differential regulation of G protein alpha subunit trafficking by mono- and polyubiquitination. The Journal of biological chemistry *280*, 284-291.

Watson, N., Linder, M. E., Druey, K. M., Kehrl, J. H., and Blumer, K. J. (1996). RGS family members: GTPase-activating proteins for heterotrimeric G-protein alpha-subunits. Nature *383*, 172-175.

Wedegaertner, P. (2012a). G Protein Trafficking. In GPCR Signalling Complexes – Synthesis, Assembly, Trafficking and Specificity, D. J. Dupré, T. E. Hébert, and R. Jockers, eds. (Springer Netherlands), pp. 193-223.

Wedegaertner, P. B., Bourne, H. R., and von Zastrow, M. (1996). Activation-induced subcellular redistribution of Gs alpha. Molecular Biology of the Cell *7*, 1225-1233.

Westfield, G. H., Rasmussen, S. G. F., Su, M., Dutta, S., DeVree, B. T., Chung, K. Y., Calinski, D., Velez-Ruiz, G., Oleskie, A. N., Pardon, E.*, et al.* (2011). Structural flexibility of the Gαs α-helical domain in the β2-adrenoceptor Gs complex. Proceedings of the National Academy of Sciences *108*, 16086-16091.

Whiteway, M., Hougan, L., Dignard, D., Thomas, D. Y., Bell, L., Saari, G. C., Grant, F. J., O'Hara, P., and MacKay, V. L. (1989). The STE4 and STE18 genes of yeast encode potential beta and gamma subunits of the mating factor receptor-coupled G protein. Cell *56*, 467-477.

Wilkinson, L. E., and Pringle, J. R. (1974). Transient G1 arrest of S. cerevisiae cells of mating type alpha by a factor produced by cells of mating type a. Experimental cell research *89*, 175-187.

Willars, G. B. (2006). Mammalian RGS proteins: multifunctional regulators of cellular signalling. Seminars in cell & developmental biology *17*, 363-376.

Winget, J. M., and Mayor, T. (2010). The diversity of ubiquitin recognition: hot spots and varied specificity. Molecular cell *38*, 627-635.

Winters, M. J., Lamson, R. E., Nakanishi, H., Neiman, A. M., and Pryciak, P. M. (2005). A membrane binding domain in the ste5 scaffold synergizes with gbetagamma binding to control localization and signaling in pheromone response. Molecular cell *20*, 21-32.

Winzeler, E. A., Shoemaker, D. D., Astromoff, A., Liang, H., Anderson, K., Andre, B., Bangham, R., Benito, R., Boeke, J. D., Bussey, H.*, et al.* (1999). Functional characterization of the S. cerevisiae genome by gene deletion and parallel analysis. Science *285*, 901-906.

Wise, A., Gearing, K., and Rees, S. (2002). Target validation of G-protein coupled receptors. Drug discovery today *7*, 235-246.

Wittinghofer, A. (1994). The structure of transducin Gαt: More to view than just Ras. Cell *76*, 201-204.

Wu, M., Su, R. Q., Li, X., Ellis, T., Lai, Y. C., and Wang, X. (2013). Engineering of regulated stochastic cell fate determination. Proceedings of the National Academy of Sciences of the United States of America *110*, 10610-10615.

Yashiroda, H., Oguchi, T., Yasuda, Y., Toh, E. A., and Kikuchi, Y. (1996). Bul1, a new protein that binds to the Rsp5 ubiquitin ligase in Saccharomyces cerevisiae. Molecular and cellular biology *16*, 3255-3263.

Yu, J., Xiao, J., Ren, X., Lao, K., and Xie, X. S. (2006). Probing gene expression in live cells, one protein molecule at a time. Science *311*, 1600-1603.

Yu, R. C., Pesce, C. G., Colman-Lerner, A., Lok, L., Pincus, D., Serra, E., Holl, M., Benjamin, K., Gordon, A., and Brent, R. (2008). Negative feedback that improves information transmission in yeast signalling. Nature *456*, 755-761.

Yuan, T. L., Wulf, G., Burga, L., and Cantley, L. C. (2011). Cell-to-cell variability in PI3K protein level regulates PI3K-AKT pathway activity in cell populations. Current biology : CB *21*, 173-183.

Zhang, H., and Chen, Y. (2012). Noise propagation in gene regulation networks involving interlinked positive and negative feedback loops. PLoS One *7*, e51840.

Zhang, Y., Luo, C., Zou, K., Xie, Z., Brandman, O., Ouyang, Q., and Li, H. (2012). Single cell analysis of yeast replicative aging using a new generation of microfluidic device. PLoS One *7*, e48275.

Zheng, B., Lavoie, C., Tang, T.-D., Ma, P., Meerloo, T., Beas, A., and Farquhar, M. G. (2004). Regulation of Epidermal Growth Factor Receptor Degradation by Heterotrimeric Gαs Protein. Molecular Biology of the Cell *15*, 5538-5550.

Zhong, H., and Neubig, R. R. (2001). Regulator of G protein signaling proteins: novel multifunctional drug targets. The Journal of pharmacology and experimental therapeutics *297*, 837-845.

Zhou, Z., Gartner, A., Cade, R., Ammerer, G., and Errede, B. (1993). Pheromone-induced signal transduction in Saccharomyces cerevisiae requires the sequential function of three protein kinases. Molecular and cellular biology *13*, 2069-2080.

Zhu, M., Torres, M. P., Kelley, J. B., Dohlman, H. G., and Wang, Y. (2011). Pheromone- and RSP5-dependent Ubiquitination of the G Protein β Subunit Ste4 in Yeast. Journal of Biological Chemistry *286*, 27147-27155.

Zong, H., Kaibuchi, K., and Quilliam, L. A. (2001). The Insert Region of RhoA Is Essential for Rho Kinase Activation and Cellular Transformation. Molecular and cellular biology *21*, 5287-5298.